Addendum to Master Engineering Science Thesis

Title: " A Synchronous Generator Monitoring System Utilizing Air-Gap Flux Signals"

Author: Dev Randhawa

(A) On Page 7,
The synchronous machine rating should read 7.5kVA, not 5kVA.

(B) Replace on Page 89,

Under short circuit condition, and making the assumption that the stator resistance is insignificant when compared to the synchronous inductance, the line current is a direct axis current.

with

The stator resistance of 1.05Ω is insignificant, 3.8%, when compared to the synchronous inductance of 27.6Ω. Hence the line current can be considered a direct axis current under short circuit conditions.

(C) Add new subsection on Page 171

E.5 The Per-Unit System.

The per unit system was used extensively in this thesis. In this system, the various machine quantities are expressed as dimensionless quantities. These dimensionless quantities are obtained by representing the machine quantities as a fraction of predefined base units. In this system there are two main base units. The first is the Volt-Amp rating, VA_{rating} of the machine and second is the rated line-line terminal voltage, $V_{terminal(l-l)}$. From these quantities other base units are derived. For example :-

$$Base\ current = \frac{VA_{rating}}{\sqrt{3}V_{terminal(l-l)}}$$

$$Base\ impedance = \frac{V_{terminal(l-l)}{}^2}{VA_{rating}}$$

Substituting the rated machine quantities the following base quantities are obtained

$$\begin{aligned} Base\ VA_{rating} &= 7.5kVA \\ Base\ V_{terminal(l-l)} &= 415V \\ Base\ current &= 10.5A \\ Base\ impedance &= 22.8\Omega \end{aligned}$$

To represent a machine quantity in per unit terms, it is a simple task of dividing it by the appropriate base value. For example:-

$$\begin{aligned} X_d &= 27.6\Omega \\ &= \frac{27.6}{22.8} \\ &= 1.21\ per\ unit \end{aligned}$$

(D) Add on Page 106 after Equation: 9.9

A good opportunity exists at this stage to compare the results obtained here with results obtained in previous tests detailed in this thesis. In the sudden 3-phase short circuit test performed in Chapter 8, Figure 8.4, the following machine quantities were derived:-

$$\begin{aligned} X_d &= synchronous\ reactance &&= 1.243\ per\ unit \\ X'_d &= transient\ reactance &&= 0.1807\ per\ unit \\ T'_d &= transient\ time\ constant &&= 0.1039s \end{aligned}$$

These quantities are related to each other by the equation shown below [1]:-

$$X'_d = \frac{T'_d}{T'_{d0}} * X_d$$

with

T'_{d0} = the direct axis transient open circuit time constant as defined above.

This equation yields a value of 0.715s for T'_{d0}. This value differs by 9% from that value obtained above from the frequency response test. A possible source of this error could the the actual frequency resolution of the frequency response tests. A variation of only 0.02Hz in the frequency measurement will account for this difference. In the frequency response tests performed here, small absolute errors in frequency could lead to very large relative errors. Considering this, the difference in the two quantities obtained above of only 9% is acceptable, and gives rise to confidence in the various instrumentation systems designed.

(E) On Page 111, Insert new paragraph after ".....and produced very good results.

The monitoring system used in this thesis was designed with a worst case accuracy of 5%. This accuracy is governed mainly by the inherent accuracy of the analogue components used and not on the design. As the accuracy of the components has a direct relationship to its cost, a trade-off has to be made between cost and accuracy depending on the particular need.

A Synchronous Generator Monitoring System Utilizing Air-Gap Flux Signals

by

Dev Randhawa

Thesis submitted for the degree of
Master of Engineering Science
in
The University of Adelaide,
Faculty of Engineering,
Department of Electrical and Electronic Engineering.

February 1995

Contents

List of Tables

List of Figures

Abstract

Measuring synchronous machine characteristics in real time when the machine is on-line is not the easiest thing to do. This thesis describes the development of a prototype machine monitoring system that allows just that. The monitoring station developed consists of three main transducers.

The first of these transducers is an Air-Gap flux transducer. This transducer was used to determine the air-gap flux in the synchronous machine in real time with high accuracy and minimal cost. The transducer design was an adaptation of a new approach that was proposed to measure the air gap fluxes in an induction machine.

The second transducer designed was a Park's Transform transducer. This transducer was used to transform, in real time, the sinusoidally varying machine quantities as viewed from the stator frame of reference to a rotor frame of reference. The machine quantities that were transformed were the line currents, the terminal voltages and the air-gap flux signals.

The last of the three transducer designed was a Rotor Angle transducer. This transducer enables the measurement of the machine's rotor angle in real time and with high accuracy. The design is also very robust and will provide accurate results even when subjected to unbalanced voltage supplies.

The practicality of the monitoring system was then tested by applying it to various tasks using a modified 5kVA laboratory synchronous machine. The monitoring station was tested with the machine running under both steady state and transient conditions.

Declaration

This work contains no material which has been accepted for the award of any other degree or diploma in any university or other tertiary institution and, to the best of my knowledge and belief, contains no material previously published or written by another person, except where due reference has been made in the text.

I give consent to this copy of my thesis, when deposited in the University Library, being available for loan and photocopying.

SIGNED: DATE: 30/01/95

Acknowledgements

I wish to express my appreciation to my supervisor, Dr A.M. Parker, for his guidance, assistance and encouragement through the course of this project and preparation of this thesis. He was always able to find time in his busy schedule to help, and for that, I am very grateful.

I also wish to thank the technical staff in the department. In particular, I would like to thank Mr P. Roberts and Mr. I. Linke for all their time, help and advise in the construction of the hardware. Thanks has to also go to Mr. G. Pook, for etching all the printed circuit boards used, and to Mr. W. Foid, for helping me solve all my computer related problem, which were numerous. A special mention has to also go to Mr. A. Schueller for all his help procuring the various devices used in this project.

I would also wish to acknowledge the generosity of the Australian Electricity Supply Industry Research Board for their financial support, by way of a research grant and for providing funds for equipment purchases.

My family have always been very supporting, understanding and full of encouragement throughout my studies. Thank you all for being there, for understanding and for putting up with me.

Chapter 1

INTRODUCTION

1.1 Measurements in Synchronous Machines

In the performance of power systems, the role of the synchronous generators and their associated controllers is of crucial importance. As well as providing all the real power requirements and a portion of the reactive power requirements of the system under normal loading conditions, it is the electromechanical behaviour of the generator when perturbed from a steady-state operating point which dominates the dynamic response of the system as a whole. It is thus vital that the operational parameters of the generators are know under conditions as close as possible to those that will be encountered in daily duty.

There are two principal uses to which operational information on synchronous generators can be applied. The first is to provide input data for mathematical modelling studies, and the second to synthesize control signals which may be used on-line to enhance system stability or to improve dynamic response.

Machine modelling is very important in power engineering. In the design of power systems, almost all the design and testing work is done with the use of computer simulations. As with all work done on computers, the output results or data are only as good as the input data. If the model used in the simulation is inaccurate, the results obtained will also be inaccurate. Hence

there is at present a lot of work being done to develop more accurate models to represent synchronous machines.

The existing tests used to determine machine parameters are numerous. Traditionally, the short and open circuit test and the sudden 3-phase short circuit test [13] have been used. However, in recent times, other more accurate tests have been developed. These include the stationary d.c. decay test [19] [18] [4] [20], the frequency response test at standstill or reduced speed [6] [12] [8] [7] and small signal tests on load [10] [14] [11] [16] just to name a few.

The obtaining of the machine parameters is not easy. There are a lot of machine intricacies that have to be considered in order to properly represent the the machine in a computer model. These intricacies include the fact that the parameters obtained for a stationary machine are different from those when rotating due to different contact pressures on the rotating parts, and that the model developed when the machine is off-line can be somewhat different than what is experienced on-line due to different flux paths and levels. The small signal model of a machine can also be vastly different from large signal analysis.[16]

When controlling a synchronous generator, machine quantities are usually used in a negative feed back loop to control various aspects of the machine's performance. As a minimum requirement in all working generators, it is essential to feed-back the frequency of the output voltage in order to control the governor of the turbine to modulate the shaft power and to use the terminal voltage to control the field excitation in AVR systems. It is becoming increasingly common to provide additional signals to controllers to improve the overall system dynamics, and in particular to increase the damping on the major oscillatory modes following a disturbance. A significant body of work exists on the formal design methods for those augmented controllers, which are usually termed power system stabilizers [5] [9]. Thus in addition to the measurement of the shaft speed and terminal voltage, there is a need to provide a range of additional measurands under operational conditions.

The ability to take accurate real time measurements from a synchronous generator, when the machine is on-line, will hence be very useful to power engineers. The task undertaken in this work was to design a monitoring

system that is able to measure various synchronous machine operating quantities accurately and in real time. The monitoring system has to be fairly cheap to build in order to make it economically viable, must also be easy to install and operate, and to be robust to changes in operating conditions. It should also be capable of extracting the required information in the presence of real-world imperfections such as noise, waveform distortion and phase unbalance.

The choice of what quantities to measure in the synchronous machine has to be carefully considered. The basic quantities like terminal voltage, line current, field excitation current and shaft speed are readily available and are easily incorporated into a measurement system. However some strategically chosen derived quantities should be added to improve the usefulness of the unit. In this work three additional features are to be provided which in combination with the conventional terminal quantities, form a powerful facility for both parameter identification and on-line control work.

The first feature is instantaneous air-gap flux. This is the essential medium for energy transfer between the stator and the rotor in any rotating machine, and information about its magnitude and spatial distribution at any instant in time is a very valuable aid in determining the exact machine operating condition. Also, from a knowledge of this flux and the stator current, a signal proportional to instantaneous developed electromagnetic torque can be readily synthesized which can form a vital component in a fast-acting control strategy.

The great majority of work done on the modelling of power systems utilize machine quantities expressed in Park's (d,q) frame of of reference, in which all the stator three-phase quantities are resolved into their equivalents along axes fixed with respect to the rotor. The second major element is this work is to design a unit which will take quantities measured on the stator (voltage, current and air-gap flux) and transfer them into their d-q components in real time. Again, the results of this stage can be used either to improve the accuracy of machine models or to act as inputs for control schemes based on d-q model formulations.

The third aspect of this work is the provision of an accurate measurement

of instantaneous rotor angle. The quantity is the normal descriptor for the stability of a generator or of a complete system, and must be included in any comprehensive measurement package.

1.2 Arrangement of the Thesis

This thesis deals with the design and construction of a prototype monitoring system for synchronous machines, that is capable of synthesising accurate measurements of the machine quantities in real time and with the machine on-line.

In chapter 2, the experimental environment for this work is described. The specifications of the rotating equipment; the d.c. machine, the synchronous machine and the shaft encoder are detailed. Included in this chapter is a section on the data acquisition and processing real time computer, AMLAB. The intended use of AMLAB, the limitations encountered and the eventual role of AMLAB is discussed.

In the next 3 chapters, the design, construction and initial testing of the monitoring system; air-gap flux transducer (chapter 3), the Park's transform unit (chapter 4) and the rotor angle transducer (chapter 5), is covered. In each of these chapters, the development of each transducer, including the various abortive designs and modifications, is covered.

Having designed and constructed the monitoring system, some applications of the system are demonstrated. The first set of tests, or applications, performed were the steady state tests. In chapter 6, the open circuit test is detailed with the field excitation current, I_{fd}, quadrature axis voltage, V_q, and the direct axis flux linkage, ψ_d, used as parameters.

The second component of the steady state tests is the load test, which is covered in chapter 7. In this test, the synchronous machine is connected in a single machine infinite busbar, SMIB, configuration. The machine is made to operate at various load points, characterized by its real and reactive power output. At each of the load points, the machine quantities are measured

with the monitoring station, as well as conventionally with multimeters and wattmeters. The results are then analyzed with the real and reactive power and torque measurements synthesized by the monitoring system being compared with those produced by the wattmeter. The results are also used in parameter identification, to try and determine quantitatively the saturation that exists in the direct and quadrature axis inductances in the synchronous machines.

The last section of chapter 7 demonstrates the capability of the transducer to determine the spatial distribution of flux in the rotor. The flux distributions obtained for 3 distinct operating conditions will be reported.

Having completed a demonstration of the steady state capabilities of the monitoring system, some transient capabilities will be reported in chapter 8. The transient tests performed are divided into 2 sections. The first section deals with the identification of the dynamic parameters of the synchronous machine by the sudden 3-phase short circuit test. In the second section, step changes were placed on the synchronous machine in view of determining the suitability of using the transient signals, produced by the monitoring system as control signals, as part of a feedback control strategy for synchronous machines.

In chapter 9, frequency response tests are performed on the synchronous machine. A gain/phase analyzer is used to obtain the frequency response of the direct axis flux linkage, ψ_d, with respect to the field excitation voltage, V_f, at various operating conditions. First order transfer functions are then generated to fit the results obtained.

Chapter 2

THE EXPERIMENTAL ENVIRONMENT

2.1 Introduction

The clear focus of the project was to produce a monitoring system which demonstrably performs in the environment of a real machine system, subject to real-world imperfections and constraints. In this chapter, the experimental environment for the work will be described, identifying the major components of hardware and data acquisition facilities.

One obvious point to be made is that the principle of the monitoring system proposed are intended to be sufficiently general to allow its use on full-scale generators, even though its experimental development is carried out on laboratory-scale equipment. In a number of respects the latter equipment poses a more stringent test of methodology, for example having shorter time constants than those found in large generators.

2.2 The Experimental Machine Set

The layout of the basic experiment set-up is shown in Figure: 2.1.

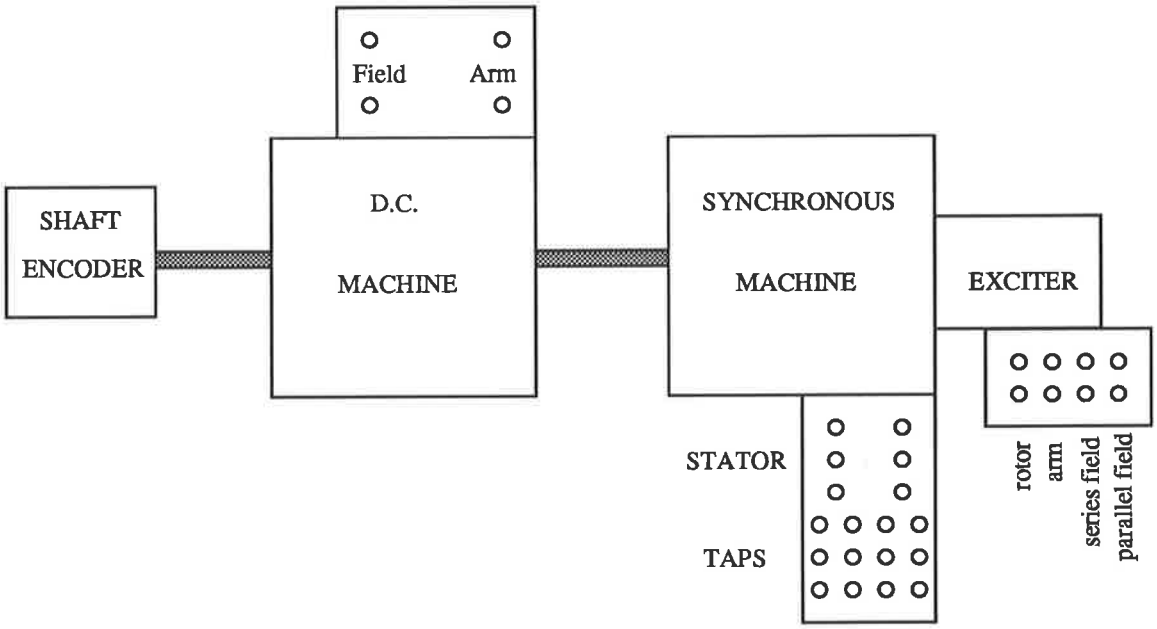

Figure 2.1: Machine Set

2.2.1 The Synchronous Generator

This machine is a modified 2 pole pair salient pole synchronous machine rated at 5kVA, 415volts. It has a 48 slot stator that incorporates 48 coils in a double lap winding configuration. The rotor has a damper cage incorporating bars embedded in the pole faces. The 2 pole pairs determine a synchronous speed of the machine at 1500rpm. A major difference between this machine and a "standard" machine are the tap windings. A tap is taken off successive coils in a phase belt of all 3 phases. These taps provides access to the voltage induced in the individual stator coils. The purpose of these taps will be

explained in detail later. The generator has an integral shaft-driven exciter, but for most tests an independent d.c. supply was used.

2.2.2 The D.C. Drive Motor

The d.c machine is a 7kW standard laboratory d.c. machine and acts as the prime mover or the load for the synchronous machine. It is used to run the synchronous machine up to synchronous speed. When the synchronous machine is synchronized to the mains supply, the d.c. machine is used as a prime mover when generating or the load when motoring. In most of the tests performed here, the synchronous machine is generating with the d.c. machine acting as a prime mover. The machine has a separately excited field winding.

2.2.3 The Shaft Encoder

The shaft encoder is used for position sensing. For the design of many of the proposed transducers, it is important to know the exact position of the rotor shaft. The shaft encoder used was a Litton Model 76, 8 bit gray code shaft encoder. The encoder produces a gray code for 256 discrete positions of the shaft. The shaft encoder was oriented on the shaft in such a way that it resulted in it counting the gray code backwards. This backwards counting is not a problem at all, but should be noted when analyzing the designs of the Park's and rotor angle transducers. The inherent resolution of the encoder corresponds to 2.8 electrical degrees.

2.3 The Real Time Data Acquisition and Analysis Computer - AMLAB

2.3.1 Description of the System

AMLAB is a data acquisition and analysis system produced by Associative Measurement Pty. Ltd. The AMLAB system consists of hardware and soft-

ware components housed in an IBM 486 personal computer.

The hardware consists of three pc cards and an analogue module. The analogue module fits into any spare 5.25 floppy disk drive slot and it is the link to the outside world. Various digital and analogue input and outputs are provided to link AMLAB to the real world. The analogue signals can be sampled into AMLAB at a rate up to 40kHz. The pc cards are the heart of the AMLAB system. It has all the data acquisition and signal processing hardware used by AMLAB. In the configuration available for this project, AMLAB has a complement of 8 analogue and 16 digital input channels

The above hardware is controlled by its own software package. This software package runs in a Windows-like environment. Various icons can be selected, from the icon library, and connected to form various schematics, or projects as it is called in AMLAB. The icons represent various functions to be implemented in AMLAB. Functions like analogue inputs, filters, fast fourier transforms, various display options are available. When the project is executed, the software interprets the project and controls the hardware accordingly. Also included in the software are various printing and saving options. Projects and waveforms obtained can be printed on any laser printer. The waveforms can also be saved for future analysis. Another function that proved to be valuable is the ability to export the waveforms to a third party software for analysis.

2.3.2 Limitations of the AMLAB System

From the specifications of the system, it was hoped that the facilities in AMLAB could be utilized to do the vast bulk of the processing involved in synthesising the various transducers. However, it was established at an early stage that there were some severe constraints imposed by the combination of sampling rate and computational capabilities.

Theoretically AMLAB's analogue inputs can be sampled at a rate up to 40kHz. However, if projects of any complexity are used, the maximum sampling rate drops fairly significantly. The sampling rate had to be reduced to

prevent AMLAB from experiencing DSP over-run errors.

This slow sampling rate led to difficulties. The slow sampling rate required the input signals, in the Park's transform transducer, to be sampled and held. This was done to give the project time to perform the transform. A example of the sample and hold signal used is shown in Figure: 2.2. However, when

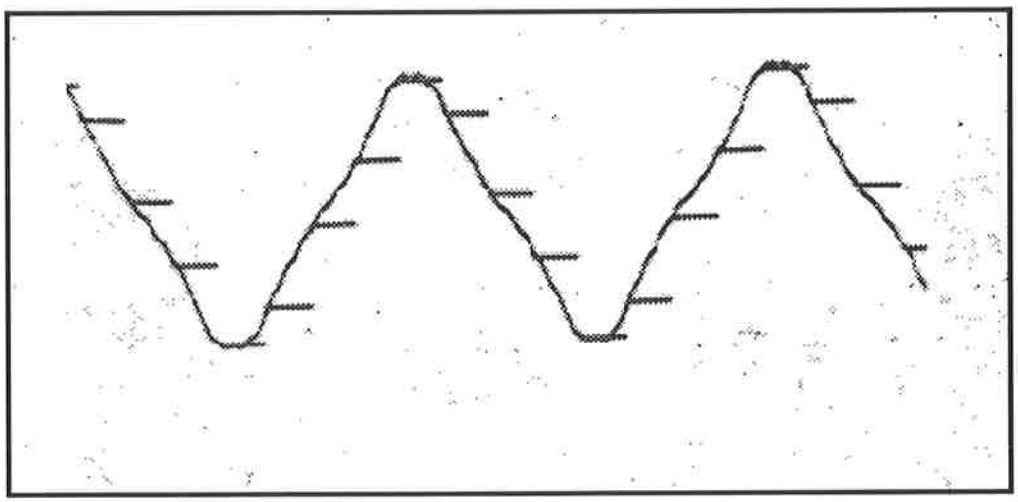

Figure 2.2: Photograph of a sampled and hold signal superimposed on the original signal

the signals were viewed on AMLAB, it was found that the AMLAB signal

did not match the actual signal very well. The results obtained are shown in Figure: 2.3 and Figure: 2.4. Using a sampling rate of 1kHz results in the filtering of all of the sample and hold steps. Using an excessive value of 10kHz does produce the stepping. However, there is an exponentially decreasing sinusoid on each transition. Both these two signals are unsatisfactory.

As a further constraint, the generic library of icons was very limited, with digital functions seriously under-supplied. For example, if an 8 bit digital word was to be input, there is no simple way to convert it back to an analogue signal. The absence of a digital counter was also a big limitation.

The hardware used in AMLAB can only be controlled by its own software. When the limitations above were encountered, there was no way to write or create user defined functions. The user is restricted to what was available in the AMLAB software.

Finally, the reference or zero level for the analogue to digital (A/D) converters used in AMLAB was found to drift when the system was first turned on. The amount of drift was quite significant and only settled down about 3 hours after the AMLAB system was first energised. The exact reason for this drift is not known but a good guess could be that is a thermal effect acting on the A/D converters.

2.3.3 The Eventual Role of AMLAB

As a result of the limitations described in the last section, it is clear that there was no prospect of implementing the operational units of the transducers in AMLAB. The only solution was to build the transducers in hardware.

It was hence decided to use AMLAB as a data acquisition system. The input signals were exported to a file in a "comma separated variable" file format. This file was then imported into MATLAB for processing, analysis and display.

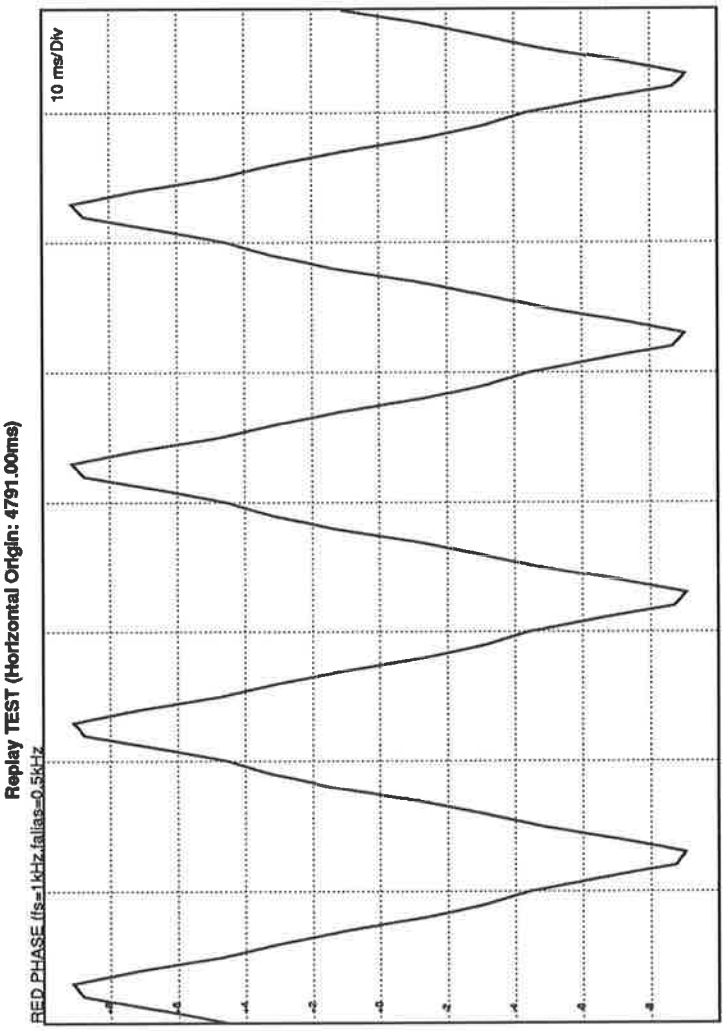

Figure 2.3: The sampled and hold signal viewed on AMLAB with a sampling frequency of 1kHz

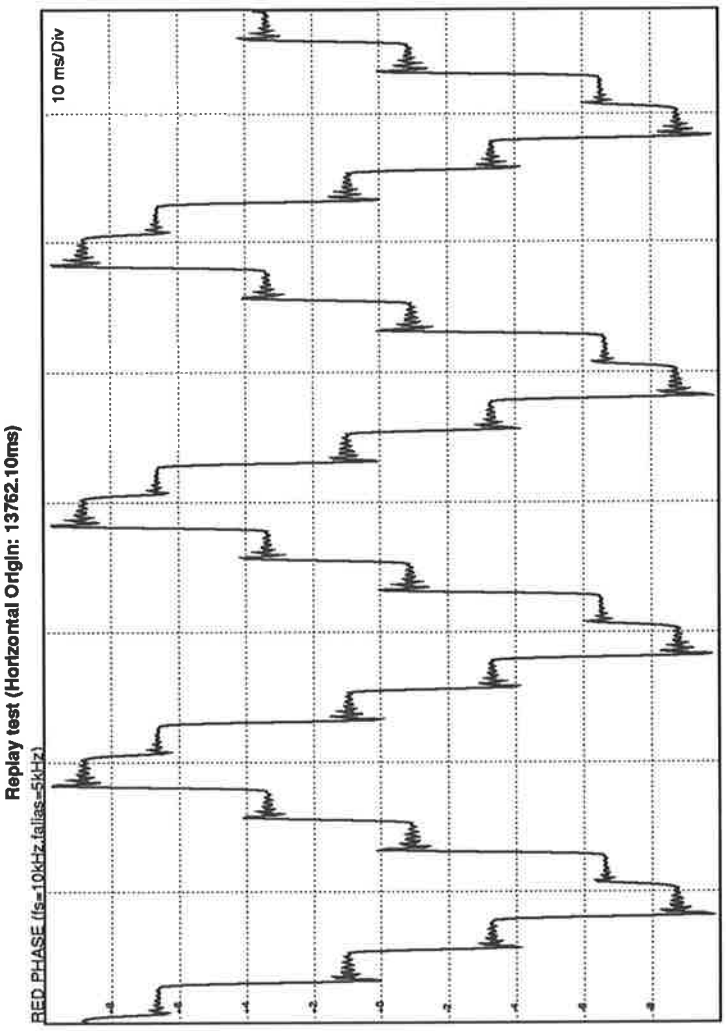

Figure 2.4: The sampled and hold signal viewed on AMLAB with a sampling frequency of 10kHz

2.4 The Use of MATLAB

MATLAB is a commercial software produced by The Math Works Inc. This software was used extensively in the development of the monitoring system. Various programs could be written in MATLAB's own script. Programs were easy to write in MATLAB when compared to other languages. It's predefined routines and graphical interface made it very useful as programs could be written very quickly with very few of the problems associated with traditional programming.

In the designing phase, MATLAB was used to simulate the transducers. Transducer designs were verified, prior to construction in hardware, by running computer simulations written in MATLAB script. These simulations were useful in two ways. Firstly, they enabled the validity of various measurement schemes to be tested and verified before any hardware was required to be built. Secondly, the effects that "real world" intricacies had on the measured signals were easily verified. When unexplainable results were obtained from the output of the transducers, various hypothetical causes could be simulated to easily verify the cause.

In the testing phase, MATLAB was used extensively as the analysis and display medium for the results obtained. As explained above, the original system did not fulfill its purpose. The transducer signals captured in AMLAB were exported into MATLAB for analysis and display. Its predefined routines and easy to use graphical interface made it ideal for this application.

Chapter 3

MEASURING THE AIR-GAP FLUX

3.1 The Need for an Air-Gap Flux Transducer

The air-gap is defined as the region between the stator and the rotor. This region is the most critical part of the machine and hence most of the machine theory is mainly concerned with the conditions in or near the air-gap. If a reliable and cheap way can be found to measure the conditions in the air-gap, a better understanding of the dynamics of the synchronous generator could be obtained. Since this flux plays an important role in determining the level of saturation in several parts of the machine, its knowledge will will assist in assigning appropriate values to those parameters which are sensitive to saturation levels. Also, as has been noted earlier, an estimate of instantaneous developed electromagnetic torque may be synthesized from the air-gap flux signal in conjunction with the stator current.

3.2 Conventional Approach to Air-Gap Flux Sensing

This transducer has to measure the air-gap flux in the synchronous generator accurately and in real time. At present, the method of measuring air-gap flux is to either use search coils or hall sensors. There are various problems associated with each of these methods. A brief description of the operation of these sensors and their limitations are discussed below.

3.2.1 Search Coils

Search coils are very thin gauge wire that are placed around the slots of the stator of the machine. The flux linking the coil induces a voltage in the coil from Faraday's law. If this induced voltage is then integrated, a measure of the air-gap flux will be obtained.

Installing the search coil requires extra work when the armature windings are being installed. This extra work leads to extra cost and hence makes the search coil uneconomical. However the major problem with search coils is the thin wire that is needed to be used. The excessive thin wire used makes it very prone to breakage due to vibration and constant flexing. Repair or replacement of the thin wire would have to await a period of routine maintenance on the stator winding and so this is clearly not suitable for situations where the flux signal is an integral part of an on-line control strategy.

3.2.2 Hall Sensors

Hall sensors work in a similar way to the search coils. The Hall sensors are placed close to the to the stator windings to detect the air-gap flux. However this method also suffers from reliability problems. Hall sensors are very temperature sensitive and since the stator coils tend to be the hottest part of the machine, this method of flux sensing would be prone to error.

3.3 A Novel Approach to Air-Gap Flux Sensing

The design of the proposed transducer is based on work originally reported by Lipo and Chang [15] in the context of vector control of an induction motor. This method is different in that it does not require external detection devices to be used to measure the air-gap flux, but uses the stator coils themselves as the sensing medium. In this way the flux sensor can be implemented with limited additional cost being incurred. The same concept is to be used to determine the air-gap flux in the synchronous machine.

3.3.1 Theory of Proposed Method

The principle behind this method is quite simple. Coils connected to the same stator phase and located in the same part of consecutive slots are called a phase belt. In the case of the machine here, the phase belt is associated with 4 coils. A phasor diagram for the various voltages encountered in the coils of phase A of the stator is shown in Figure: 3.1.

The voltages Vn1, Vn2, Vn3 and Vn4 are made up of 3 components. The first component is the voltage induced by the air-gap flux and is proportional to the rate of change of that flux. The second component is the voltage drop due to the leakage flux. The third component is due to the resistive voltage drop in the coil. The second and third components are only dependent on the current that flows in the coil and are independent of some other coil mutually coupled to it. The coils in a phase belt are always connected in series in order to result in phasor addition of the induced voltage. This implies that the current in all four coils are equal.

In this flux sensing scheme, taps are placed on individual coils in the phase belt. The taps are placed so that the voltages in 2 coils in a phase belt can be accessed. These taps are made for the corresponding phase belt for all 3 phases. The voltage from one coil is subtracted from the voltage in the other coil. The resultant voltage is then integrated. This integrated voltage rep-

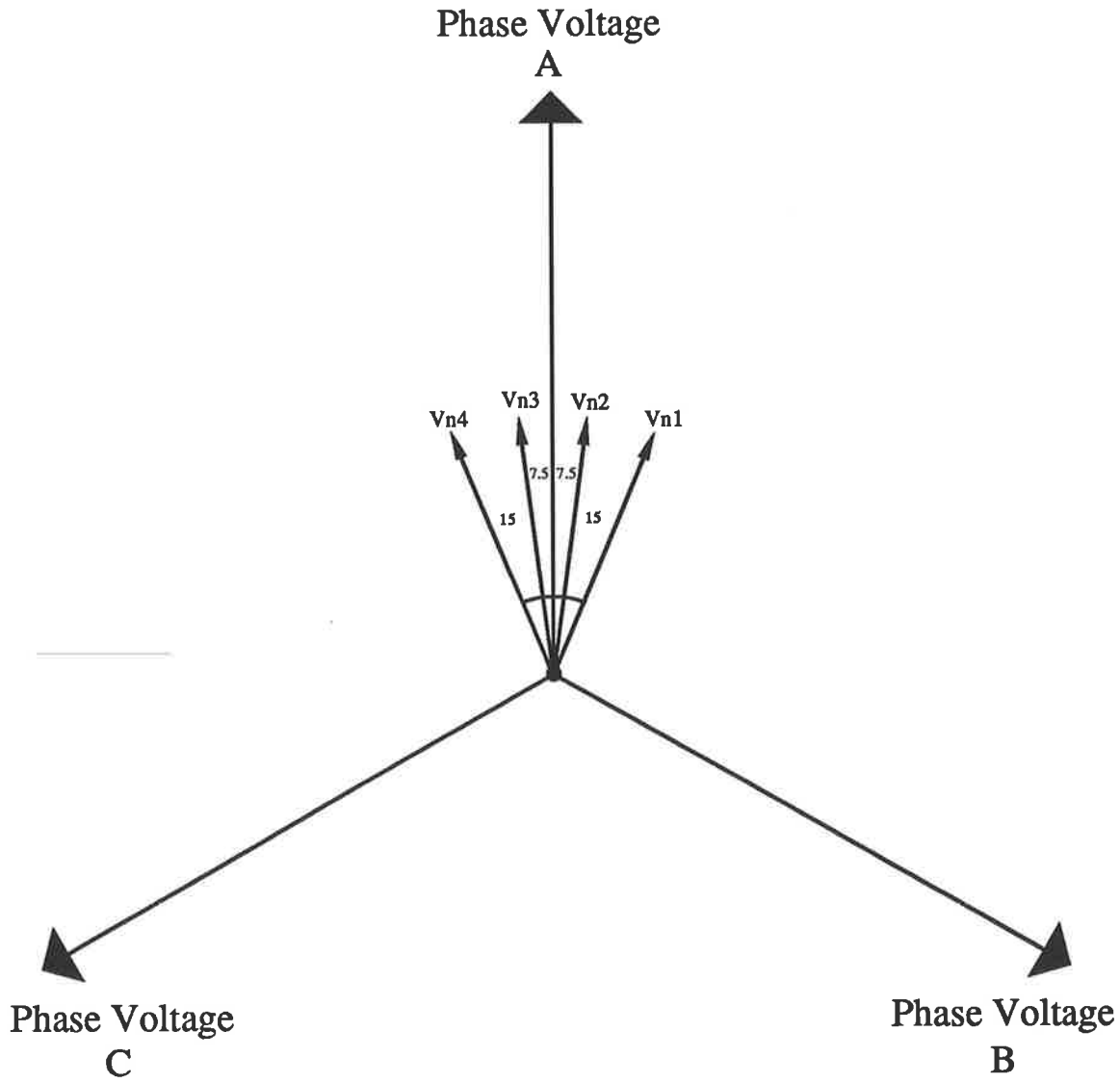

Figure 3.1: Phasor Diagram of Phase Voltages and Coil Voltages

resents the instantaneous air-gap flux linking with that phase. The phasor diagram shown in Figure: 3.2 illustrates this method best.

This method of flux sensing has the following advantages

1. The additional cost of adding taps to the machine is minimal.
2. The quantity measured is air-gap flux and parasitic terms like leakage reactance and resistances in the coil are eliminated by the subtracting process. If the two coils chosen for the subtracting process are symmetrically placed within the phase belt (for example coil 1 and 4), then the leakage flux paths will be similar, so minimizing errors in this process.

Hence this flux sensing scheme will provide a cheap accurate way of measuring air-gap flux in real time.

3.3.2 Hardware Construction and Testing

A schematic of the method described above is shown in Figure: 3.3. This transducer was constructed in hardware by translating each of the modules into hardware directly using standard analogue designs. The full circuit diagram of the hardware constructed is provided in Appendix A with accompanying text describing the various intricacies of the design.

The hardware was then tested. This test was performed to detect errors and to test unreliable aspects of the hardware. The transducer was connected to the stator taps of the synchronous machine via 6 ARLEC AL7VA/30 transformers. These transformers were used for two reasons. The first was to step down the tap voltages to a level suitable for the transducer. The other reason was to provide electrical isolation between the transducer and the synchronous machine.

The synchronous machine was run up to synchronous speed and the inputs into and the output from the air-gap flux transducer were viewed with the machine on open circuit. A photograph taken of both the input and output signals is shown as Figure: 3.4. Two points are worthy of note in this Figure. The first is the harmonic distortion present on the coil voltage signals, a feature of the "real world" measurement environment present in experimental

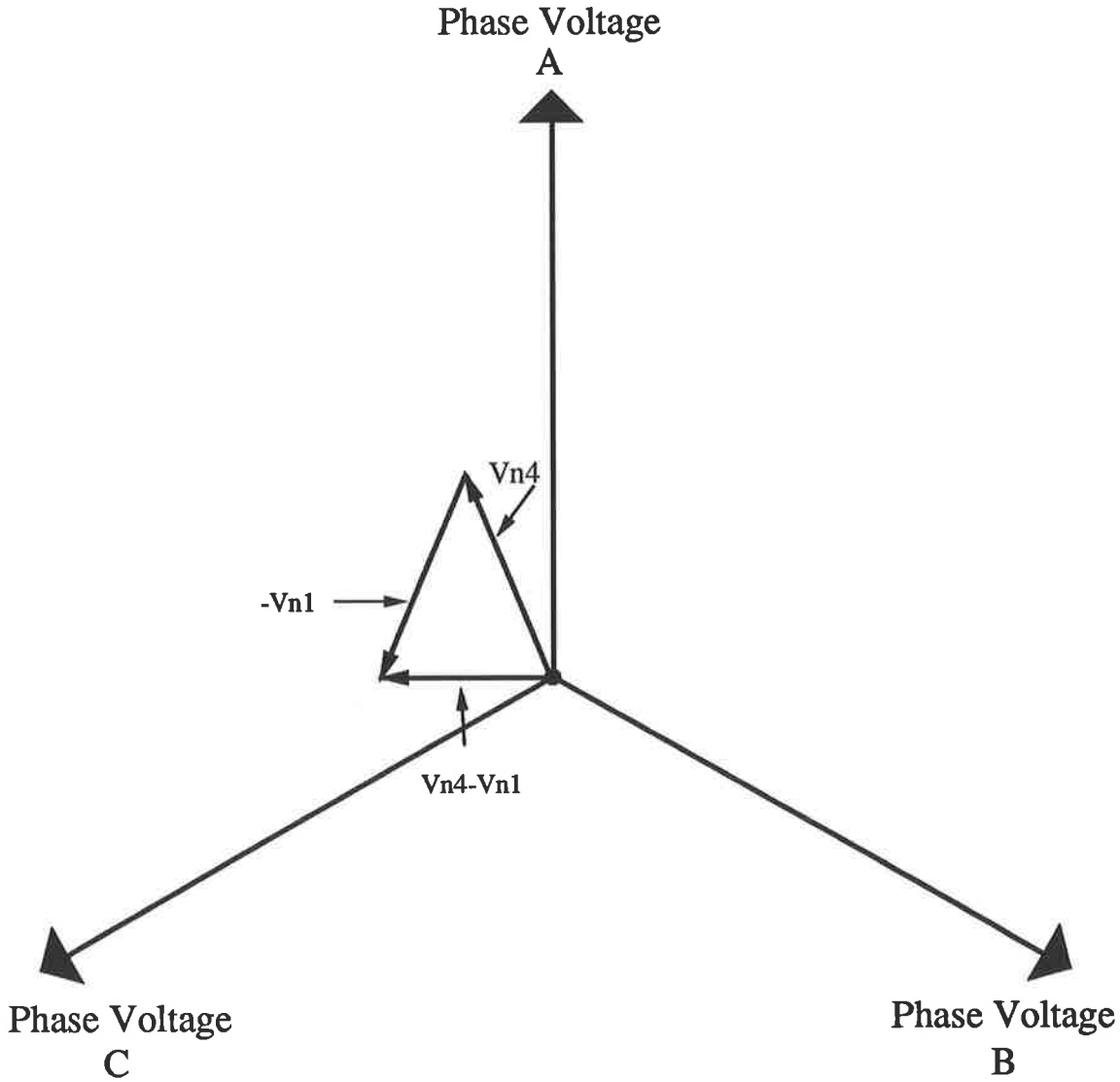

Figure 3.2: Phasor Diagram of Phase Voltages and Coil Voltages

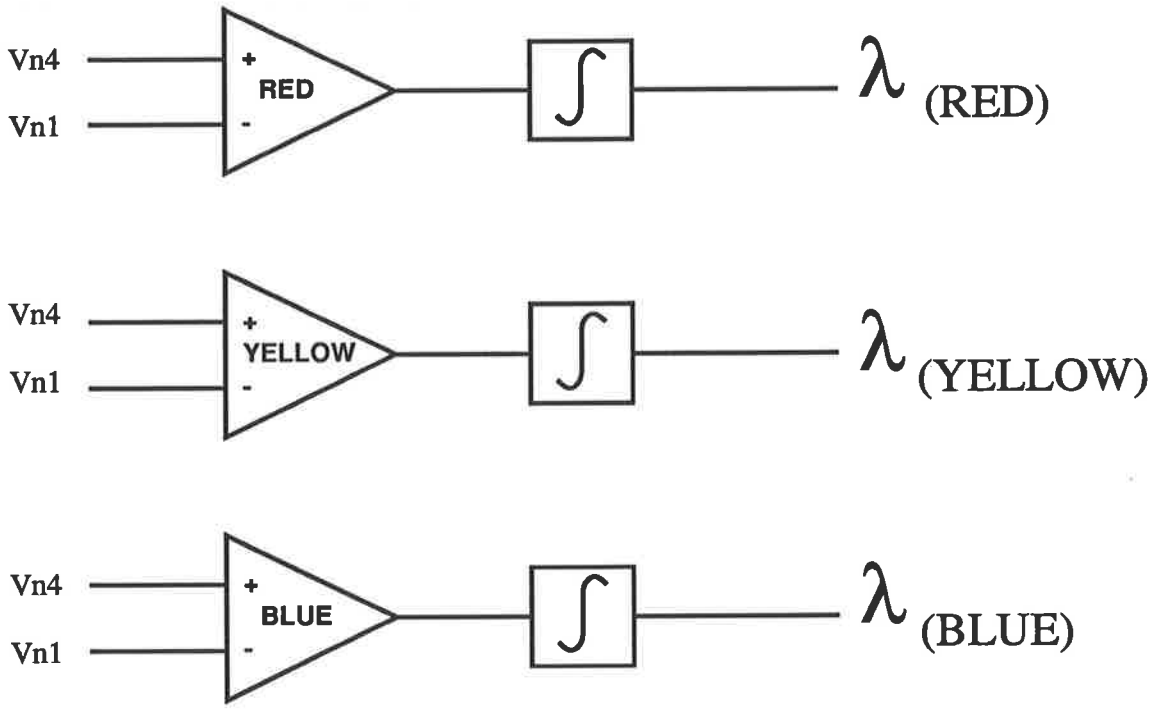

Figure 3.3: Schematic of proposed method of air-gap flux sensing

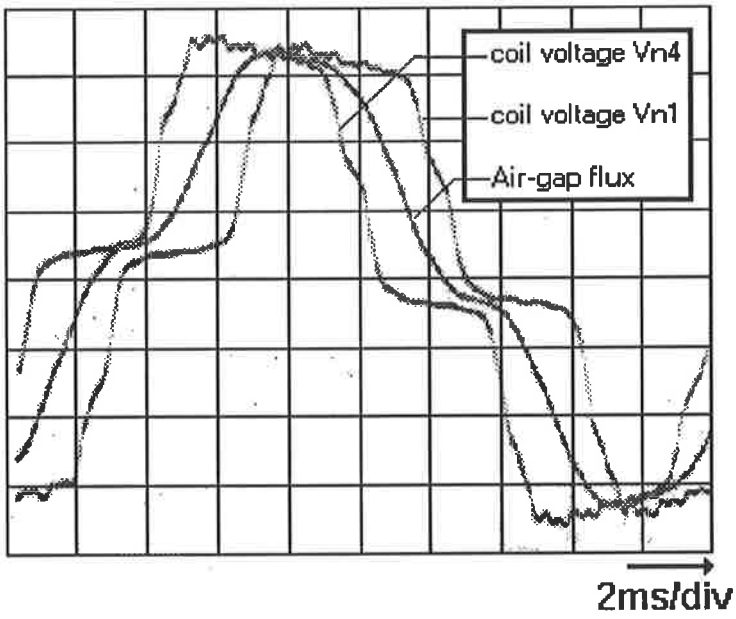

Figure 3.4: Photograph of the inputs and output into the air-gap flux transducer

work, and second is that the fundamental of the air-gap flux signal is in phase with that of the mean coil voltages. This is brought about by the subtracting process which first produces a phase shift of 90^o in the result (as in Figure: 3.3) and the subsequent integration which of course introduces a further 90^o shift.

A spectral analysis performed on the coil voltage signal showed a very significant 3^{rd} (18%) and 5^{th} (17%) harmonic and a less significant 7^{th} (2.5%) and 9^{th} (4.8%) harmonics. There are also 2 other components at 75Hz (1.2 %) and at 125Hz (1.9 %), probably caused by rotational eccentricity in this 4-pole generator.

3.3.3 Extracting the Fundamental Component

For the majority of applications, it is required to extract the fundamental component of the air-gap flux (for example to isolate direct and quadrature axis flux linkages). An attempt was therefore made to filter the individual coil voltages before any further processing occurred.

The design of the filters proved to be a bigger problem than was first anticipated. There are six voltage signals, two per phase, to be used in the transducer. This implied the need for six filters. To maintain accuracy in the transducer, these filters had to be almost identical. Small variations in the filters, like the amount of phase shift or attenuations, could decrease the accuracy of the transducer significantly and hence limit the applications possible with the transducer.

Building six identical transducers the conventional way, with discrete components, is next to impossible. A possible solution surfaced in the form of the MF4. This device is a capacitive switched 4^{th} order butterworth low-pass filter in a single package. In this filter, the cut-off frequency of the filter is determined by an external clock and is accurate to 0.3%. Hence six identical filters can be built, with all of then being controlled by the same clock. If the clock frequency should drift, all the filters will drift by identical amounts, hence minimizing errors.

If this filter is used with a cut-off frequency of 75Hz, the filters will be able to provide an attenuation of 20dB for the 3^{rd} harmonic and 40dB for the 5^{th} harmonic without modifying the main signal by any great amount. The filters were built and incorporated into the air-gap flux transducer.

The tap voltage obtained after filtering is shown in Figure: 3.5. The signal

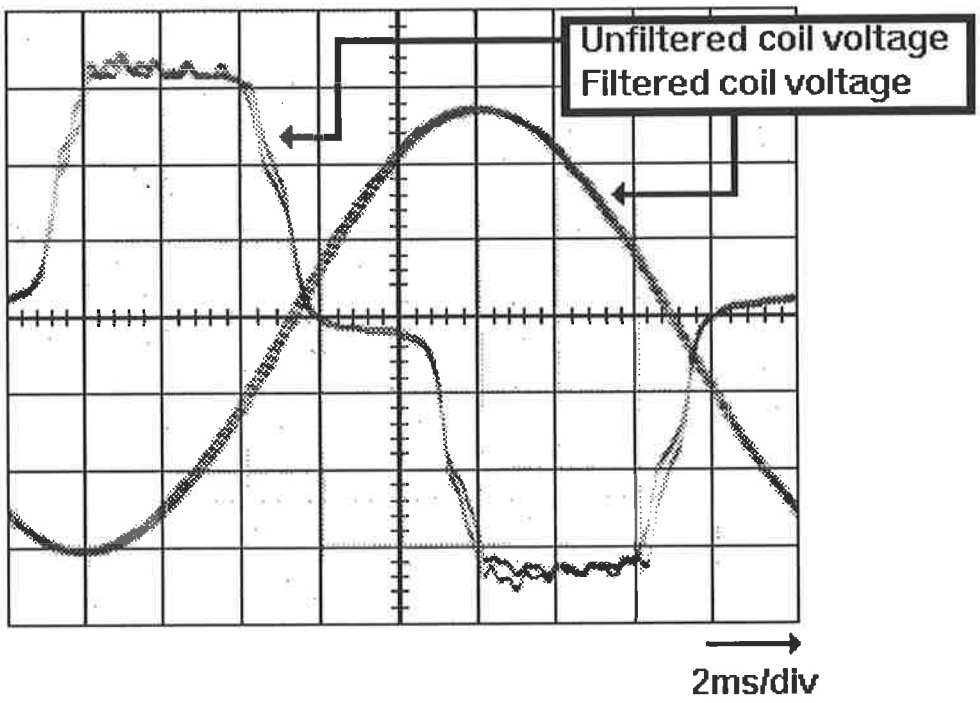

Figure 3.5: Photograph of the filtered input into the air-gap flux transducer

appears fairly clean. The stepping observed on the signal, caused by capacitive switching, gave rise to some problems in the later stages. The integrators used in the design of the transducer, like any analogue integrator, had to be

compensated against d.c. offsets in the input signals. The steps, in the filtered signal, are not stationary and react with the compensation system in the integrator making the output of the transducer drift with time.

In the final version of the measurement package, the filter location was shifted until after the Park's Transform stage with highly satisfactory results, as reported later.

Chapter 4

PARK'S TRANSFORMATION UNIT

4.1 Background to Park's Transform

The primary instrumentation on the machine measures three-phase voltage, current and flux linkages from the viewpoint on the stator winding. When modelling and analyzing the dynamic behaviour of machines, it is customary to treat each machine as an integrated system as suggested by the form of Figure: 4.1, in which the electrical and mechanical sub-systems co-exist simultaneously. Coupled circuit equations can be written to show the interactions between the voltage, flux and current in the various circuits in the synchronous machine. Consider the general equation for the k^{th} electrical circuit in the machine

$$V_k = R_k i_k + \rho \psi_k \tag{4.1}$$

$$\text{but } \psi_k = \sum_{j=1}^{N} L_{kj} i_k = \text{flux linking the circuit k} \tag{4.2}$$

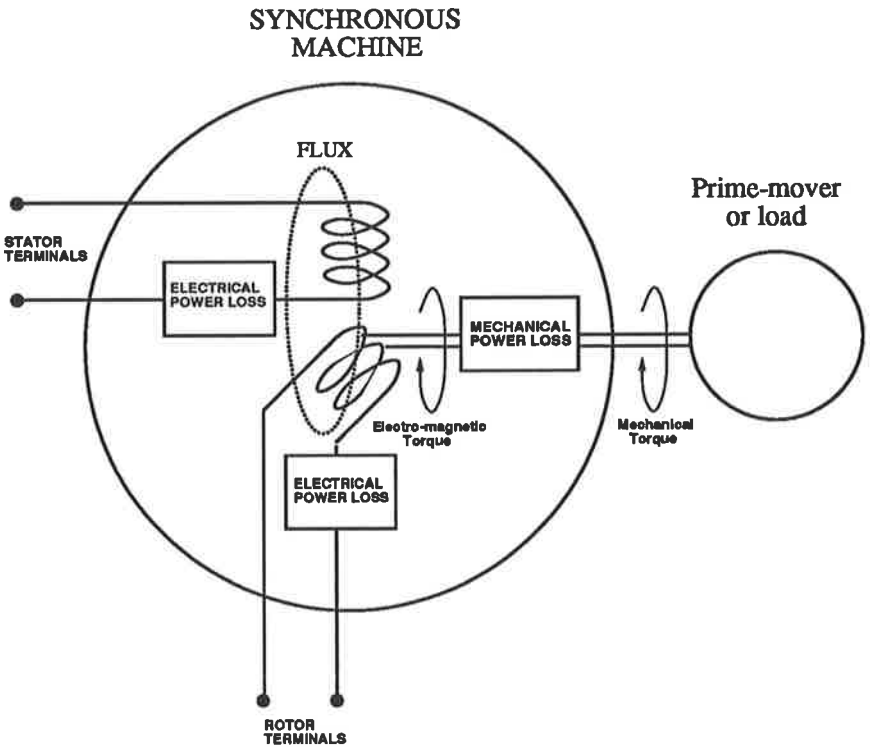

Figure 4.1: Internal Structure of a Synchronous Machine

$$\text{Therefore } V_k = R_k i_k + \sum_{j=1}^{N} (\rho L_{kj}) i_j + \sum_{j=1}^{N} (L_{kj}) \rho i_j \tag{4.3}$$

Where

R_k = the resistance in circuit k

i_k = the current in circuit k

L_{kj} = the mutual inductance between circuit k and circuit j

V_k = the voltage across circuit k

$\rho = \frac{d}{dt}$

N = the total number of circuits

As can be clearly seen from Equation: 4.3, the general equations of the machine reduces to a set of 1^{st} order differential equations in i. If these quantities are expressed in the holonomic reference frame (i.e. with each physical circuit directly modelled), the inductance coefficients are nearly all periodic functions of time. Solving these time varying coefficients, in real time, is technically possible but it is very computationally intensive. The solution is hence to express these machine quantities in a form that makes analysis easier.

Park's transformation provides the means to express these machine quantities in a form that is easy to analyze. In a Park's transform, stator variables, like terminal voltage V_a, V_b and V_c are transformed to their equivalents viewed from the rotor, namely the direct, V_d, and quadrature axis, V_q, components. The direct axis acts through the rotor pole and the quadrature axis acts electrically 90^o to it. To preserve generality, there is a third component; the zero sequence component. This component is strictly necessary if the three stator quantities are all independent (for example line currents to a star connected load in the presence of a neutral conductor).

4.2 Properties of Park's Transform

The signals when viewed in the Park's frame of reference have many beneficial properties. These properties are detailed below.

1. All machine variables are viewed from the rotor, and hence are stationary with respect to rotor saliency.
2. Under steady state operations, all variables are d.c.
3. The impedance elements are all stationary. The equations do not have the problem of time varying coefficients, although of course provisions may be made for variation with operating point due to magnetic saturation.

4.3 Form of Park's Transform

As discussed before, Park's transform is used to represent the machine quantities in a form that is easy to analyze. The transformation matrix will be easier to implement if it is subdivided into its 2 component transformations.

The first transform is when the machine quantities are transformed from a 3-phase stationary frame of reference to a 2-phase stationary frame of reference. This transform can be represented by the transformation matrix, shown in Equation: 4.4.

$$\begin{bmatrix} m_d \\ m_q \\ 0 \end{bmatrix} = \begin{bmatrix} 2/3 & -1/3 & -1/3 \\ 0 & 1/\sqrt{3} & 1/\sqrt{3} \\ 1/3 & 1/3 & 1/3 \end{bmatrix} * \begin{bmatrix} R \\ Y \\ B \end{bmatrix} \tag{4.4}$$

Where

$$\begin{aligned} \text{R, Y and B} &= \text{the 3-phase stator stationary signals} \\ m_d \text{ and } m_q &= \text{the 2-phase stationary signals} \\ 0 &= \text{the zero sequence component} \end{aligned}$$

The second transform is when the 2-phase stationary frame of reference signals, obtained above, are transformed to the desired 2-axis rotating frame of

reference. This transform can be represented by the transformation matrix, shown in Equation: 4.5.

$$\begin{bmatrix} d \\ q \\ 0 \end{bmatrix} = \begin{bmatrix} cos(\theta) & -sin(\theta) & 0 \\ sin(\theta) & cos(\theta) & 0 \\ 0 & 0 & 1 \end{bmatrix} * \begin{bmatrix} m_d \\ m_q \\ 0 \end{bmatrix} \tag{4.5}$$

Where

d and q = the 2-axis rotating signals

θ = the instantaneous angle (in electrical degrees) between the axis of stator winding R and the direct axis of the rotor

To perform a continuous Park's transform in real time will be too computationally intensive. The 3-phase stationary $\rightarrow$ 2-phase stationary transformation can be performed continuously but 2-phase stationary $\rightarrow$ 2-axis rotating transformation is complicated due to the continuously changing parameters. It was decided here to perform Parks transform at discrete intervals thus restricting the computational time needed.

4.4 Implementation in Hardware

For the purposes intended for this transducer, it will be sufficient to perform Park's transform at regular intervals of 45^o electrical. This means that the transformation matrix has to be evaluated 8 times every cycle. This gives a sampling frequency for the d and q based variables of 400Hz. In view of the fact that the nature of the transformation means that all machine transients are based on d.c. steady-state levels, and that typical generator modes have characteristic frequency considerably lower than 400Hz, this was considered to be a satisfactory specification. The implementation process therefore relied on capturing the time instant when the instantaneous shaft position, θ, passed through 45^o increments (electrical) using the shaft encoder and implementing Equation 4.5 using the appropriate sine and cosine values which

are pre-calculated.

Symbolically, the hardware can be described by Figure: 4.2. The sample and

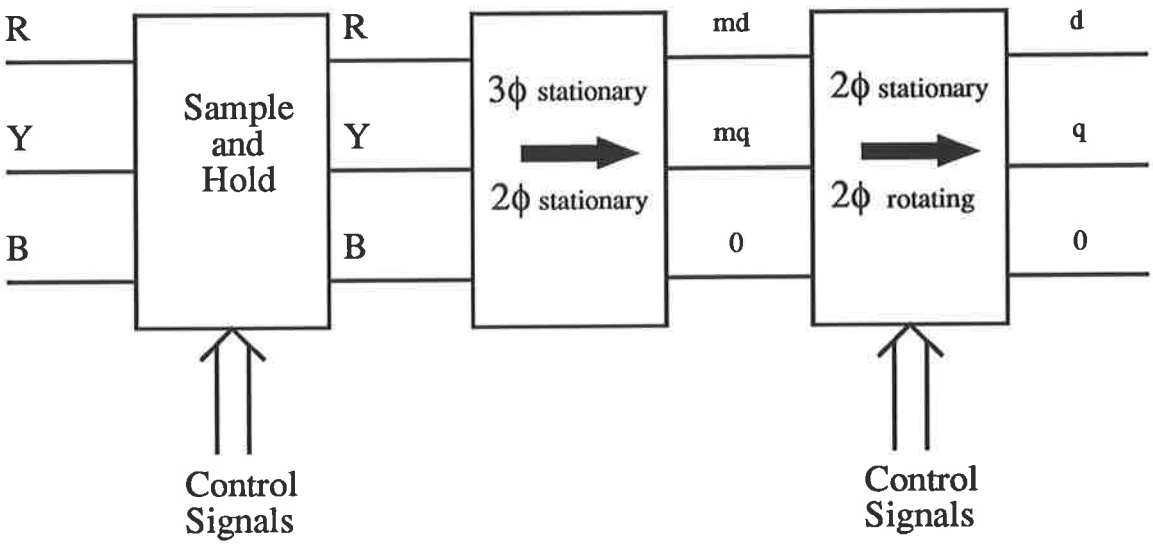

Figure 4.2: Symbolic diagram of Park's transform circuit

hold stage is required because Park's transform is being carried out discretely. The input signal is kept constant for the 8 discrete evaluation positions as shown in Figure: 2.2. The design of the hardware to implement Equation: 4.4 is straight forward, using standard operational amplifier based adding and subtracting amplifiers. In the case of Equation: 4.5, the design of the hardware is a little more involved due to the changing coefficients. As mentioned above, Parks transform is to be performed discretely 8 times a cycle at 45° intervals. Due to the symmetrical nature of the 45° intervals, evaluating the sine and cosine terms at these angles, produces only 5 coefficients for the transformation matrix in Equation: 4.5; 0, 0.707, -0.707, 1 and -1. In the first part of the hardware, the m_d and m_q signals were attenuated by the 4 non-trivial coefficients; the 0 attenuation is provided for by a ground connection. Four analogue multiplexers, one for each element of the transformation matrix, are then used to switch between the various attenuated signals at the

8 evaluation points. As an example, Table: 4.1 shows the switching sequence required for element (1,1) of the transformation matrix shown in Equation: 4.5.

θ	magnitude of element (1,1)
0^o	$1*m_d$
45^o	$0.707*m_d$
90^o	$0*m_d$
135^o	$-0.707*m_d$
180^o	$-1*m_d$
225^o	$-0.707*m_d$
270^o	$0*m_d$
315^o	$0.707*m_d$

Table 4.1: Switching sequence required for element (1,1) of the 2-phase stationary to 2-axis rotating transformation matrix

The full circuit diagram of the hardware constructed is provided in Appendix B. A brief explanation of the circuit, together with any of the non trivial aspects of the circuit, accompanies the circuit diagram.

4.5 Testing the Unit

The synchronous machine was synchronized to the mains in a single machine infinite busbar (SMIB) configuration, shown in Figure: 4.3. The machine was made to generate into the infinite busbar. Park's transform was performed on the stator voltages. The direct and quadrature axis voltages were viewed on the CRO and a photograph of this shown in Figure: 4.4.

There appears to be a 100Hz component superimposed on the d.c. direct and quadrature axis voltages. This was traced down to the unbalanced 3 phase voltage. An unbalanced 3 phase voltage can be divided into positive and negative sequence components. The negative sequence is 100Hz when viewed with respect to the positively rotating Park reference frame, and is

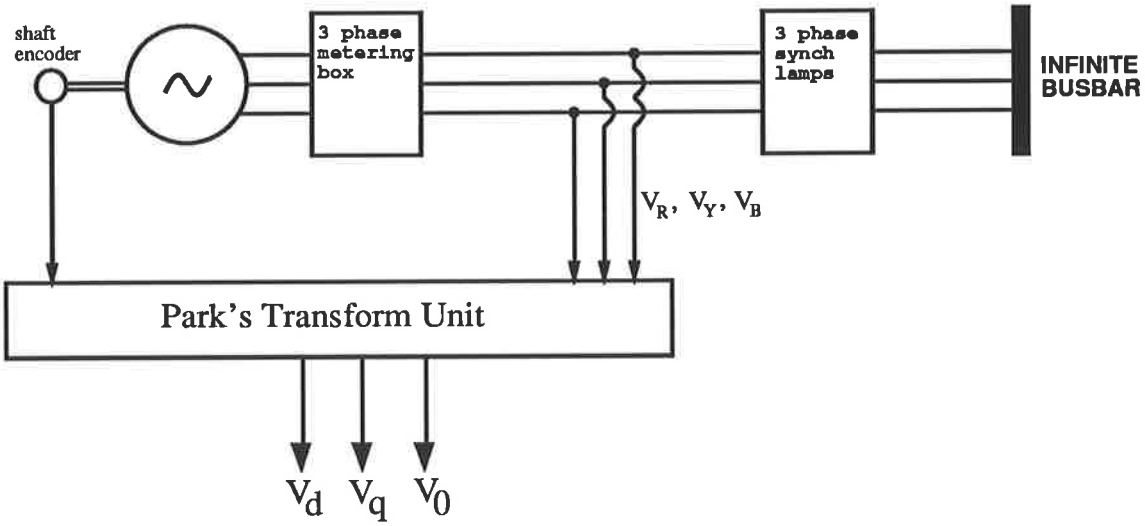

Figure 4.3: Single machine infinite busbar configuration (SMIB)

the cause of the 100Hz component.

This was confirmed when a MATLAB routine, simulating this system, was run. The results obtained, shown in Figure: 4.5, are very similar to the experimental results obtained. The symbol "n" in Figure: 4.5, is the ratio of the magnitude of the negative voltage sequence to the positive voltage sequence. The size of the ripple is dependent on the value of "n", and hence on the degree of the unbalance.

To test the accuracy of the transducer, the terminal voltages, line currents and power factor were measured. From these values, phasor diagrams were drawn and the values obtained from the phasor diagrams were compared with the values obtained with the transducer. The magnitudes of these values showed good agreement. An initial concern was that the sign of the direct axis voltage of the transducer, expected to be positive when it is generating, was found to be negative.

This was tracked down to a sensing problem in measuring the rotor position.

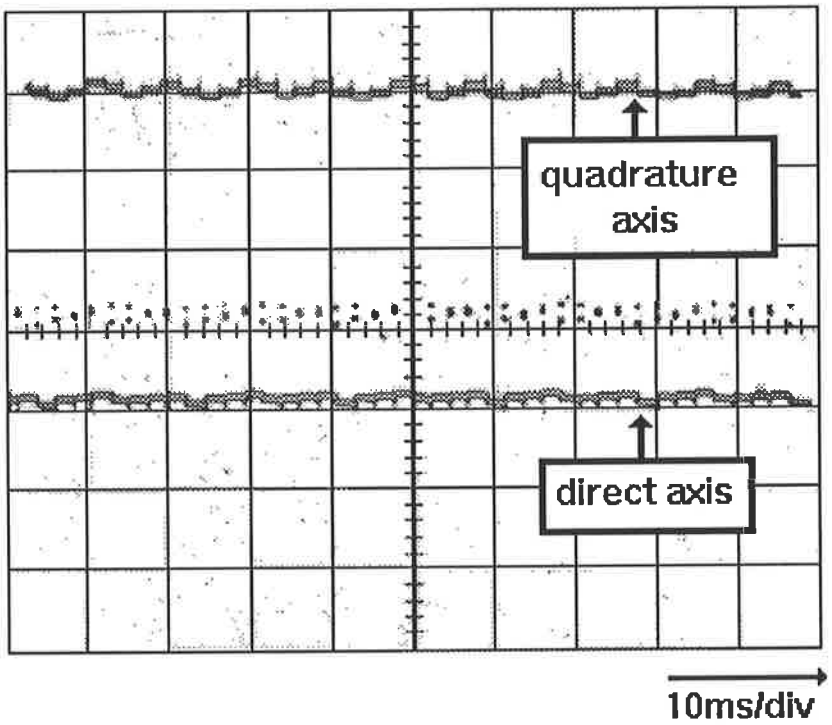

Figure 4.4: Photograph of the direct and quadrature axis voltage at an arbitrary load

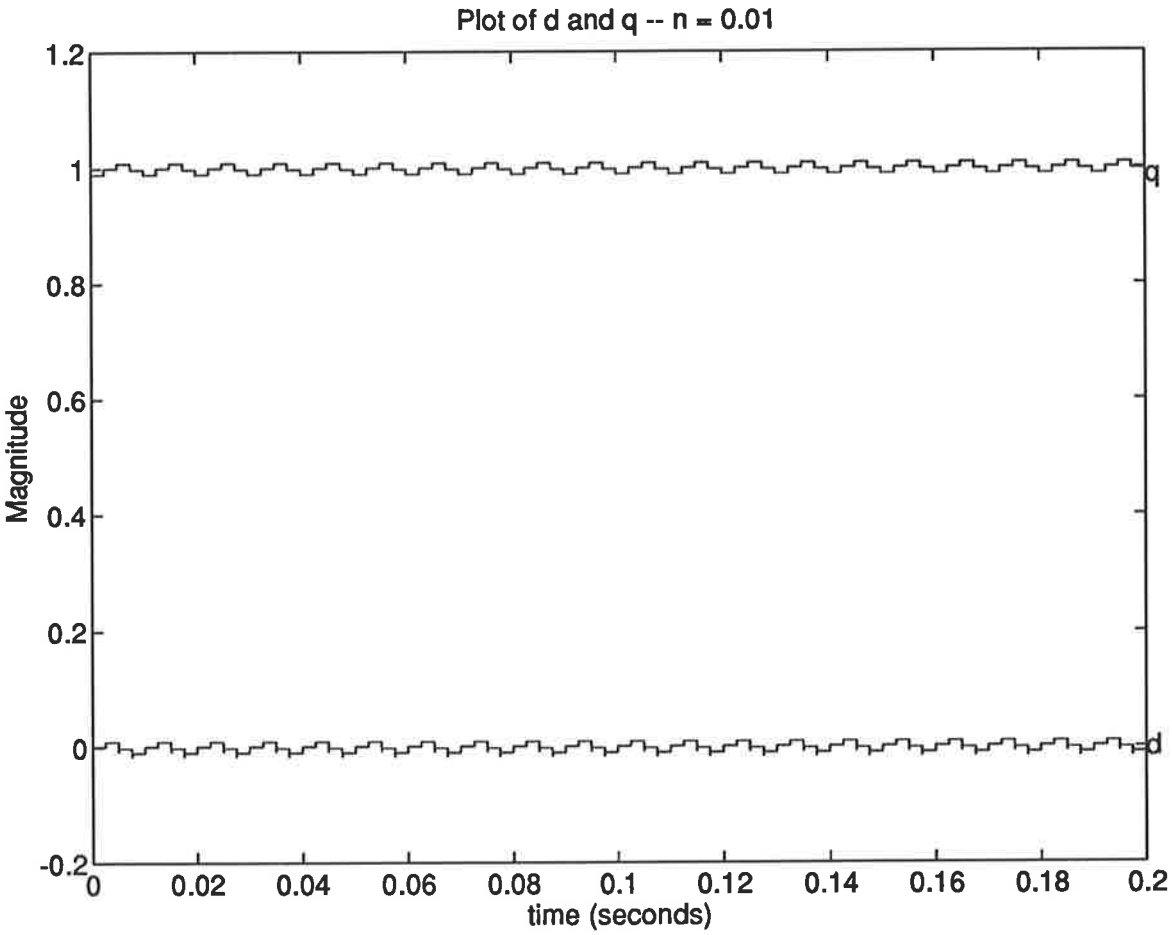

Figure 4.5: Output of a MATLAB routine simulating parks transform

In the theory for Park's transform, rotor position is defined as being the rotor pole axis relative to that of a stator phase. However in the set up, with the shaft encoder, the rotor position comes out to be defined as that of the stator with respect to the rotor pole axis. This is not considered a problem as long as the convention is noted.

Chapter 5

ROTOR ANGLE UNIT

5.1 Introduction

The rotor angle is an internal parameter in the synchronous machine. It is defined as the departure of the rotor structure from its rotational position on no load when the machine is connected to an external a.c. network. By definition a positive rotor angle is when the machine is feeding real power into the network. This quantity is introduced in the steady state power equations (in per-unit):

$$P = \frac{E_o V}{X_d}\sin(\delta) + \frac{V^2}{2}\left(\frac{1}{X_q} - \frac{1}{X_d}\right)\sin(2\delta) \tag{5.1}$$

$$Q = \frac{E_o V}{X_d}\cos(\delta) - V^2\left(\frac{\cos^2(\delta)}{X_d} + \frac{\sin^2(\delta)}{X_q}\right) \tag{5.2}$$

Where

P = real power output

Q = reactive power output

$$
\begin{aligned}
E_o &= \text{internal machine voltage} \\
V &= \text{external network voltage} \\
X_q &= \text{total direct axis inductance} \\
X_d &= \text{total quadrature axis inductance} \\
\delta &= \text{rotor angle}
\end{aligned}
$$

When the machine is connected to a large external a.c. network, the terminal voltage phasor, V, acts as a synchronously rotating reference phasor. E_o is the internal voltage phasor of machine and is fixed relative to the rotor. The separation between these two phasors is by definition the rotor angle.

The ability to measure the rotor angle will hence provide another different perspective in the machine performance analysis and will give vital information on the dynamic performance of power systems, giving a prime indication of the ability of a generator or a group of generators to remain in synchronization This quantity can be inferred from the measurements of voltage, power and current. However it is highly desirable to design and construct a transducer to measure rotor angle independently.

5.2 Basis for the Design

The rotor angle transducer to be designed had to meet the following criteria.

1. The transducer must be able to measure rotor angles in the range of $\pm 180^o$.

2. The rotor angle measured must be accurate to $\leq 0.5^o$

3. The sampling rate of the transducer must be at least 50Hz.

The principle behind the method of measuring the rotor angle was based on a paper written by Ahson and Ali [2] . The method can best be explained by Figure: 5.1. A fixed position on the shaft was determined by the shaft encoder. A datum pulse is generated every time this position is reached. One phase voltage from the system reference point is then selected. A point on

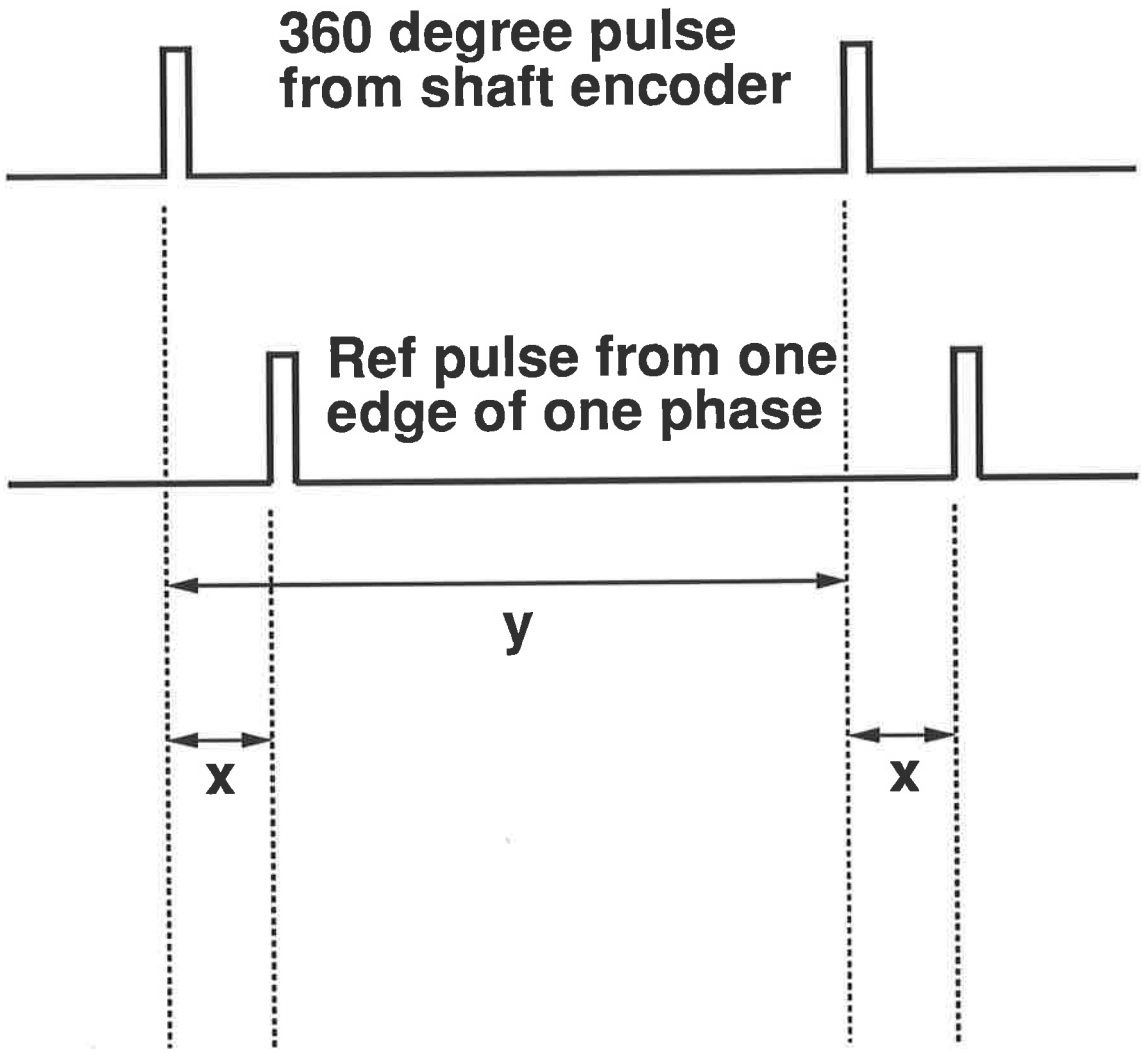

Figure 5.1: Method behind rotor angle transducer

this reference phase was determined by detecting the positive zero crossing. This zero crossing generated another pulse. A counter is used to generate a timing pulse sequence. The number of timing pulses encountered between the two pulses from the shaft encoder is measured, giving "y". The number of timing pulses encountered between the shaft encoder pulse and the pulse generated by the positive zero crossing edge of a stator phase is also measured. This count is "x". A phase shift is then calculated using the formula shown in Equation 5.3

$$\phi = \frac{x}{y} * 360^o \tag{5.3}$$

When the machine is on no load, the phase shift is calculated, ϕ_{offset}. The same thing is repeated when the machine is on load, generating ϕ_{raw}. Subtracting these two values should give rotor angle, δ.

$$\delta = \phi_{raw} - \phi_{offset} \tag{5.4}$$

In the design implemented for the transducer, the counting pulses were provided by the least significant bit of the shaft encoder. This was done to reduce the complexity of the design. The shaft encoder generates 256 codes per revolution of the shaft. That means that 256 states represents 720^o electrical. The 2^0 output of the gray encoder generates pulses that are 4 states long, 2 states "off" and 2 states "on". That means pulse counted above represents an angle of 11.25^o. Hence to measure ϕ, all that is required is to measure the number of pulses occurring in time "x" and multiply the number by 11.25^o. This method does away with the need for complex digital dividers as y is always 128 counts.

The resolution of the rotor angle transducer as it stood was 11.25^o, and so obviously needed to be improved to meet the specifications.

5.3 Enhancement 1: Increasing the Angular Resolution

It was decided to use a phase lock loop to increase the frequency of the shaft encoder pulses. The principle behind this method can be illustrated by a schematic of the phase lock loop system shown in Figure: 5.2. The

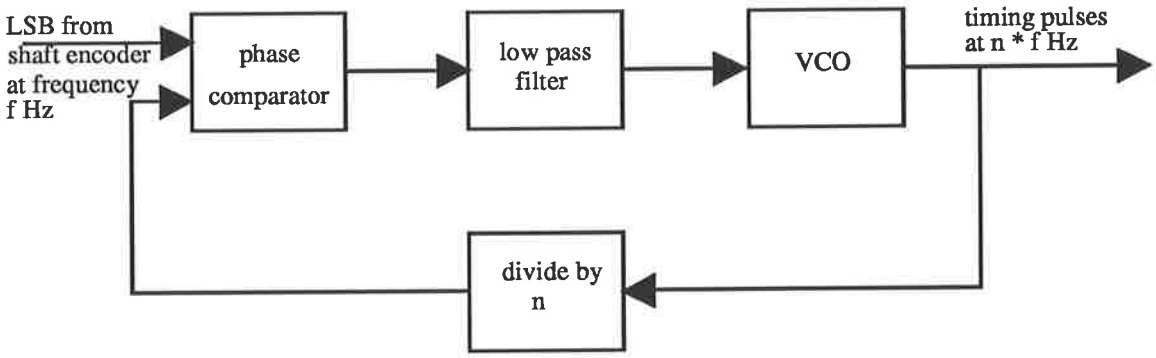

Figure 5.2: Schematic of the PLL system used to increase the frequency of the shaft encoder pulses

VCO center frequency is set at "**n**" times the input signal when the shaft is rotating at 1500rpm. This signal is divided by "**n**" and compared to the input signal. The phase lock loop should lock on to the input signal and produce an output "**n**" times the frequency of the input signal.

Choice of n in the divide by n circuit

To get an accuracy of $\leq 0.5^o$, n needs to be at least 32. This will give an accuracy of 0.35^o. This value of accuracy will require all the circuitry to follow, like latches and counters, to be 10 bits wide. As most of this circuitry comes in lots of 4 bits, it was decided to make n = 128, to utilize the full 12 bits that will be present.

5.3.1 Testing the Enhanced Transducer

The synchronous machine was made to generate into an infinite busbar. The terminal voltages, line currents and power factor were measured. Phasor diagrams were drawn and a value of rotor angle was obtained using conventional steady-state theory. This angle was compared with the value obtained from the transducer. When this was done it was found that the transducer did not give the correct value of rotor angle.

The error was tracked down to the unbalanced nature of the terminal voltage. As explained earlier, if the terminal voltage is unbalanced, the direct and quadrature axis voltages will have a 100Hz component on them. The magnitude of this component depends on the extent of the unbalance. The rotor angle, δ, when expressed with respect to the machine's terminal busbar, can be represented in terms of V_d and V_q as shown in Equation 5.5.

$$\delta = \arctan \frac{V_d}{V_q} \tag{5.5}$$

From this equation, it is fairly obvious that δ will have a 100Hz ripple on it as well. Using the above method to measure rotor angle, δ is evaluated at only one point in a 50Hz cycle. This means that the value measured can vary by the size of the ripple. For example, if the value of δ is 10^o with a ripple of 2^o peak, the value of δ measured with the transducer can range from 8^o to 12^o depending on the nature of the unbalance.

On its own, this ripple will not cause the error. If the degree of unbalance of the voltage remains constant, there will be no problem. This is because the error on ϕ_{raw} will be identical to the error on ϕ_{offset}, thus cancelling during the subtracting process. The error is due to the fact that the unbalanced nature of the system is not stationary or predictable. The unbalanced nature of the system is different off-line (measuring ϕ_{offset}) when compared to the unbalanced nature of the system when the machine is synchronized to the mains (measuring ϕ_{raw}).

A MATLAB routine was written to simulate the rotor angle transducer in software. The above effects were noticed and verified in the simulation. It was noticed that the unbalanced stator voltages caused the zero crossing

of the stator voltage to shift. The amount of shift was observed, in the MATLAB simulation, to be different for each phase. It was also observed that the average of these shifts, taken over the three phases was zero. This last effect suggested a solution to the problem. A method had to be found to average out the shifts on the three phases prior to counting.

5.4 Enhancement 2 : Allowance for Unbalanced Voltages

A paper written by Ainsworth [3] provided the solution to this problem. In this paper a method using a phase locked loop to provide accurate timed firing pulses for static converters, from a distorted a.c. line voltage, was discussed. A similar system was used to perform the averaging process desired here. A block diagram of the system used for the averaging process is shown in Figure: 5.3.

5.4.1 Steady-State Tests

The modified rotor angle transducer was re-tested under steady state conditions feeding into an infinite busbar. The averaging process was viewed on the CRO and worked well. The results obtained from the steady state test were as expected, with the experimentally obtained value of δ having good agreement with the theoretically calculated value.

5.4.2 Transient Tests

The synchronous machine was connected to the infinite busbar as shown in Figure: 5.4. with the 3-phase switch closed, short circuiting the inductors. The 3-phase switch was then opened, switching in the inductors and hence producing a step change in the line impedance.

When the transient test was performed it was found that that the phase locked loop in the rotor angle transducers lost lock giving random ± 120 de-

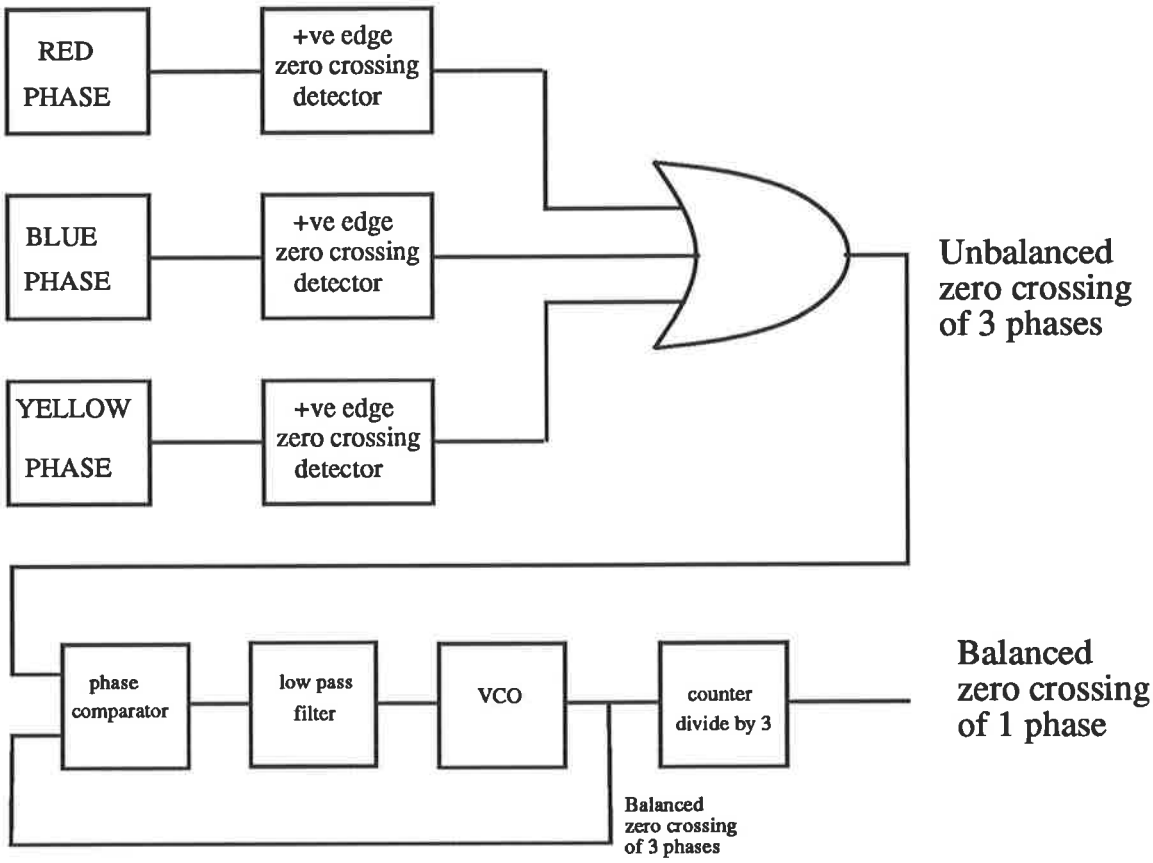

Figure 5.3: Schematic of the PLL system used to average out the zero crossings of the 3 phases

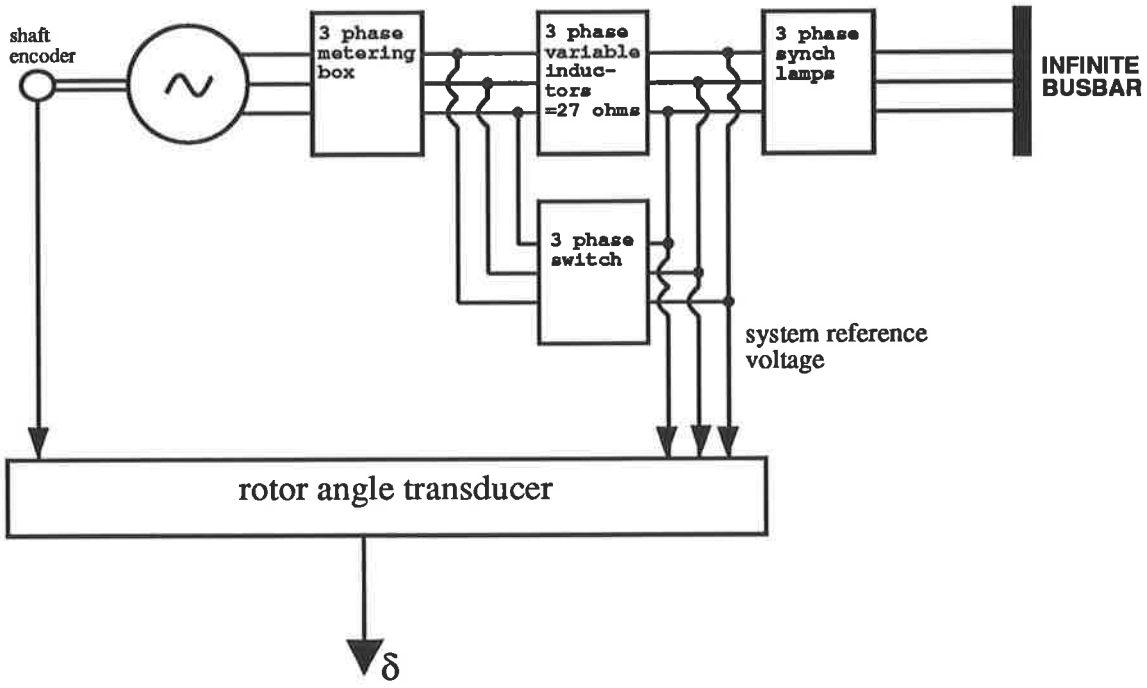

Figure 5.4: Testing the rotor angle transducer with a transient load

gree shifts from the expected output.

The low pass filter needed to be redesigned in order to improve the tracking of the transducer and hence remove the "loss of lock" problem. The solution to this problem is a catch 22 situation. The bandwidth of the filter has to be increased to enable tracking of the transients. However doing this will result in jitter in the averaging process of the 3 phase zero crossing pulses.

The only option that seems possible is to use a microprocessor or microcontroller of some description to determine the rotor angle using each phase individually and then averaging out the values. Building such a transducer using individual discrete components is not practical as the size and complexity of the design will make the transducer very unreliable.

5.5 Final Version Using a Microcontroller

The microcontroller chosen for this purpose was the MOTOROLA MC68HC811E2 microcontroller. This microcontroller is based on the MOTOROLA 6800 family of microprocessors, and was chosen for the following reasons:-

- It has 256 bytes of RAM and 2 Kbytes of EEPROM on board the chip. This greatly reduces the complexity of the final product as there is no need to design the communication and data lines for the external RAM or EPROM.
- The programming of the microcontroller is also easy. The program can be written and compiled on any IBM personal computer. Once the program is compiled it can be easily downloaded onto the microcontroller via the pc's serial port. The only extra component needed to accomplish this is a MAX232 chip. This chip is a RS232 receiver chip. It performs the necessary handshaking between the pc and the microcontroller to enable the program to be downloaded via the serial port. All the software used to compile the program, whether in C or in Assembly, and the software to download the program onto the microcontroller, is shareware and available via anonymous ftp.

- There are many users of this microcontroller. If problems should arise, as they did, in the development of the transducer, technical advice should be readily available.

The design for this transducer was the same as the discrete component version, except that a free running counter provided the timing pulses. The entire process was repeated for the other 2 phases and then the 3 rotor angles were averaged.

Before the transducer could be built, a few aspects of the design had to be considered. As discussed earlier, the rotor angle signal will have a 100Hz ripple on it. To properly detect the 100Hz ripple, the evaluation of rotor angle has to be performed 6 times a cycle, on both the positive and negative zero crossing edge of each phase. If the rotor angle was evaluated on only one zero crossing edge of each phase, the 100Hz ripple will be aliased to 50Hz.

The proposed rotor angle transducer was simulated in MATLAB to gauge the suitability and accuracy of the transducer in measuring transient rotor angles. A MATLAB routine $rotor5\_1.m$ was hence written for this transducer. A typical transient rotor angle chosen for the simulation and was of the form shown in Equation: 5.6.

$$\delta = 20 + 20(1 + e^t) * sin(2\pi * 1 * t) \tag{5.6}$$

This transient has an initial value of 20^o and a final value of 40^o. The frequency of oscillation for the transient was assumed to be 1Hz.

The results of the simulation is shown in Figure: 5.5 superimposed onto the original transient. As can be seen in Figure: 5.5, the transducer works very well. It measures the steady state rotor angle accurately. It is also able to measure the transient behaviour of the rotor angle fairly well. The 100Hz ripple can be filtered out later as with the Park's transform signals.

The most obvious way to implement the transducer is to use the input capture feature of the microcontroller.

> Physical time is represented by the count in the 16 bit free running counter. Input capture functions, used to record the time at

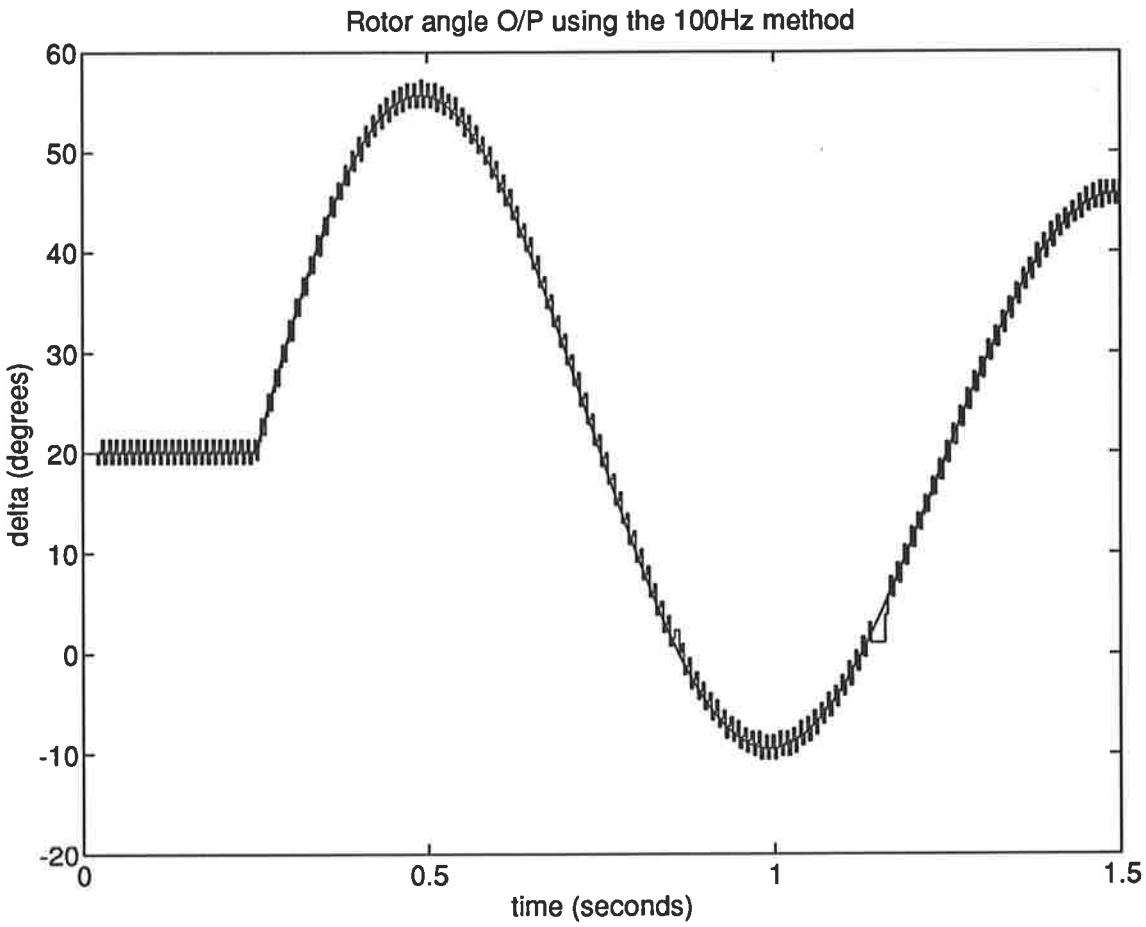

Figure 5.5: Simulating transients using the micro-controller based transducer

which some external event occurred, are accomplished by latching the contents of the free running counter when a selected edge is detected at the related timer input pin [17] .

The front end of the transducer can be represented by Figure: 5.6. The as-

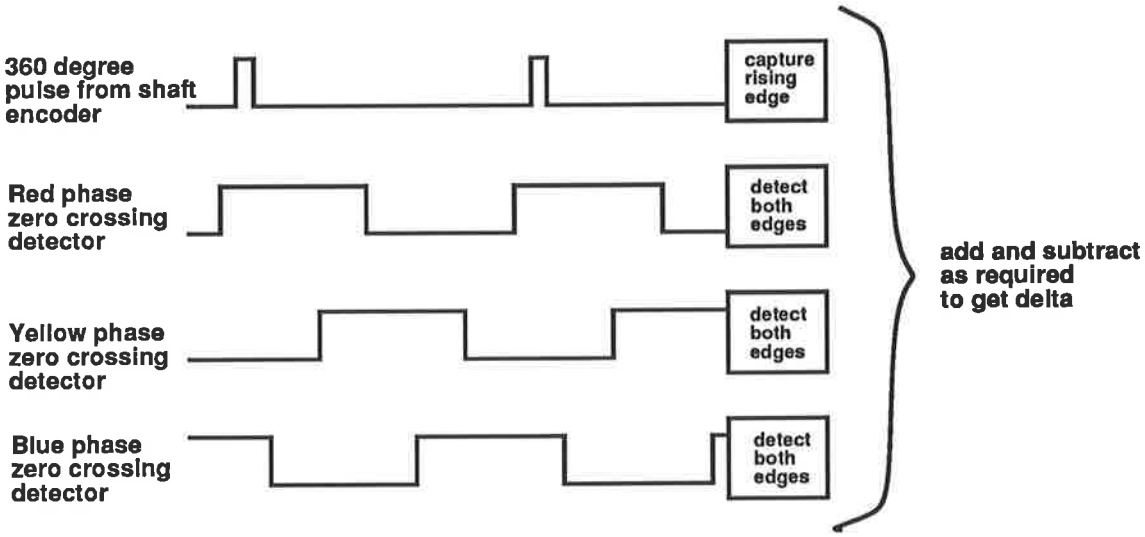

Figure 5.6: Block diagram of the front end of the transducer

sembly code that was written for the microcontroller can be described by the flow chart shown in Figure: 5.7. The flow chart shows a direct implementation of Figure: 5.1 with

$$
\begin{aligned}
(I/C1 - ref) &= y \\
(I/C2 - ref) &= x_{RED} \\
(I/C3 - ref) &= x_{YELLOW} \\
(I/C4 - ref) &= x_{BLUE} \\
FFF &= 360^{o} \text{ in hexadecimal (corresponding to the} \\
&\quad \text{12 bit word representing } \delta)
\end{aligned}
$$

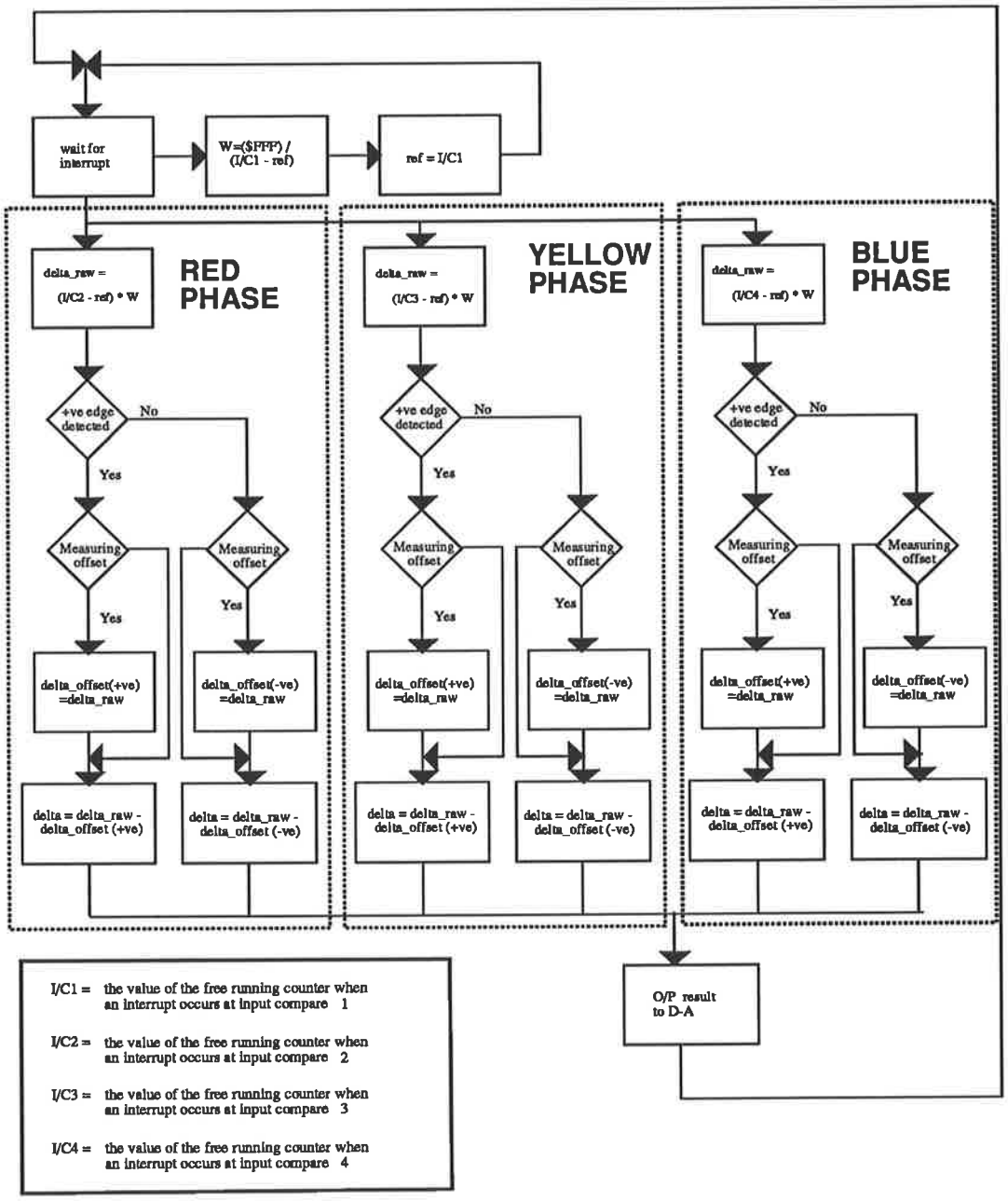

Figure 5.7: Flow chart of the program used to implement the rotor angle transducer in the microcontroller

A schematic of the hardware used for the transducer is shown in Figure: 5.8. The most significant bit of PORT B is used to trigger the latches to load the rotor angle word. A detailed circuit diagram used for the transducer is provided in Appendix C together with a full listing of the assembly code used.

5.5.1 Steady-State Tests

The rotor angle transducer was tested under steady state conditions with the synchronous machine set up in a SMIB configuration. A calculation of the rotor angle expected was also made from the voltage and power measurements. The results obtained are shown below.

case 1

$$\begin{aligned} \delta_{calculated} &= 7.84^o \\ \delta_{measured} &= 7.89^o \end{aligned}$$

case 2

$$\begin{aligned} \delta_{calculated} &= 6.78^o \\ \delta_{measured} &= 6.53^o \end{aligned}$$

case 3

$$\begin{aligned} \delta_{calculated} &= -9.61^o \\ \delta_{measured} &= -9.55^o \end{aligned}$$

The results above shows excellent agreement between the value of δ obtained with the rotor angle transducer and the theoretical value calculated for δ using circuit measurements and known machine data.

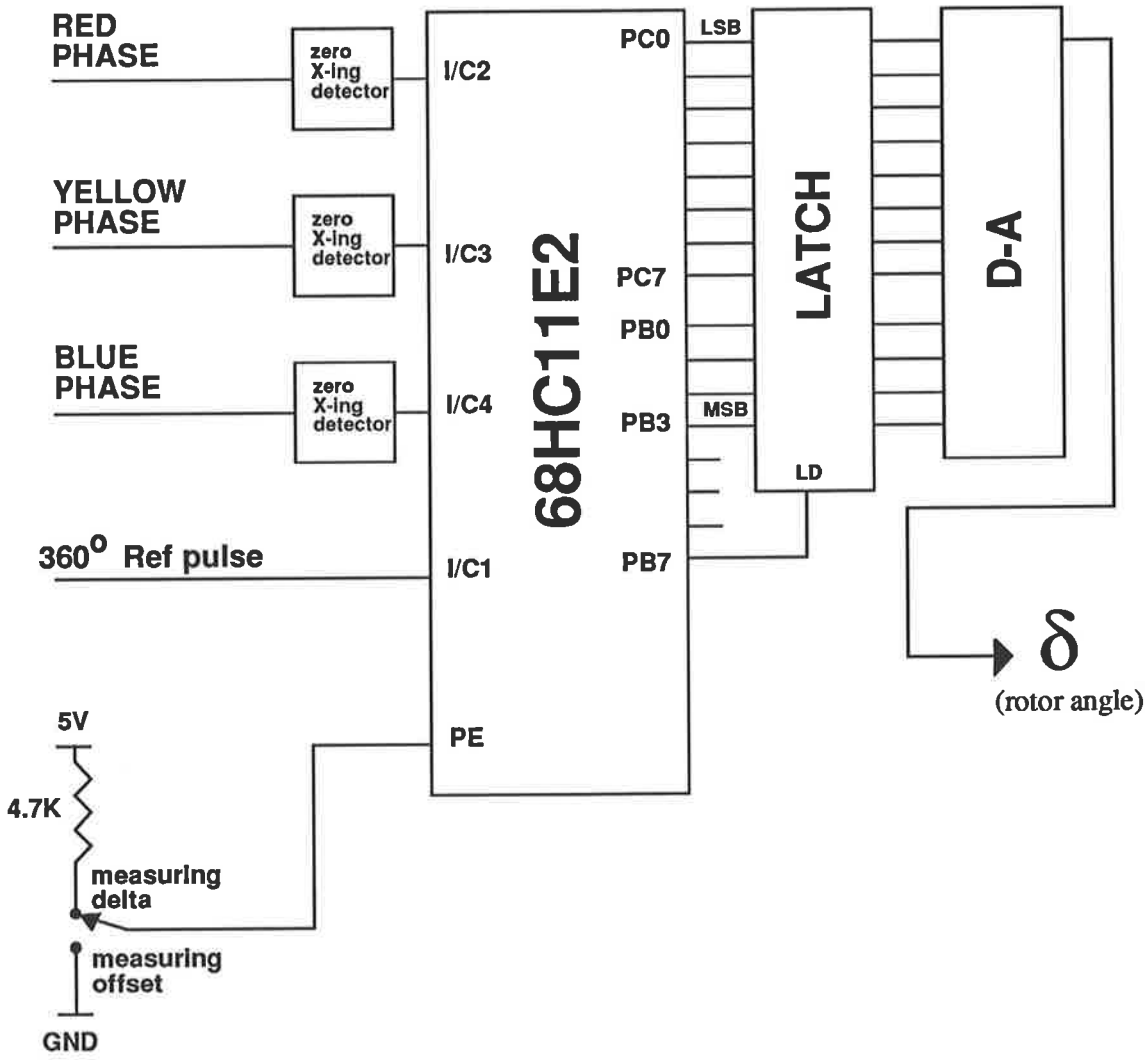

Figure 5.8: Schematic of hardware used for transducer

5.5.2 Transients Tests

The transient tests performed were the same as performed with the earlier variation of the rotor angle transducer.

The output of the rotor angle transducer was viewed on both a digital storage CRO and on AMLAB. An AMLAB project was written for this purpose. This project displays the raw output of the rotor angle transducer together with a filtered version of the output. The filter used were two 2^{nd} order Butterworth filters, of corner frequency=50Hz, cascaded together. The results obtained are shown in Figure: 5.9, Figure: 5.10 and Figure: 5.11.

The important features of the transients were measured to see if there was any difference in the transient signal when viewed on AMLAB when compared to the digital storage CRO. This was done to make sure that AMLAB can handle the transient signals. The results obtained are shown in Table: 5.1.

	CRO	AMLAB
1^{st} peak	-1480mV (44.40°) @0.237 seconds	45° @0.236 seconds
1^{st} valley	-635mV (19.05°) @0.475 seconds	19° @0.471 seconds
initial value	-230mV (6.9°)	7°
final value	-1030mV (30.9°)	31°

Table 5.1: Comparing the rotor angle transient measured with the CRO and with AMLAB

The following points may be noted from the results

1. The position and magnitude of the first peak and valley is the same when viewed on the digital storage CRO and on AMLAB

2. There seems to be a discontinuity in the AMLAB signal at the introduction of the transient. It was originally suspected that the problem was with AMLAB. This was because no discontinuity was visible in the digital storage CRO output shown in Figure: 5.10. Another transient measurement was made with the scale on AMLAB and the CRO enlarged to cover the entire 360° range. The results obtained are shown in Figure: 5.12 and Figure: 5.13.

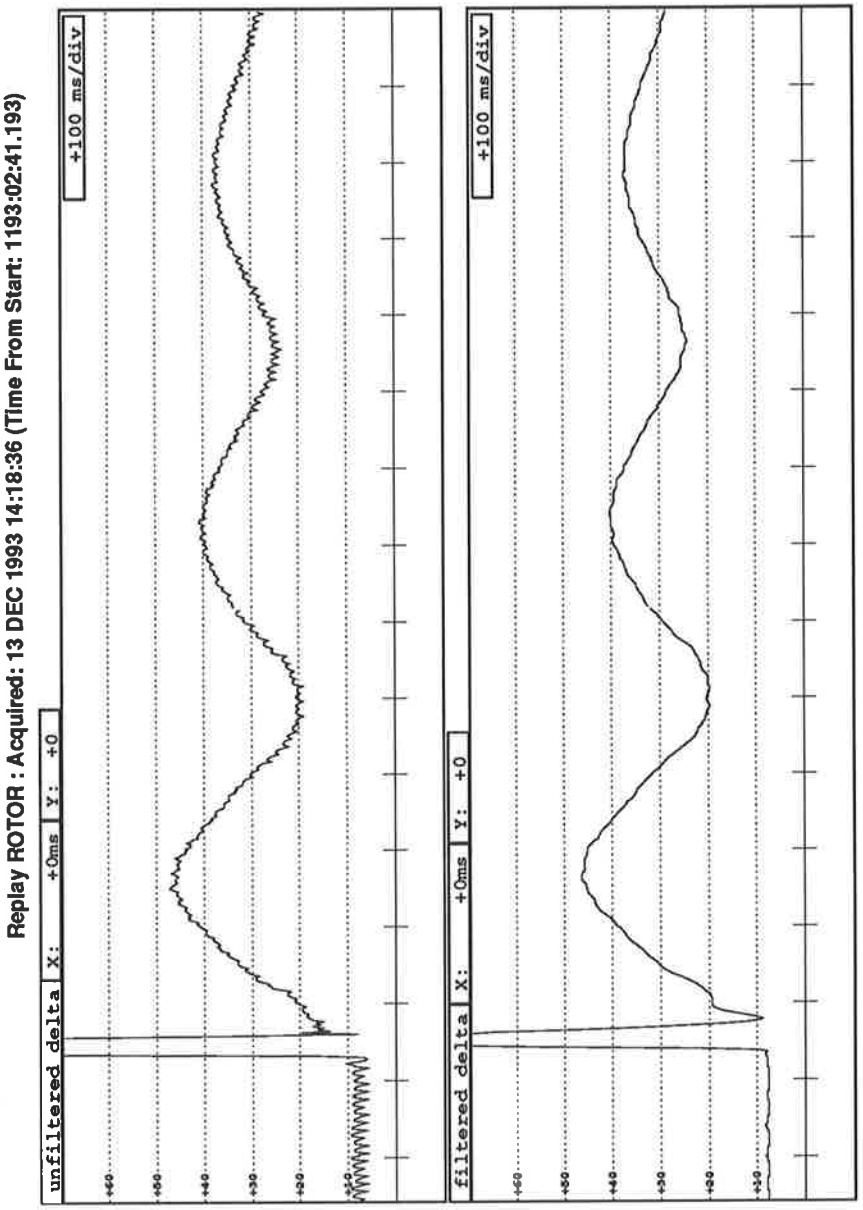

Figure 5.9: Output of the rotor angle transducer under transient conditions as viewed on AMLAB

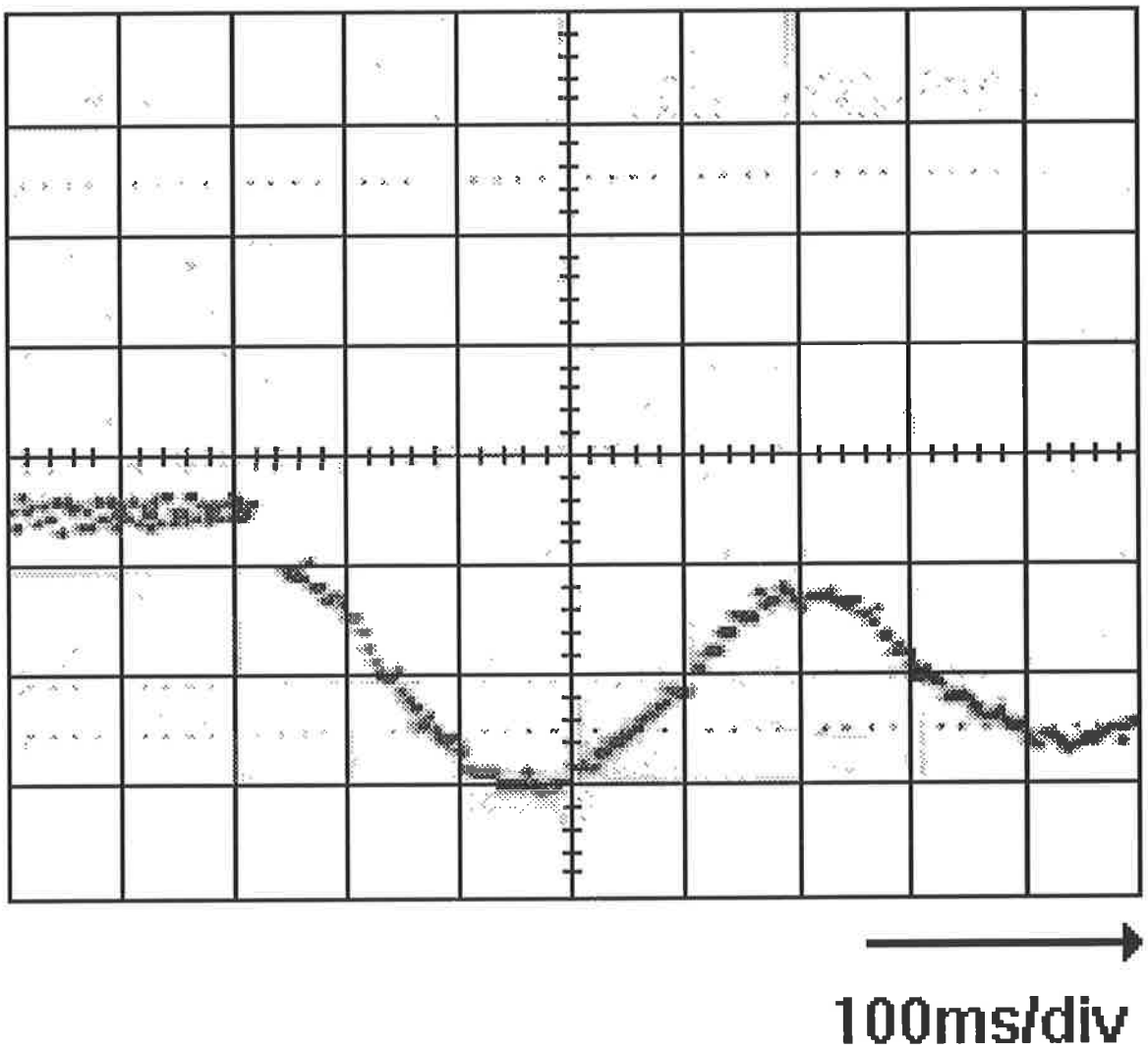

Figure 5.10: Photograph of the output of the rotor angle transducer under transient conditions as viewed on a digital storage CRO

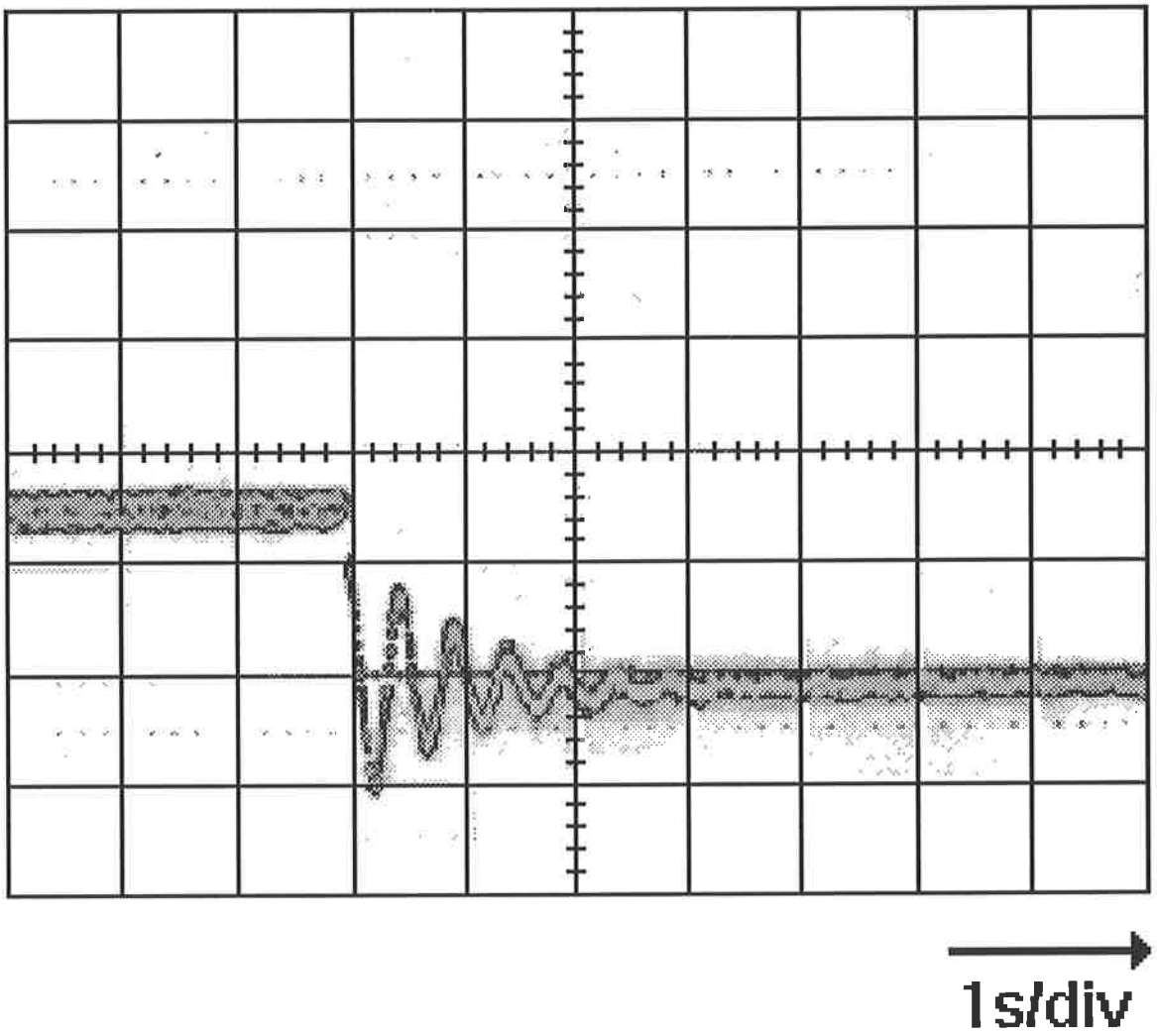

Figure 5.11: Photograph of the output of the rotor angle transducer under transient conditions as viewed on a digital storage CRO

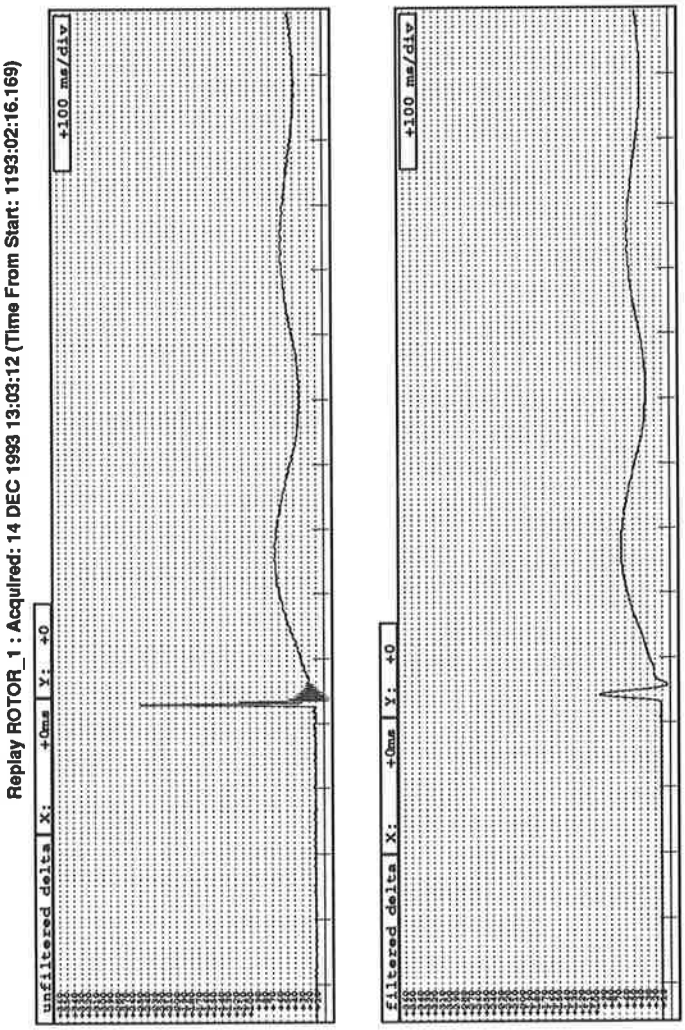

Figure 5.12: Output of the rotor angle transducer under transient conditions as viewed on AMLAB

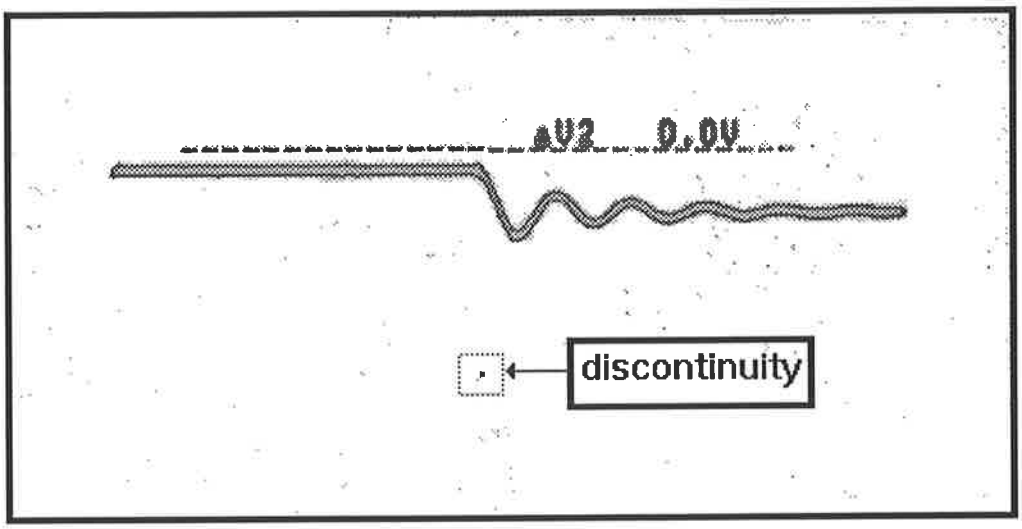

Figure 5.13: Photograph of the output of the rotor angle transducer under transient conditions as viewed on a digital storage CRO

It can be seen that the discontinuity present in the AMLAB signal is also present in the CRO signal, the only difference being that the AMLAB anti-aliasing filter exaggerates the effect of this discontinuity by introducing an RC oscillatory decay.

This discontinuity seems to occur at the start of the transient. This leads to the belief that the discontinuity is caused by the introduction of the transient. The application of the transient must put a spike on the stator voltage that causes an unwanted trigger on the rotor angle transducer.

A modification was made to the zero crossing detector as shown in Figure: 5.14 with a 470nF capacitor added. This capacitor has the effect of grounding any high frequency noise that might be present on the stator signal. Making the modification on the zero crossing detector cured the problem. This is evident in Figure: 5.15 where the discontinuity is no longer present.

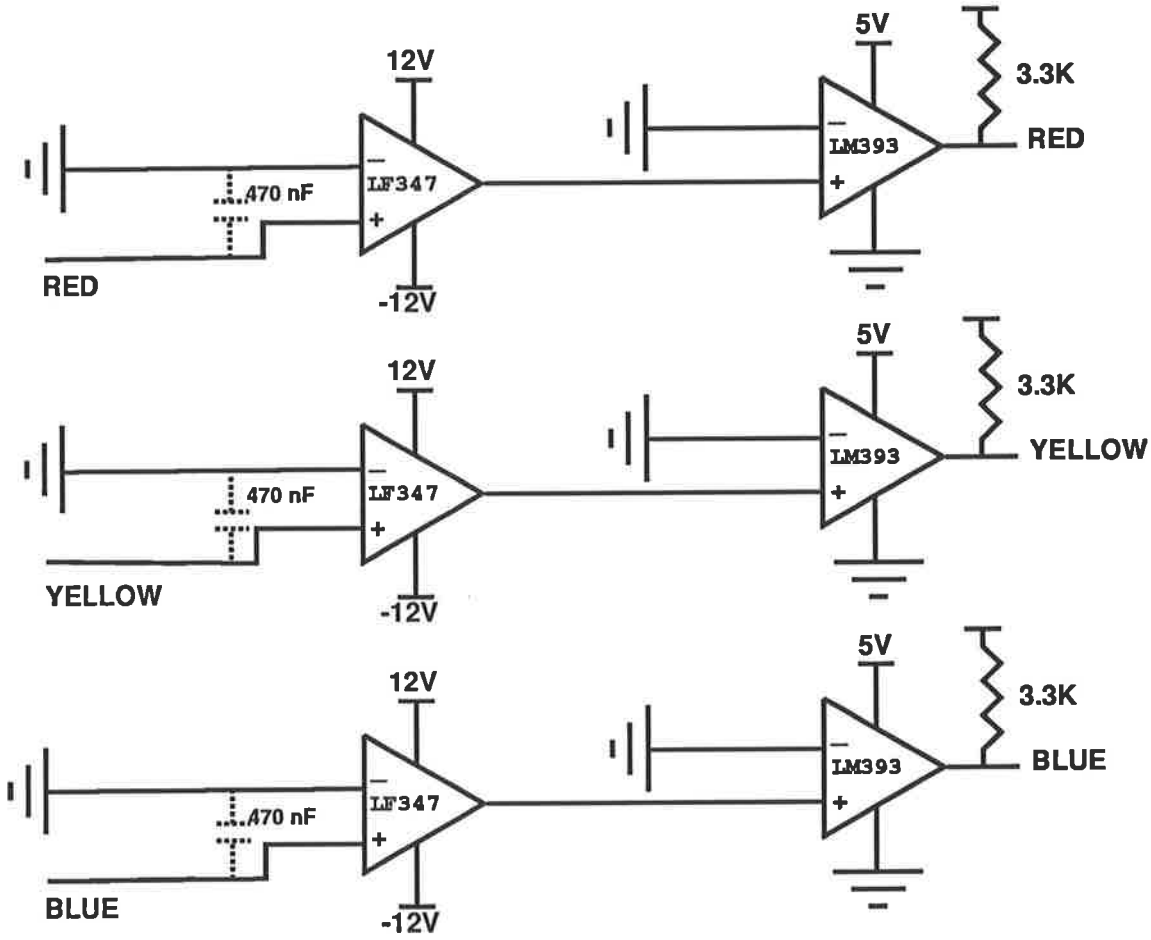

Figure 5.14: Zero crossing detector used for the the rotor angle transducer

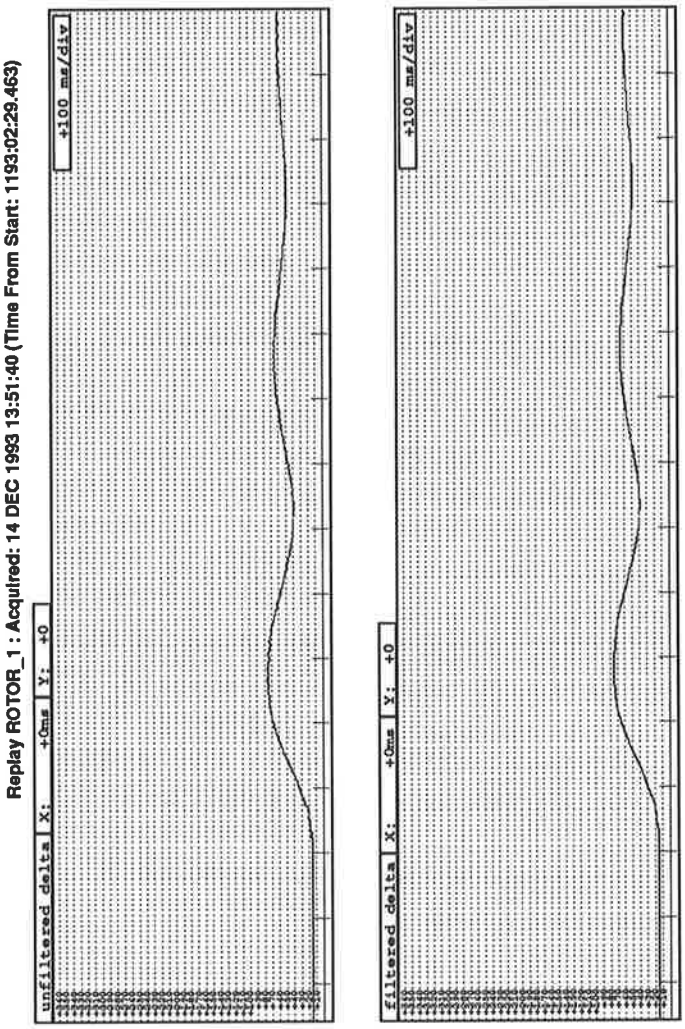

Figure 5.15: Rotor angle transient when using the modified zero crossing detector

Chapter 6

OPEN CIRCUIT TEST

6.1 Introduction

The open circuit test is a fundamental test for synchronous machines. With the machine on open circuit and at synchronous speed, the relationship between terminal voltage, V_t, and field excitation current, I_{fd}, is recorded. This relationship provides an understanding of the saturation that exists in the flux path.

When the machine is open circuit, the direct axis voltage, V_d, and quadrature axis flux, ψ_q, is zero. This means that terminal voltage and air-gap flux can be represented by Equation: 6.1 and Equation: 6.2.

$$\begin{aligned} V_t &= \sqrt{{V_d}^2 + {V_q}^2} \\ &= V_q \end{aligned} \tag{6.1}$$

$$\begin{aligned} \psi &= \sqrt{{\psi_d}^2 + {\psi_q}^2} \\ &= \psi_q \end{aligned} \tag{6.2}$$

$$Also\ V_t = \frac{d\psi}{dt}$$

Therefore in per unit terms

$$V_t = V_q = \psi_d \tag{6.3}$$

In this test, the ability of the monitoring system to be used for the open circuit test will be demonstrated, with V_t, V_q and ψ_d measured as the field excitation current was varied. V_t was measured using a digital multimeter with V_q and ψ_d being measured via the monitoring station. The results obtained are shown in Figure: 6.1. The V_t vs I_{fd} curve exhibits the typical saturation curve. At low values of field current, the curve is very linear. As the field current is increased, the flux in the rotor will also increase. However this increase in flux will be limited by the saturation of the flux path. This will lead to a tapering off of the curve. The V_q and ψ_d curves are as predicted in the theory, and exhibit the same characteristics as the V_t curve.

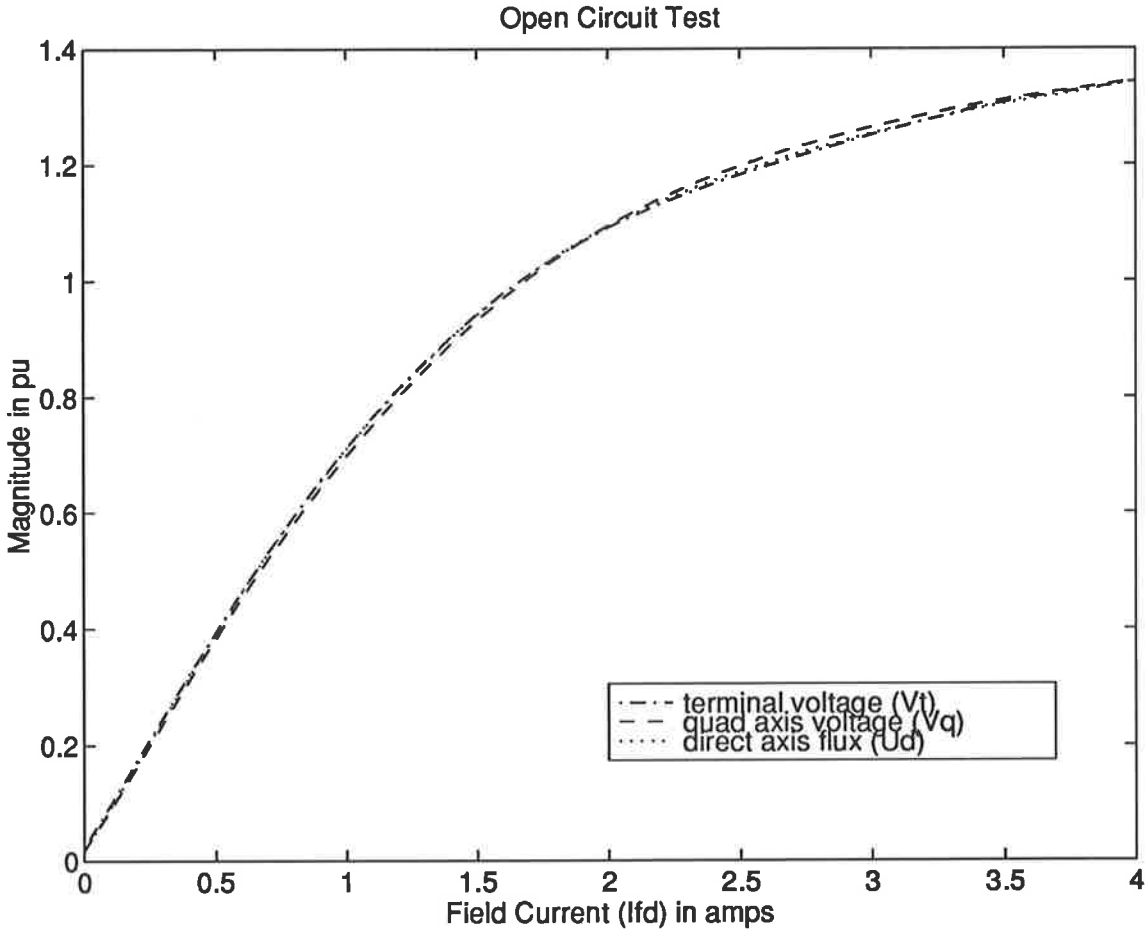

Figure 6.1: Open circuit test

Chapter 7

STEADY STATE TEST IN A SINGLE MACHINE INFINITE BUSBAR CONFIGURATION

7.1 Introduction

Having designed and constructed the monitoring system, various applications of the system for synchronous machine analysis were investigated. In this chapter some steady state applications for the monitoring system will be detailed. In these tests, the synchronous machine was connected as shown in Figure: 7.1, in a single machine infinite busbar (SMIB) configuration. The external inductance is used to simulate a transmission system and hence make the results more meaningful.

The tests performed here are to be used to analyze the synchronous machine.

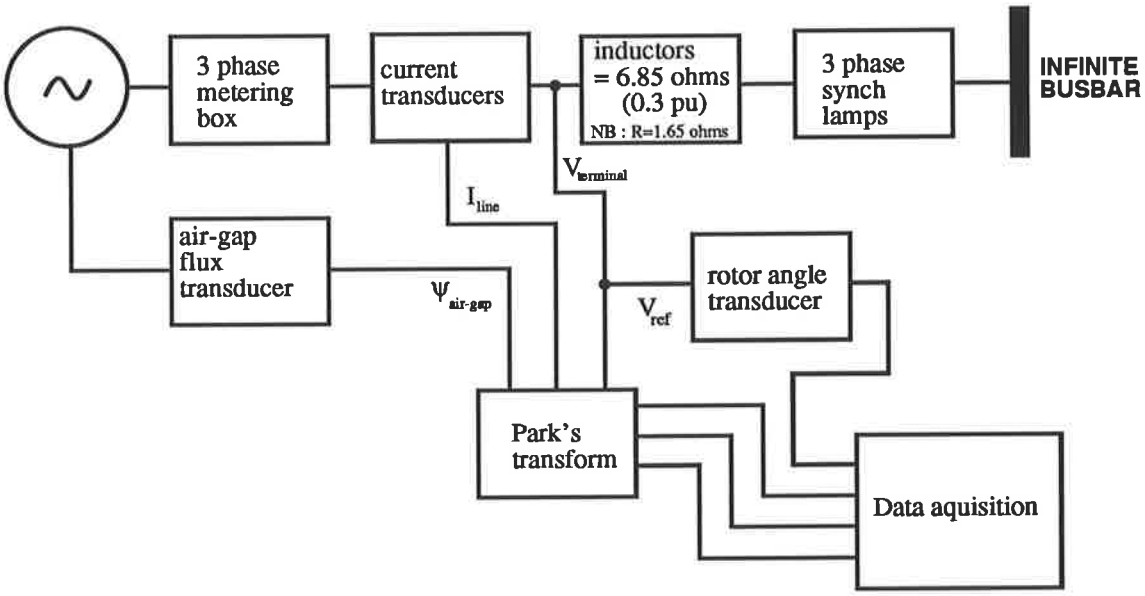

Figure 7.1: Single machine infinite busbar configuration (SMIB)

This is why, as can be seen in Figure: 7.1, all the measurements made by the monitoring station were made before the external inductance. By taking the measurements before the inductors, the effects of the inductors are not included in the measured data. The real and reactive power were measured using the 2 wattmeter method via the 3-phase metering box. The tests were performed on the synchronous generator at various operating or load points. Each load point is characterized by the real and reactive power output of the generator. The operating points were chosen such that there was an even spread over the entire operating range.

At each operating point, all the synchronous machine quantities were measured. The traditional measured values like terminal voltage, line current, field excitation current, real and reactive power and busbar voltage were measured using the appropriate meters. The quantities provided for in the monitoring station were also measured. The data obtained with the monitoring station were analyzed and compared with the data obtained with the traditional method as detailed in the proceeding sections.

7.2 Analysis of Results – Load Points

7.2.1 Introduction

The real power, P, and the reactive power, Q, can be calculated in two ways. The first is a direct measurement with the wattmeters. The second method is via the monitoring station. The monitoring station provides a measurement of V_q, V_d, I_q and I_d. From these quantities real and reactive power can be calculated using the equation shown in Equation: 7.1 and Equation: 7.2.

$$P = V_d * I_d + V_q * I_q \tag{7.1}$$

$$Q = V_q * I_d - V_d * I_q \tag{7.2}$$

The two methods were used to calculate the real and reactive power at each of the load points. The accuracy of the transducer can hence be verified by comparing the two set of values.

7.2.2 Results

A graphical interpretation of the results obtained are shown in Figure: 7.2, Figure: 7.3 and Figure: 7.4. The results obtained from the transducer

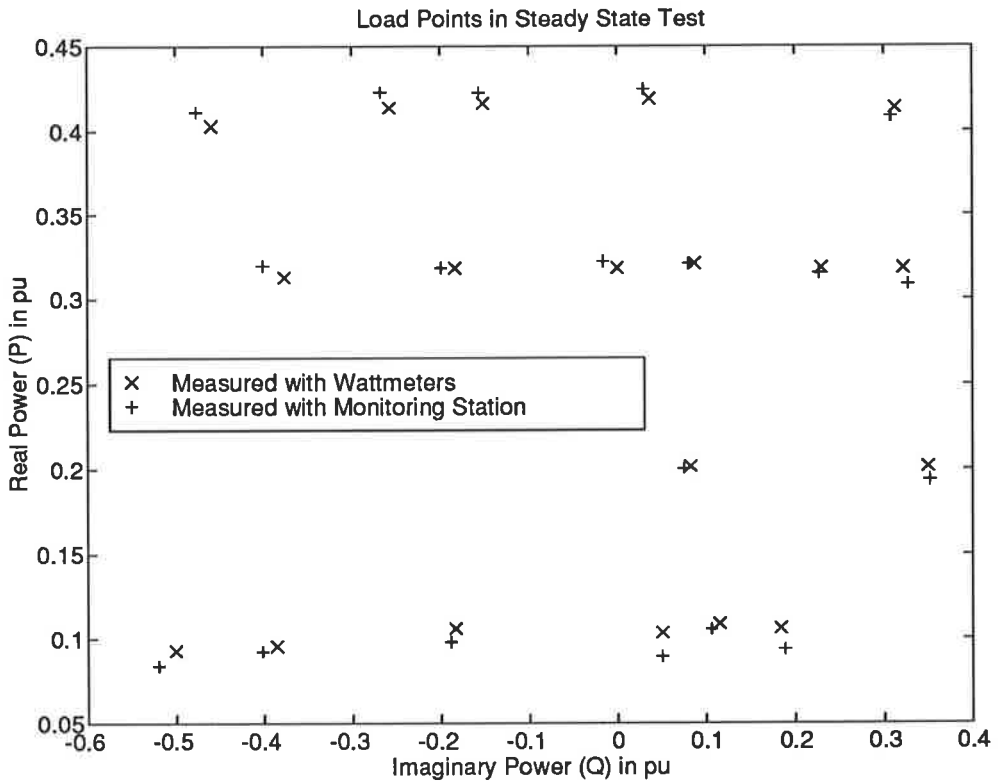

Figure 7.2: Load Points showing Real and Imaginary Power

is in good agreement with those obtained from the wattmeters. At higher power values, the real power obtained with the monitoring station is almost identical to those obtained with the the wattmeters. At low power levels, the difference between the two sets of results is more significant. This error can be attributed to the wattmeters. At low power levels, the deflection in the wattmeter needle is very small. At times, it was very difficult to accurately

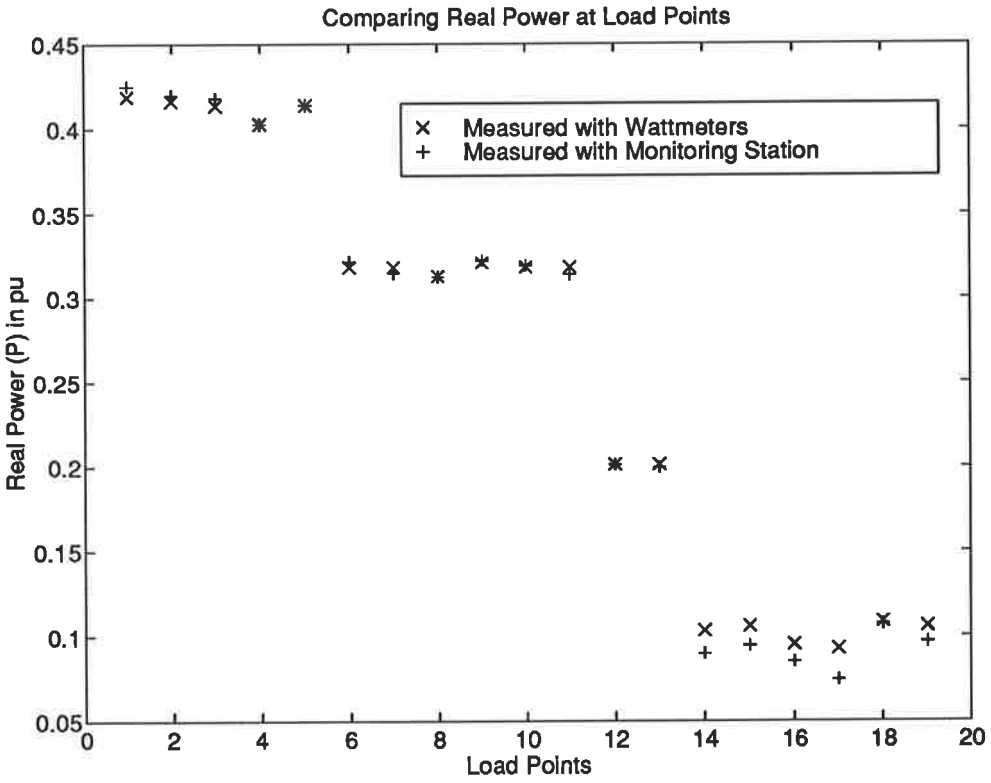

Figure 7.3: Real Power

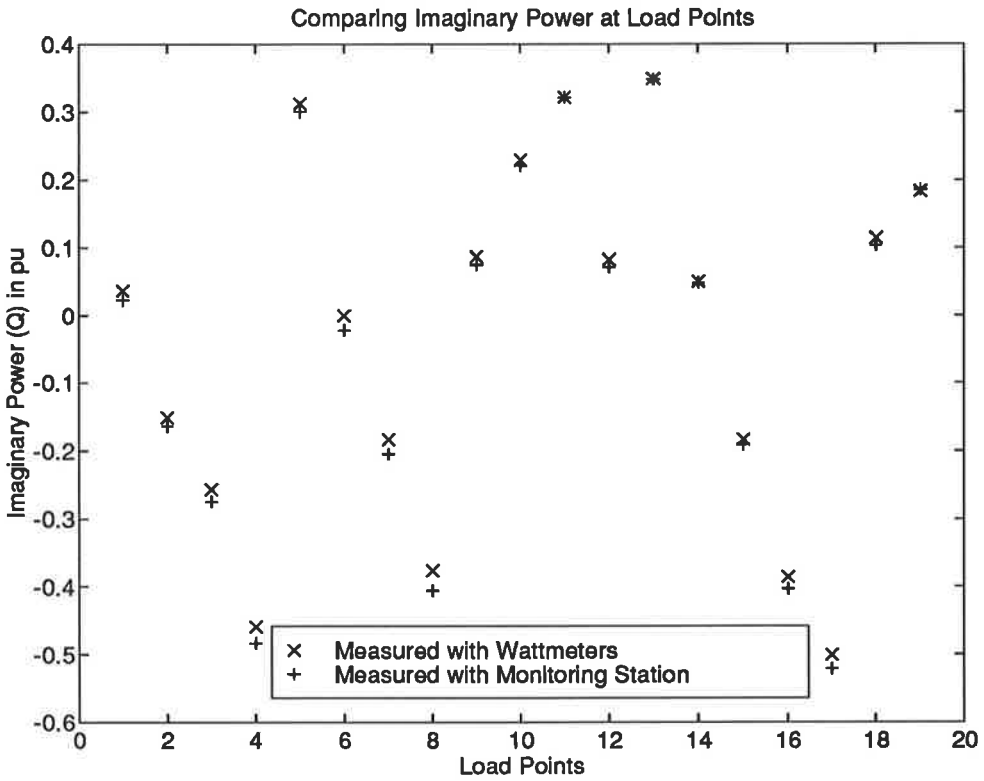

Figure 7.4: Imaginary Power

measure the small deflections on the wattmeters. A similar agreement exists in the reactive power measurements.

7.3 Analysis of Results – Torque Measurements

7.3.1 Introduction

As with the real and imaginary power, the electro-magnetic torque of the synchronous machine can be calculated from the quantities measured with the monitoring station . The flux signals, ψ_d and ψ_q, are used together with the current signals to provide a measure of the torque as shown in Equation: 7.3.

$$T = \psi_d * I_q - \psi_q * I_d \tag{7.3}$$

To test the accuracy of the torque measurements, it has to be compared with some other appropriate measurement. Real power, P, is related to torque by Equation 7.4

$$P = \omega T \tag{7.4}$$

where ω is the rotational speed of the shaft. However, all the quantities used are measured in per unit terms. This means that the above equation reduces to Equation 7.5.

$$P = T \tag{7.5}$$

Hence, the accuracy of the torque measurement can be verified by equating it to the real power measured by the wattmeters.

7.3.2 Results

A graphical interpretation of the results obtained is shown in Figure: 7.5. It is clear that the 2 sets of results are not very close. This discrepancy can

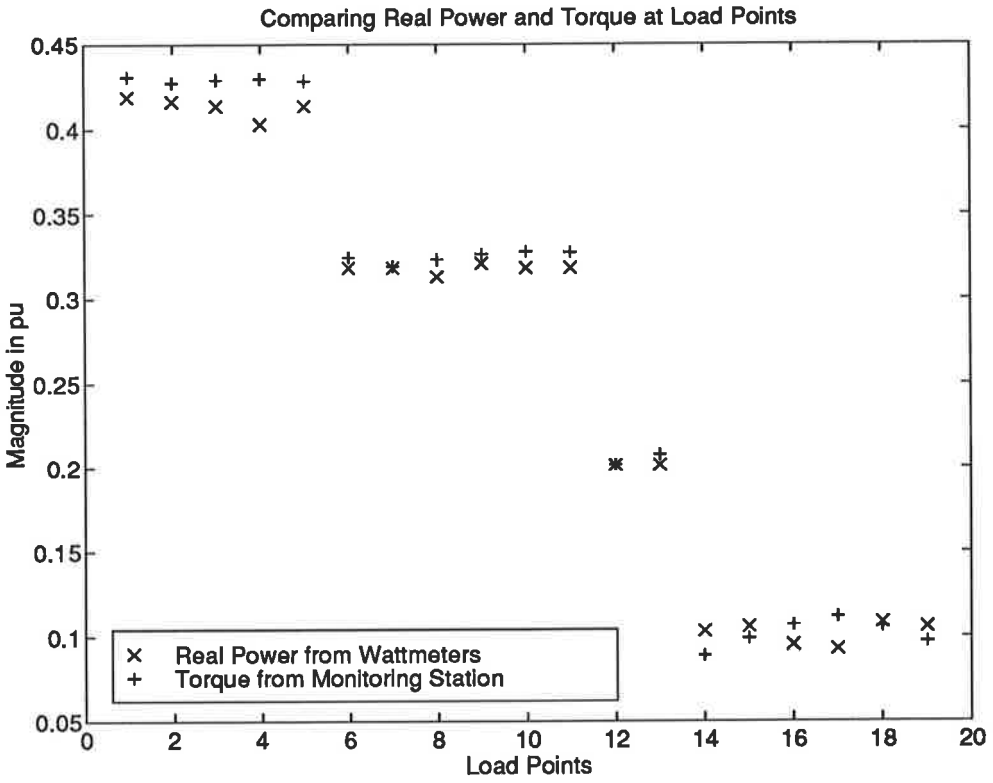

Figure 7.5: Comparing Electro-magnetic torque with real power

easily explained by considering the resistance in the stator coils. The torque is measured internally in the machine whereas the real power is measured at the machine terminals. The resistance in the stator coil of the synchronous machine is very small, when compared to the inductance, and it is usually considered insignificant. However in this case the effect of the resistance is not insignificant. The measurements for air-gap flux, used to calculate torque, had the effect of the resistance removed. However, in the power measured with the wattmeter, the effect of the resistance is included in the measurements. When the power dissipated in the resistance, I^2_{line}R, was added to the real power, as shown in Figure: 7.6, there was be a better agreement between the two sets of results.

This I^2_{line}R factor perfectly shows up the benefit of the monitoring station. Small insignificant quantities like the stator resistance, R, may not be that significant in all applications. The traditional method of equating real power output and electromagnetic torque is obviously incorrect and could be a significant source of error. By measuring torque directly, these possible sources of error are minimized.

7.4 Analysis of Results – Parameter Identification

7.4.1 Introduction

To determine the parameters of the synchronous machine is not an easy proposition. The monitoring station facilitates this measurements very easily. A few of these machine parameters will be calculated using the data measured in the SMIB test. The general equations relating the various quantities are shown in Equation: 7.6 and Equation: 7.7.

$$\psi_d = L_d * i_d + L_{kd} * i_{kd} + L_{md} * i_{fd} \quad (7.6)$$

$$\psi_q = L_q * i_q + L_{kq} * i_{kq} \quad (7.7)$$

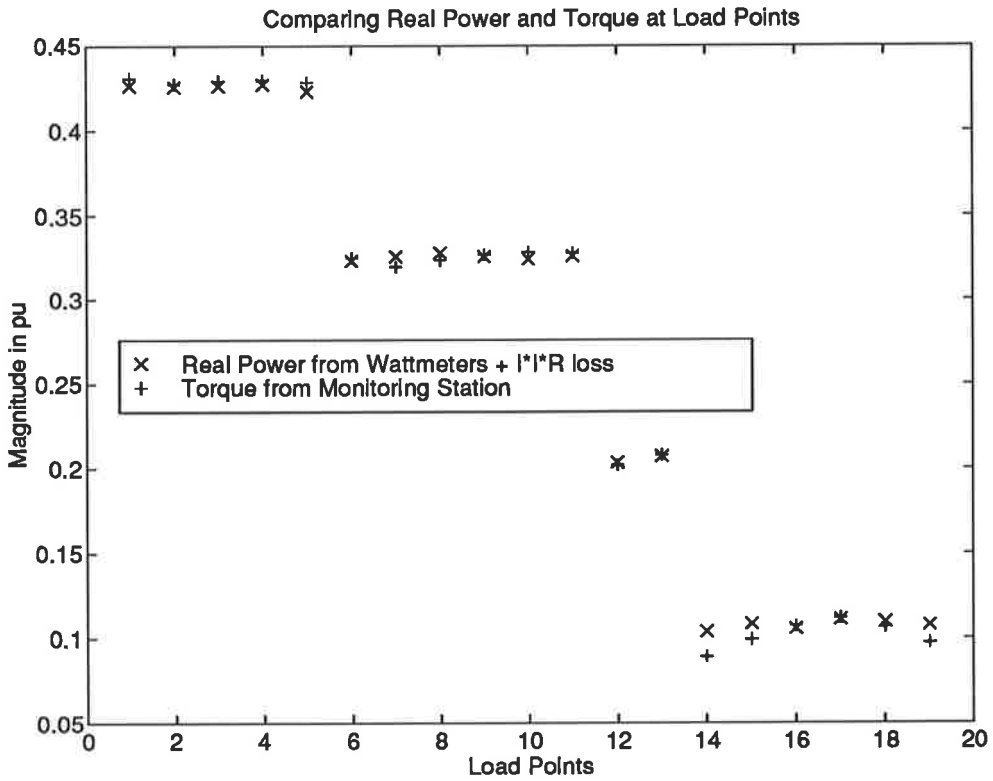

Figure 7.6: Comparing Electro-magnetic torque with real power

Where

L_{md} = mutual inductance between the field and the direct axis
L_d = the complete self-inductance in the direct axis
L_q = the complete self-inductance in the quadrature axis
L_{kd} = self inductance of the damper coil in the direct axis
L_{kq} = self inductance of the damper coil in the quadrature axis

The data set used here, was obtained under steady state conditions. This means that simplifications can be made to the above equations. Under steady state conditions the damper winding current, i_{kd} and i_{kq}, are zero. Also under open circuit conditions, there is no line current meaning that i_d and i_q are zero. The equations above can hence be simplified as shown below.

Under steady state load condition

$$\psi_d = L_d * i_d + L_{md} * i_{fd} \tag{7.8}$$
$$\psi_q = L_q * i_q \tag{7.9}$$

Under open circuit conditions

$$\psi_d = L_{md} * i_{fd} \tag{7.10}$$
$$\psi_q = 0 \tag{7.11}$$

The machine parameters can hence be isolated by rearranging the equations, as shown below.

From Equation: 7.10

$$L_{md}(\psi_d) = \frac{\psi_d(o.c.)}{i_{fd}} \tag{7.12}$$

From Equation: 7.8

$$L_d = \frac{\psi_d - L_{md}(\psi_d) * i_{fd}}{i_d} \tag{7.13}$$

From Equation: 7.9

$$L_q = \frac{\psi_q}{i_q} \tag{7.14}$$

7.4.2 Results

The machine parameter, L_d, was calculated using the data measured in the SMIB steady state test. L_{md} was calculated using the data measured in the open circuit test. The results obtained are graphically represented in Figure: 7.7 and Figure: 7.8. The results shown in the figures appear to be a little

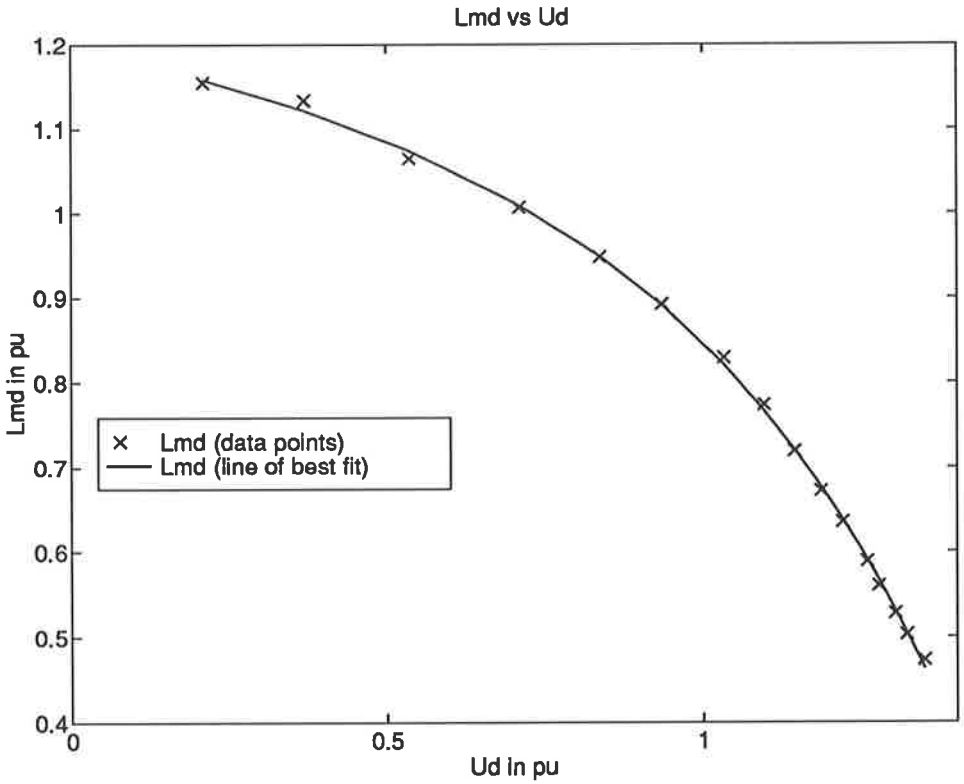

Figure 7.7: L_{md} *vs* ψ_d

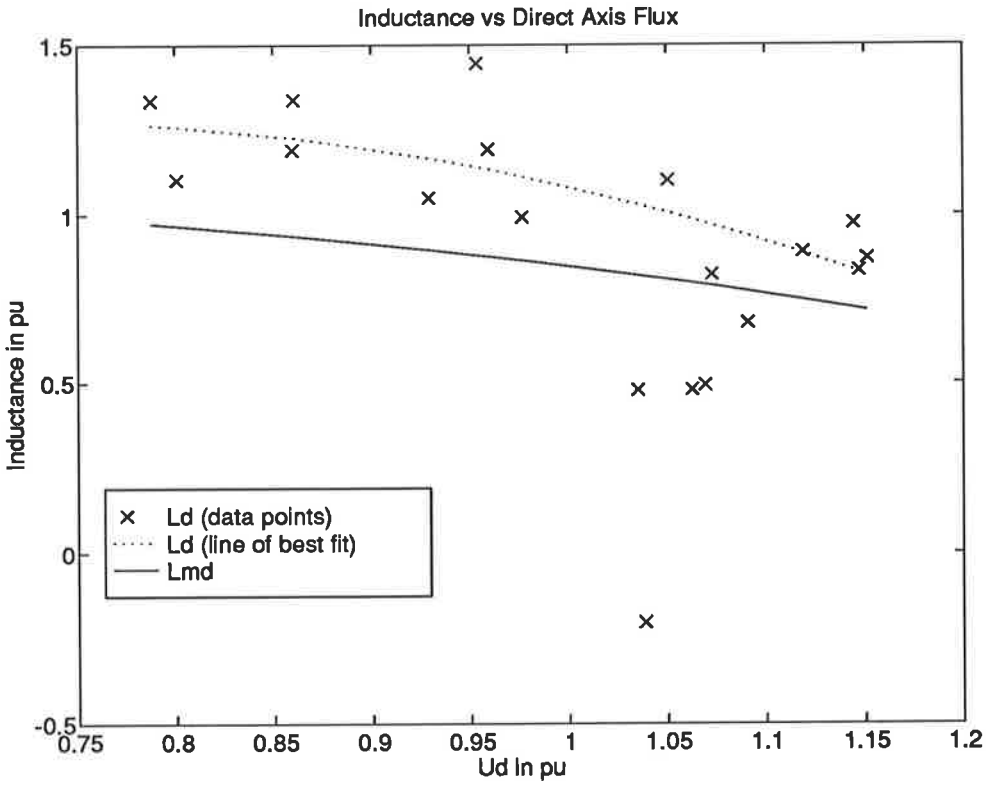

Figure 7.8: L_d *and* L_{md} *vs* ψ_d

patchy due to the lack of data points. However some meaningful results can still be derived from them.

The data points for L_d seem to be fairly well grouped together, except for 4 points that are a little low and out of place. This is caused by a numerical analysis problem. For these points, the value of the numerator and denominator of Equation: 7.13 are very small. Hence any small errors that are present in any of the quantities gets exaggerated when they are divided. Even so, a line of best fit can be drawn through the remaining data points.

Comparing this curve of L_d with that of L_{md} provides a description of the effective leakage inductance, l_a, of the synchronous machine. These three inductance quantities are related to each other by Equation: 7.15.

$$L_d = L_{md} + l_a \tag{7.15}$$

Hence the difference between the L_d and L_{md} curves represents l_a. It has always been assumed that l_a is a constant value that does not saturate. If this was the case, the separation between the L_d and L_{md} curves will be constant. However, this was not observed. It appears that l_a, is not constant but saturates at high flux levels.

There would not be any significant saturation expected in the quadrature axis of a salient pole machine. This is because the flux path in the quadrature axis is in air and air does not saturate. The data points, shown in Figure: 7.9, supports this. The straight line of best fit drawn is a good representation of the data points. The slope of this line of best fit is the value for L_q and was found to be 0.5539 pu.

Analyzing these data points directly by evaluating $L_q(= \frac{\psi_q}{i_q})$ point-by-point can produce results that are very misleading, especially at low current levels, as shown in Figure: 7.10. The points in Figure: 7.10 appear to follow some non-linear pattern, which is obviously incorrect. This is due to a practical limitation in the transducer. When i_q is zero, the value of ψ_q would be expected to be zero as well. However, this is not possible practically and consequently there is a small zero offset in ψ_q. This offset is then grossly exaggerated when ψ_q is divided by i_q.

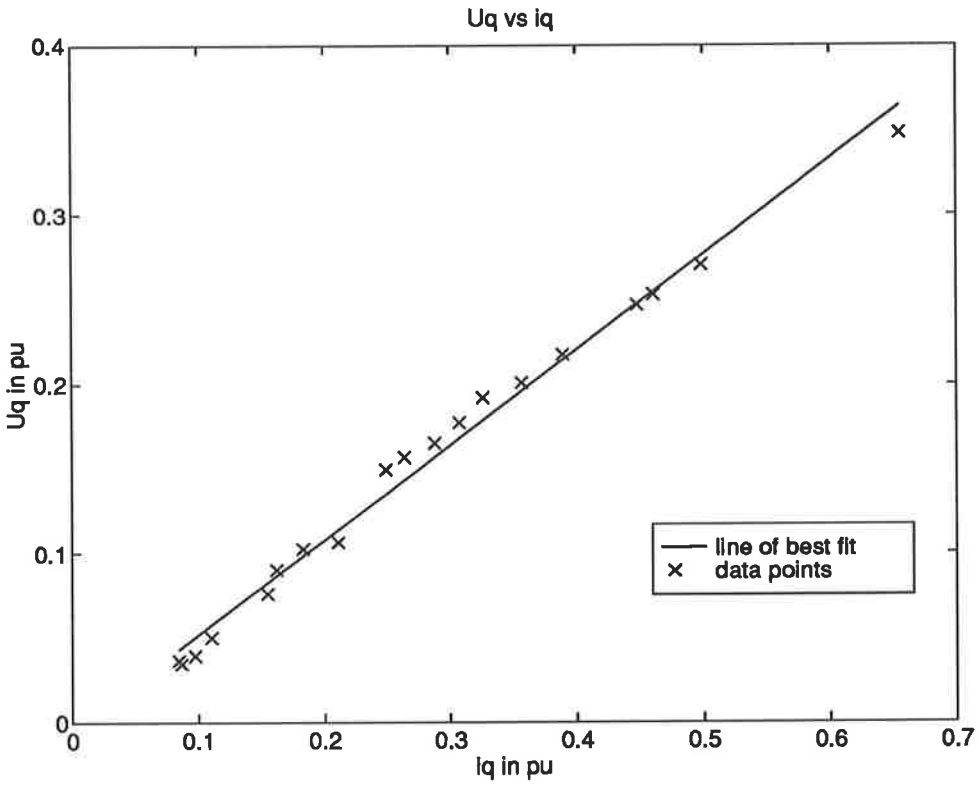

Figure 7.9: ψ_q *vs* i_q

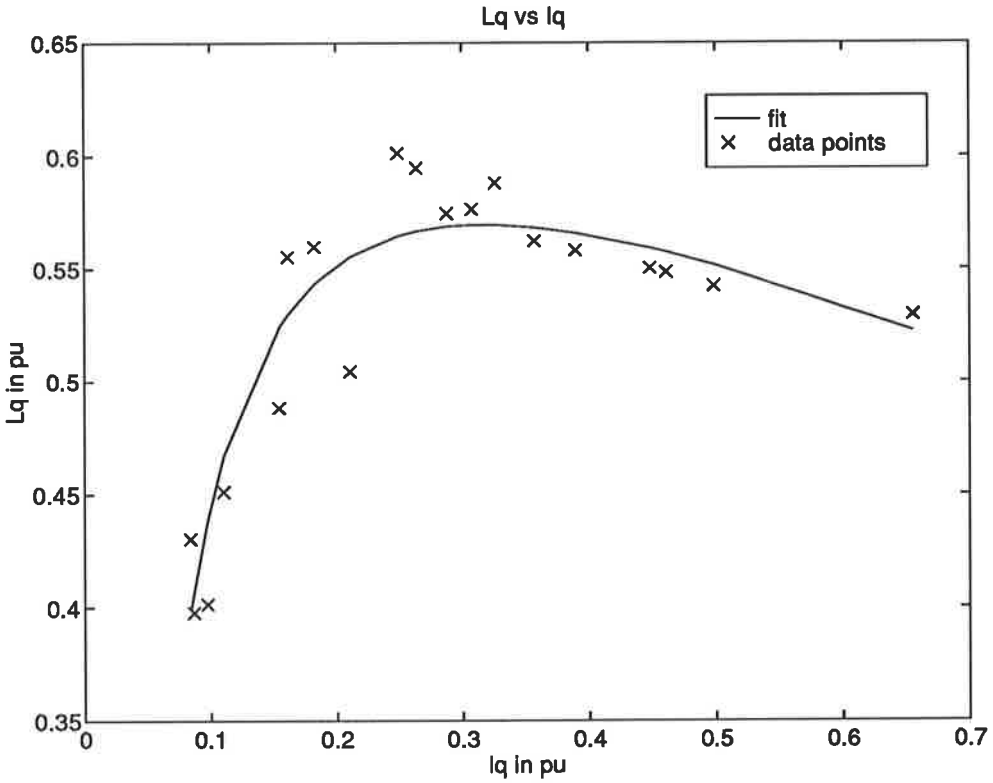

Figure 7.10: L_q *vs* i_q

7.5 Flux Distribution in Space

7.5.1 Introduction

The 3-phase flux signal from the air-gap flux transducer is transformed to the 2-axis Park's transform equivalent. Park's transform was performed at 8 discrete positions. The start point, or 0^o reference angle, of the transform was chosen such that it resulted a maximum direct axis flux, ψ_d, and a zero quadrature axis flux, ψ_q, under open circuit conditions. Hence the 0^o reference angle can be taken to represent the position in line with the rotor pole if we are considering ψ_d. Similarly 0^o would represent a position of the quadrature axis if considering ψ_q.

This 0^o reference angle was set with the use of an 8 bit dip switch. Each 8 bit binary code on the dip switch represents the corresponding 8 bit gray code for the shaft position as determined by the shaft encoder. It was found that the binary code that represents 0^o was "00001011_b". So if this code was chosen, the value of ψ_d obtained would represent the air-flux flux in a direction in line with the rotor pole, a maximum. If a code of "00001100_b" was chosen instead, the ψ_d signal measured would represent the air-gap flux at a point shifted by one code or 2.81^o from the line of the rotor pole. By using a range of codes, it would be possible to determine the spatial distribution of the air-gap flux in space.

The spatial distribution of flux was determined at 3 operating conditions.

1. The synchronous machine at synchronous speed and and on open circuit with the excitation field current set such that the rotor was unsaturated.

2. The synchronous machine at synchronous speed and and on open circuit with the excitation field current set such that the rotor was saturated.

3. The synchronous machine was connected in a SMIB configuration. The machine was made to generate into the infinite busbar so as to create a significant quadrature axis flux, ψ_q.

7.5.2 Results

The results obtained are shown graphically in Figure: 7.11, showing the var-

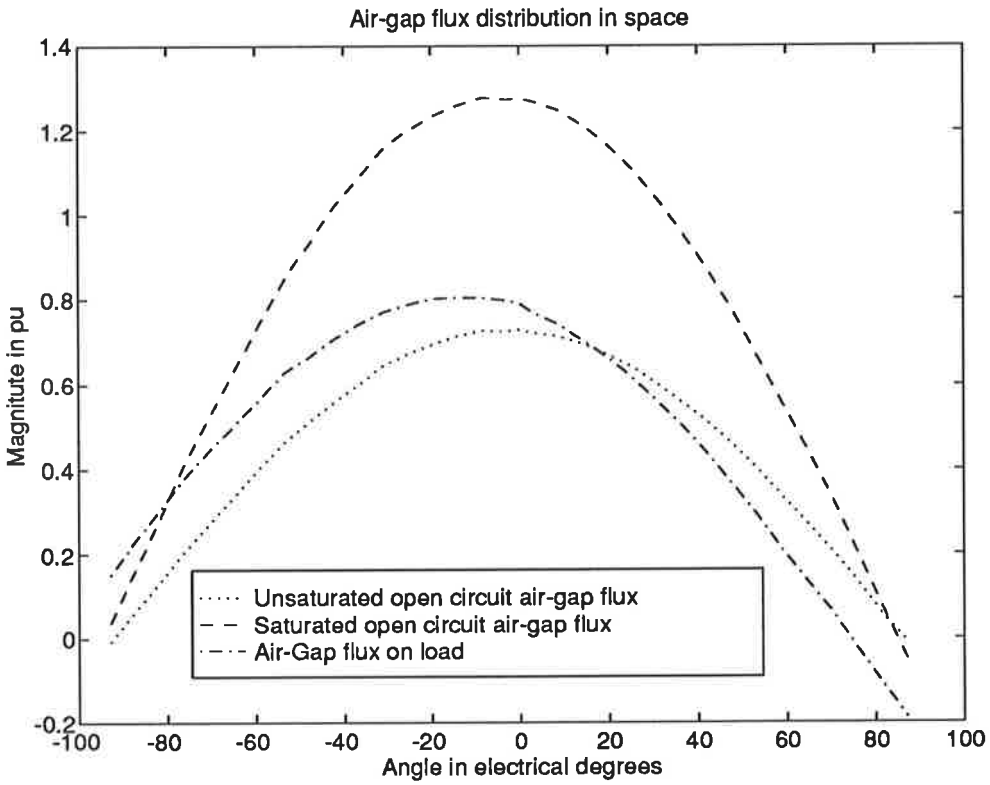

Figure 7.11: Flux distribution expressed in per unit

ious flux spatial distributions represented in per unit terms. The increased magnitude of the saturated flux signal when compared to the unsaturated case is clearly visible. For the comparisons of the relative shapes and angle shifts of the distribution it is easier to compare the normalized flux distributions as shown in Figure: 7.12. The shift between the on-load case when compared to the no-load case is very obvious. With the increase in the ψ_q component of flux, it would be expected that the overall flux distribution

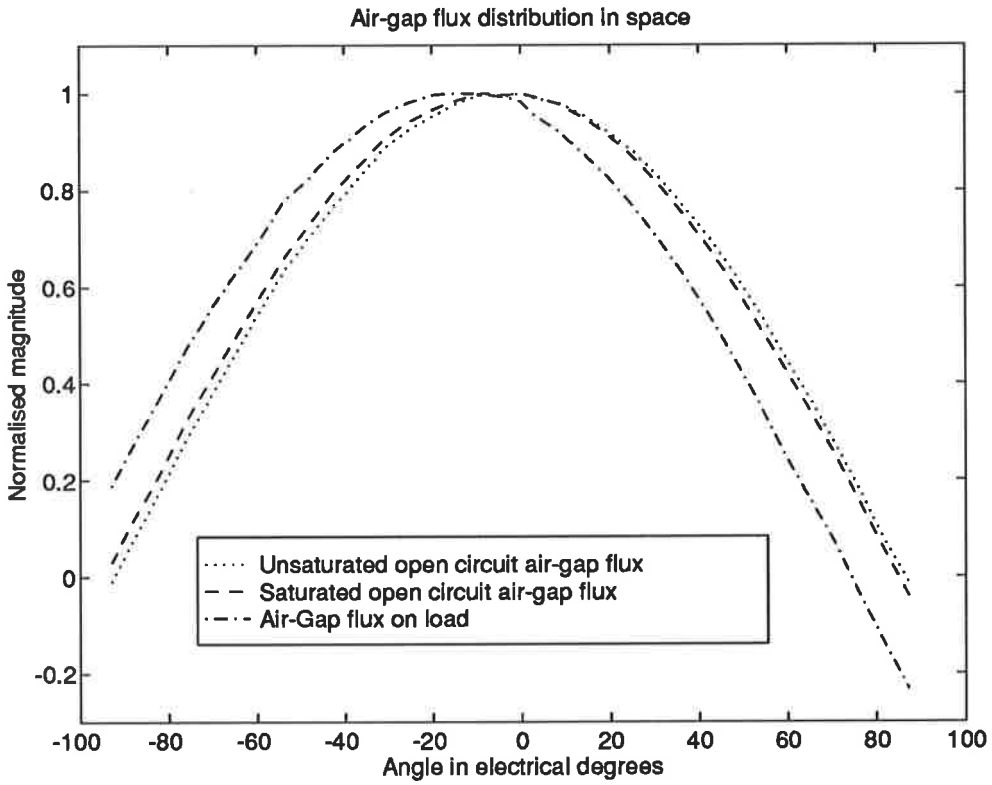

Figure 7.12: Normalized flux distributions

will be shifted towards the quadrature axis.

The effect that was unexpected was the distribution of the saturated air-gap flux when compared to the unsaturated case. There appears to be slight angle shift of the flux distribution towards the quadrature axis. The air-gap flux distribution that was expected was of the form shown in Figure: 7.13. As

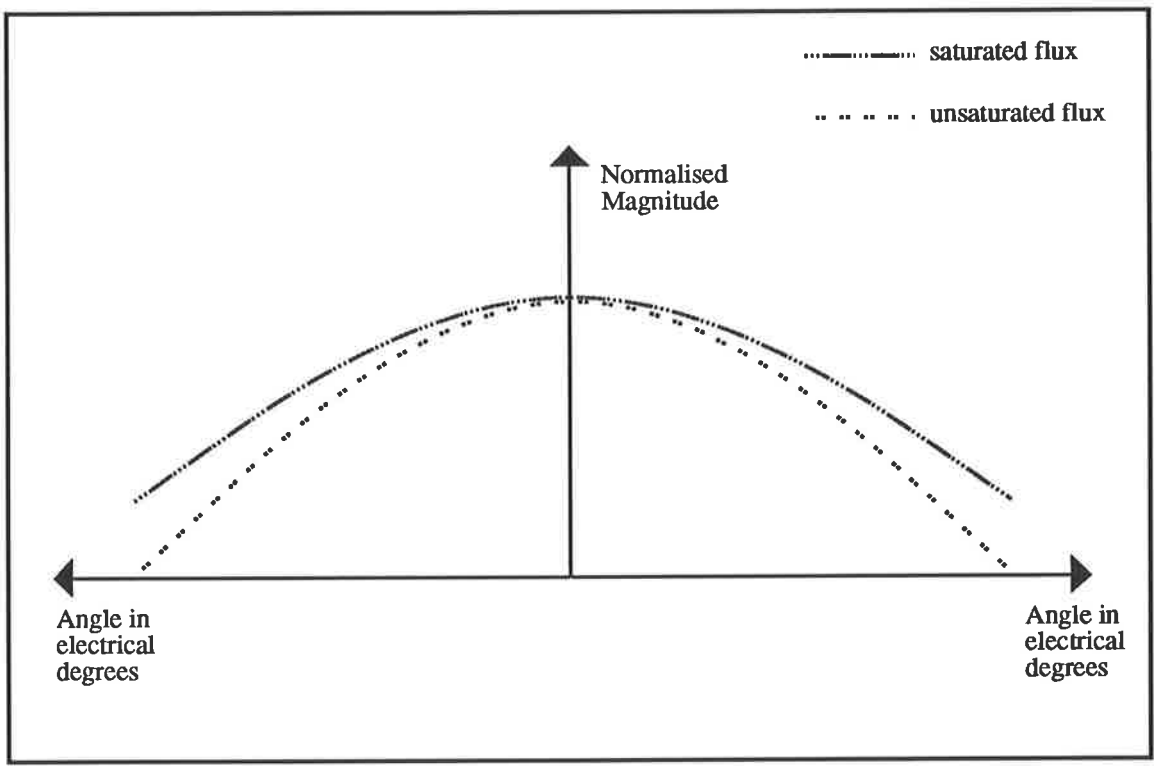

Figure 7.13: Flux distribution expected

the rotor gets saturated, the flux signal will be expected to be more uniform as it utilizes more of the rotor pole volume. However this was not seen. The effect observed here is probably due to a non-uniform saturation across the pole face of the rotor. If the pole structure is not perfectly symmetrical, the flux distribution will also not be symmetrical, producing the effect observed.

Chapter 8

TRANSIENT TESTS

8.1 Introduction

In the previous chapter, various steady state applications of the monitoring system were demonstrated. In this chapter, the focus shifts to cover the transient applications. The transient test performed here are grouped into 2 main sections. The first section deals with the identification of dynamic machine parameters from the sudden 3-phase short circuit test. In the second section, various step changes will be made to the synchronous machine's operating condition, in view of determining the suitability of using the various transient signals as part of control strategy.

8.2 Sudden 3-Phase Short Circuit Test at Reduced Voltage

8.2.1 Introduction

The sudden 3-phase short circuit test is a fundamental machine test. It is used to determine the dynamic parameters of the synchronous machine. In

this test, the machine is first run up to synchronous speed with its terminals open circuit. As the name of the test implies, a sudden 3-phase short circuit is then applied to the machine terminals, resulting in a 3-phase transient line current. Analyzing this transient current will provide a quantitative description of the dynamic or transient parameters of the machine. This current transient can be modelled by Equation: 8.1.

$$I = E[\frac{1}{X_d} + (\frac{1}{X'_d} - \frac{1}{X_d})e^{\frac{-t}{T'_d}} + (\frac{1}{X''_d} - \frac{1}{X'_d})e^{\frac{-t}{T''_d}}] \tag{8.1}$$

Where

I	=	rms short-circuit current (pu)
E	=	rms voltage before short circuit (pu)
t	=	time in seconds from the start of the short circuit
X_d	=	synchronous reactance
X'_d	=	transient reactance
X''_d	=	subtransient reactance
T'_d	=	transient time constant
T''_d	=	subtransient time constant

The current transients that are produced in this test are very large. Performing this test at rated terminal voltage often results in peak currents in the order of 6-8 pu. Apart from the safety considerations of such a high current, there is also the limitation in the instruments which are not capable of measuring this current. For these reasons, this test is usually performed at reduced terminal voltage. The test is still valid as can be seen from Equation: 8.1, the absolute magnitude of the current is not that important, but rather it is the ratio of current to open circuit voltage that is of concern.

8.2.2 Results

The machine setup used for this test is shown in Figure: 8.1 where closing the 3-phase switch produces the sudden 3-phase short circuit. The open circuit

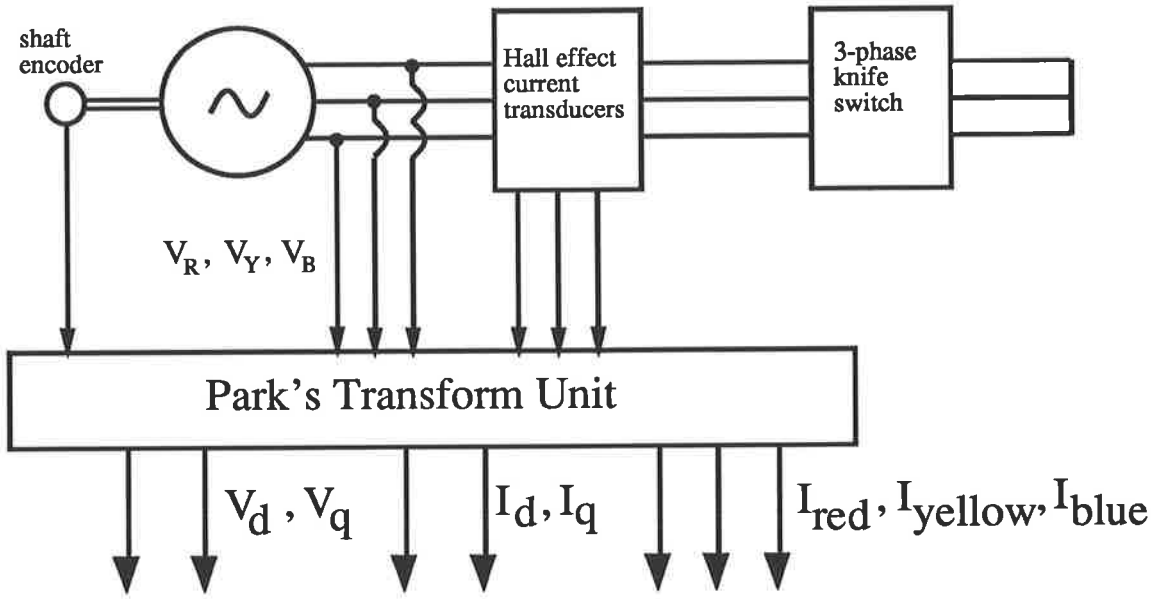

Figure 8.1: Machine set-up for the Sudden 3-phase short circuit test

terminal voltage chosen for this test was 0.171pu. The quantities shown in Figure: 8.1 were measured. The current waveform obtained for the "red" phase is shown in Figure: 8.2. The task of extracting the rms component of

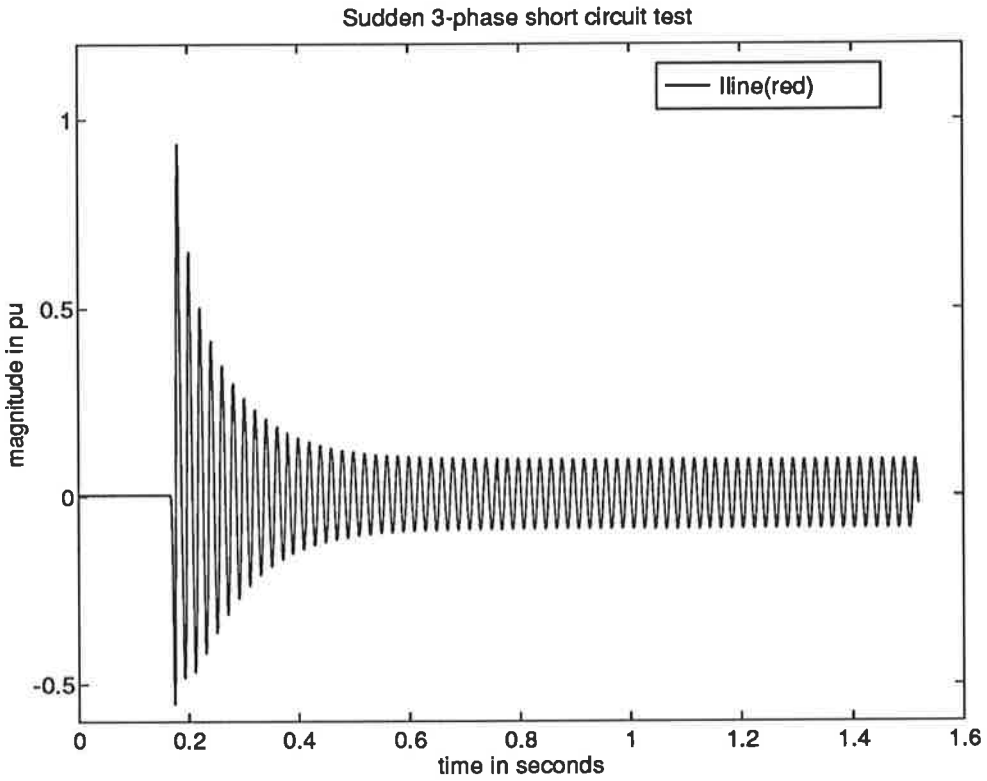

Figure 8.2: Sudden 3-phase short circuit test - Iline(red)

the transient is not an easy proposition. However, a simple solution to this problem is to use the positive peaks of the transient. These positive peaks form the positive envelope of the transient signal. In a sinusoidal signal, the rms quantity is related to the peak quantity by a factor of $\sqrt{2}$. However, this factor does not arise,in this case, because all the calculations are performed in per unit.

Using the positive envelope of the transient definitely makes the transient easier to analyze. However, using the positive envelope, which requires additional processing to obtain, results in a lowering of the resolution of signal as only one point in a 50Hz cycle is used. With the monitoring system, this problem is very quickly rectified. Under short circuit condition, and making the assumption that the stator resistance is insignificant when compared to the synchronous inductance, the line current is a direct axis current. This can be confirmed by referring to Figure: 8.3. The direct axis current signal,

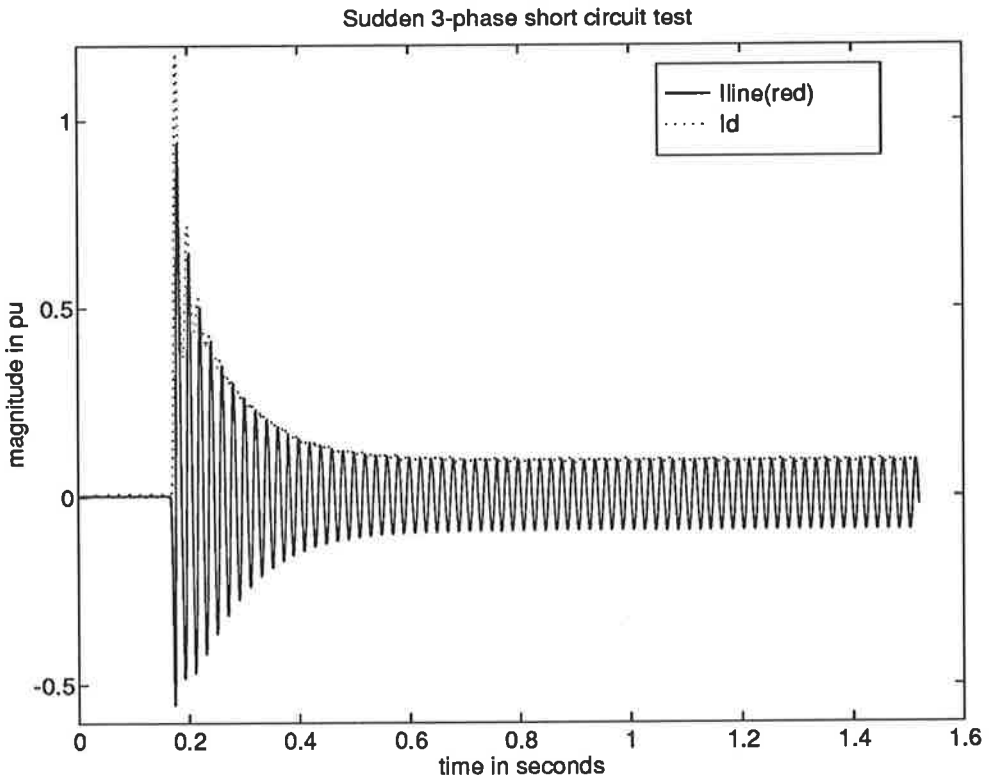

Figure 8.3: Sudden 3-phase short circuit test - Id superimposed onto Iline(red)

I_d, measured with the measuring system, corresponds to the positive enve-

lope of the line current transient. Park's transform has removed the 50Hz component. The resolution is also greatly improved with the direct axis current being evaluated 8 times in a 50Hz cycle.

A curve fitting algorithm, using a simplex least square error fit, was used to fit Equation: 8.1 to the direct axis current signal. The results obtained are shown in Figure: 8.4. Apart from the direct axis synchronous inductance, X_d,

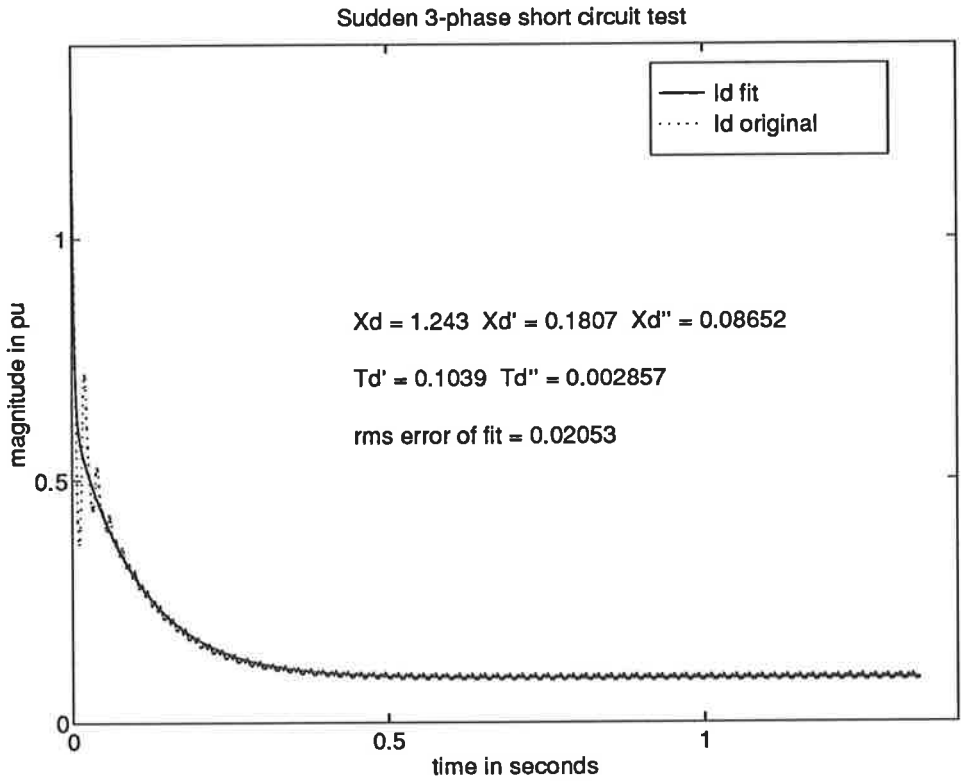

Figure 8.4: Sudden 3-phase short circuit test - Parameter identification using LMS curve fitting of Id

there is no way to compare the other parameters quantitatively. X_d, measured from this test, had a value of 1.243pu. This quantity was measured at

with the terminal voltage originally set to 0.171pu. As can be seen from the results from the open circuit test, Figure: 6.1, this means that the rotor is in its unsaturated region. Comparing the unsaturated value of X_d obtained here with that obtained from the large-signal machine tests, Appendix E, of 1.210pu, yields comparable results with a difference of only 2.8% between the two sets of results. As for the other parameters, even though a direct comparison cannot be made, a qualitative comparison can still be made. It was found that the parameters obtained here were the same order of magnitude as those obtained from an identical synchronous machine [16].

8.3 Step Change in Operating Condition

8.3.1 Introduction

In the event of a disturbance in a power system, it is the job of the power system stabilizer to keep the generators stable. As part of an automatic control system, machine quantities are used as control signals as part of a feedback control loop. To be effective as control signals, these machine quantities have to be generated in real time and have to be accurate. The base quantities measure by the measuring system are terminal voltage, V_d and V_q, line current, I_d and I_q, air-gap flux, ψ_d and ψ_q, and rotor angle, δ. As demonstrated earlier, other quantities can be derived from these base quantities, namely real power, P, reactive power, Q, and electro-magnetic torque, T.

In this section, the stable machine, generating under steady state conditions into an infinite busbar, will have various step changes placed onto it. The ability of the measuring system to cope with transient conditions and hence its suitability to provide control signals, will be determined from these tests.

8.3.2 Step Reduction in the Shaft Torque

The first of the step changes that was performed was a step reduction in the shaft torque. For this test, the SMIB setup shown in Figure: 7.1, was modified as shown in Figure: 8.5. The d.c. machine had two additional elements

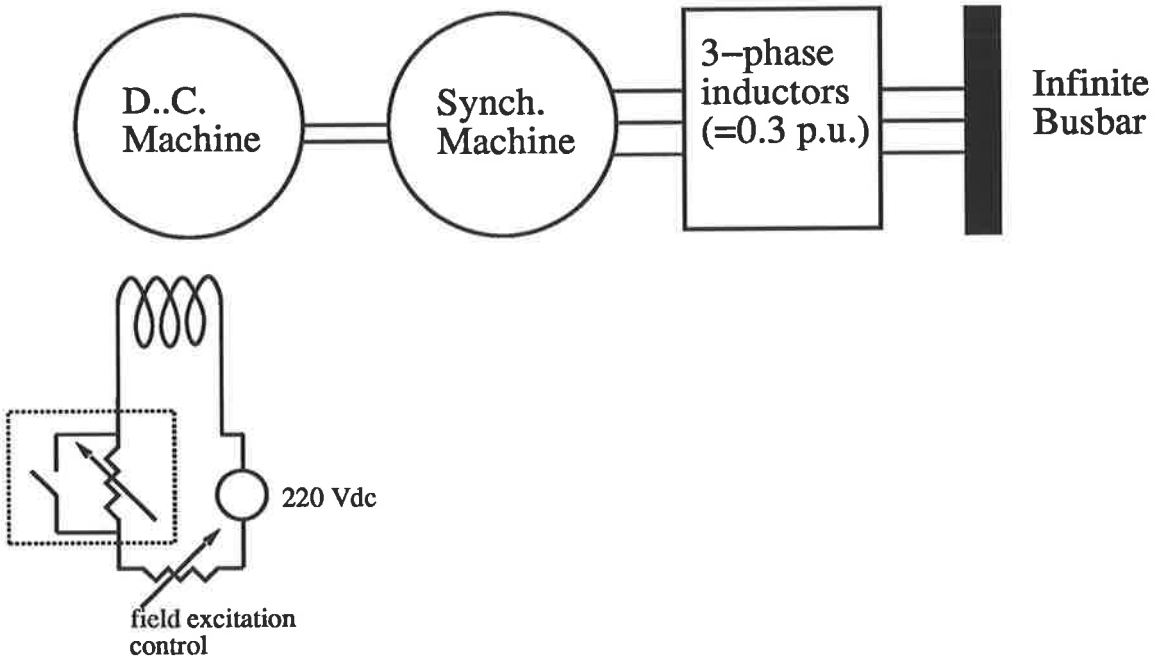

Figure 8.5: Machine set up used to perform a transient torque test

placed in its field excitation circuit, shown boxed in Figure: 8.5. These are the variable resistor and a switch placed parallel to it. When the switch, which is first opened, is closed, there will be a step increase of the field current which will in turn produce a step reduction of the shaft torque.

The steady state machine machine quantities were measured before and after the introduction of the step change, as shown in Table: 8.1. The base tran-

	Before Transient	After Transient
Real Power (P)	2.26 kW	1.28 kW
Reactive Power (Q)	-2.53 kVar	-2.08 kVar
Excitation Field Current (I_{fd})	0.992 Amps	0.920 Amps
Line current (I_{line})	5.0 Amps	3.7 Amps
Terminal Voltage (V_t)	373 $Volts_{line-line}$	377 $Volts_{line-line}$
Infinite Busbar Voltage	409 $Volts_{line-line}$	409 $Volts_{line-line}$

Table 8.1: Steady state condition before and after the transient torque

sient machine quantities synthesized by the monitoring system are shown in Figure: 8.6, with the derived quantities shown in Figure: 8.7.

8.3.3 Step Reduction in the External Line Inductance

The second test that was performed was a step reduction in the external line impedance. This test is analagous to switching in a transmission line. This test was performed with the machine set connected as shown in Figure: 8.8. When the 3-phase switch, that is first opened, is closed, the 0.3 pu impedance is removed from the circuit thus producing a step reduction in the line impedance.

As with the transient torque test, the steady state and transient quantities of the machine were measure and the results are shown Table: 8.2, Figure: 8.9 and Figure: 8.10.

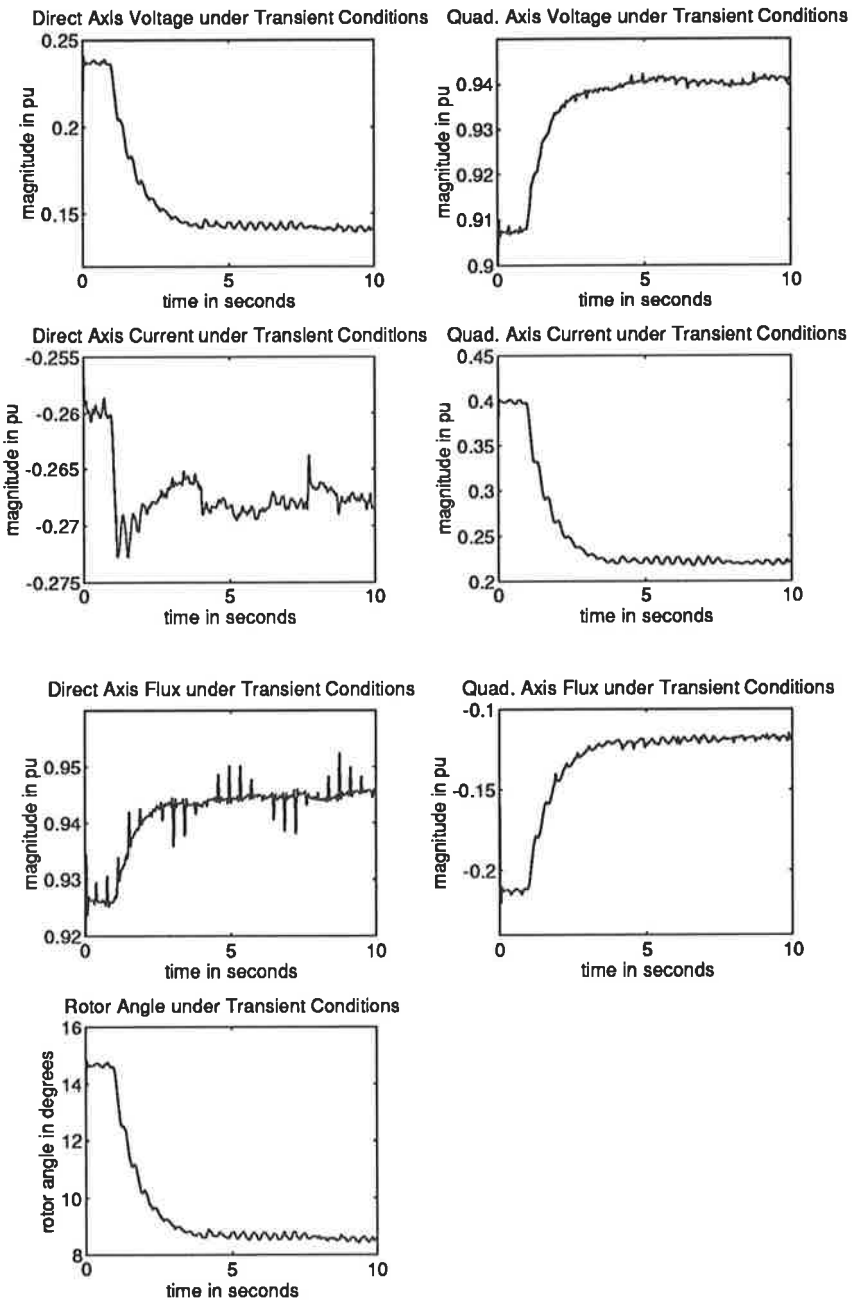

Figure 8.6: Step Reduction in the Shaft Torque - Base monitoring system quantities

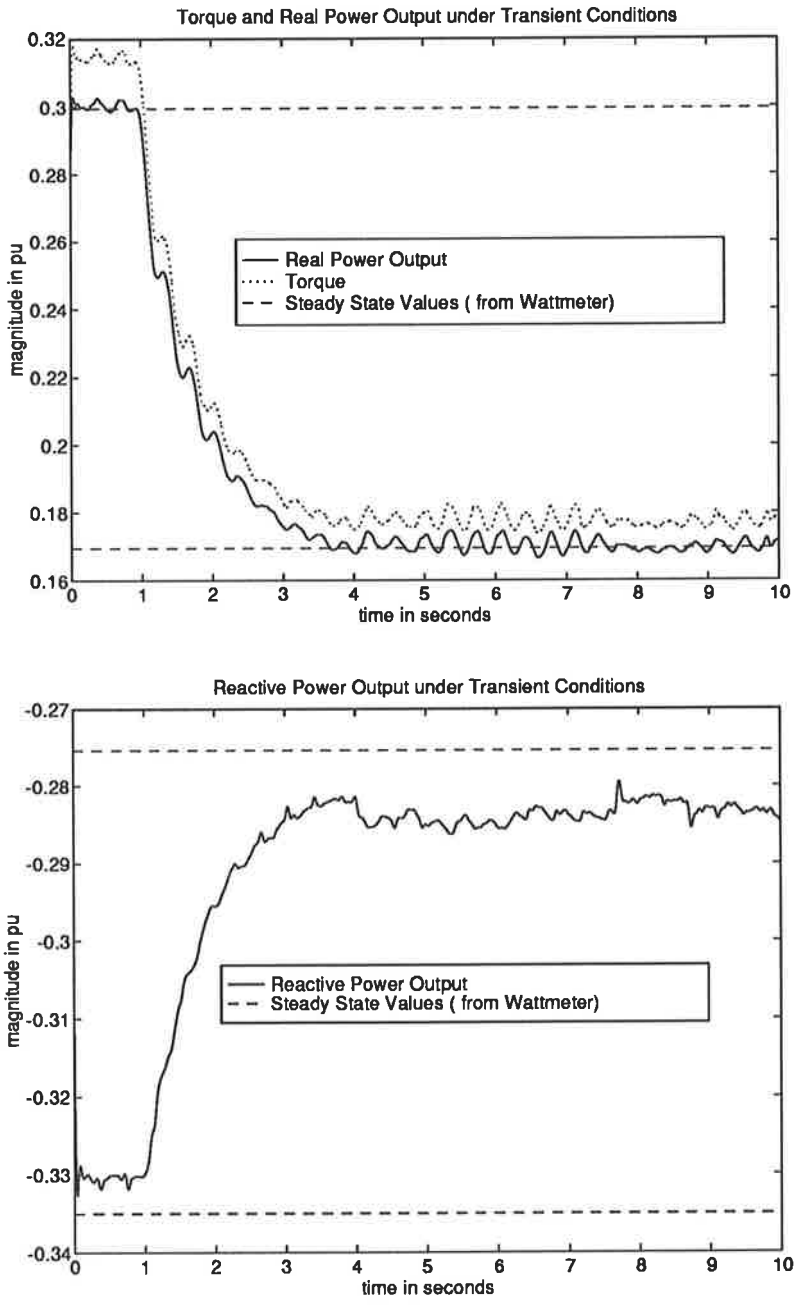

Figure 8.7: Step Reduction in the Shaft Torque - Derived quantities

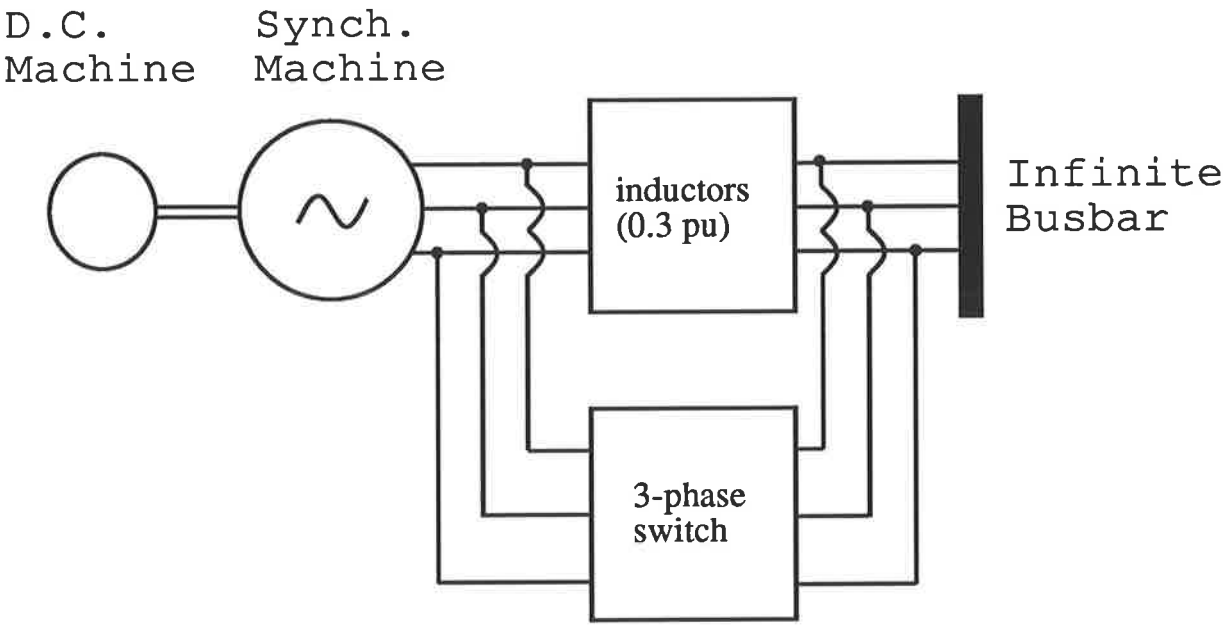

Figure 8.8: Machine set up used to perform a simulations of line switching

	Before Transient	After Transient
Real Power (P)	2 kW	2 kW
Reactive Power (Q)	2.21 kVar	3.18 kVar
Excitation Field Current (I_{fd})	0.977 Amps	0.973 Amps
Line current (I_{line})	4.3 Amps	5.1 Amps
Terminal Voltage (V_t)	377 $Volts_{line-line}$	411 $Volts_{line-line}$
Infinite Busbar Voltage	410 $Volts_{line-line}$	412 $Volts_{line-line}$

Table 8.2: Steady state condition before and after the step change of line impedance

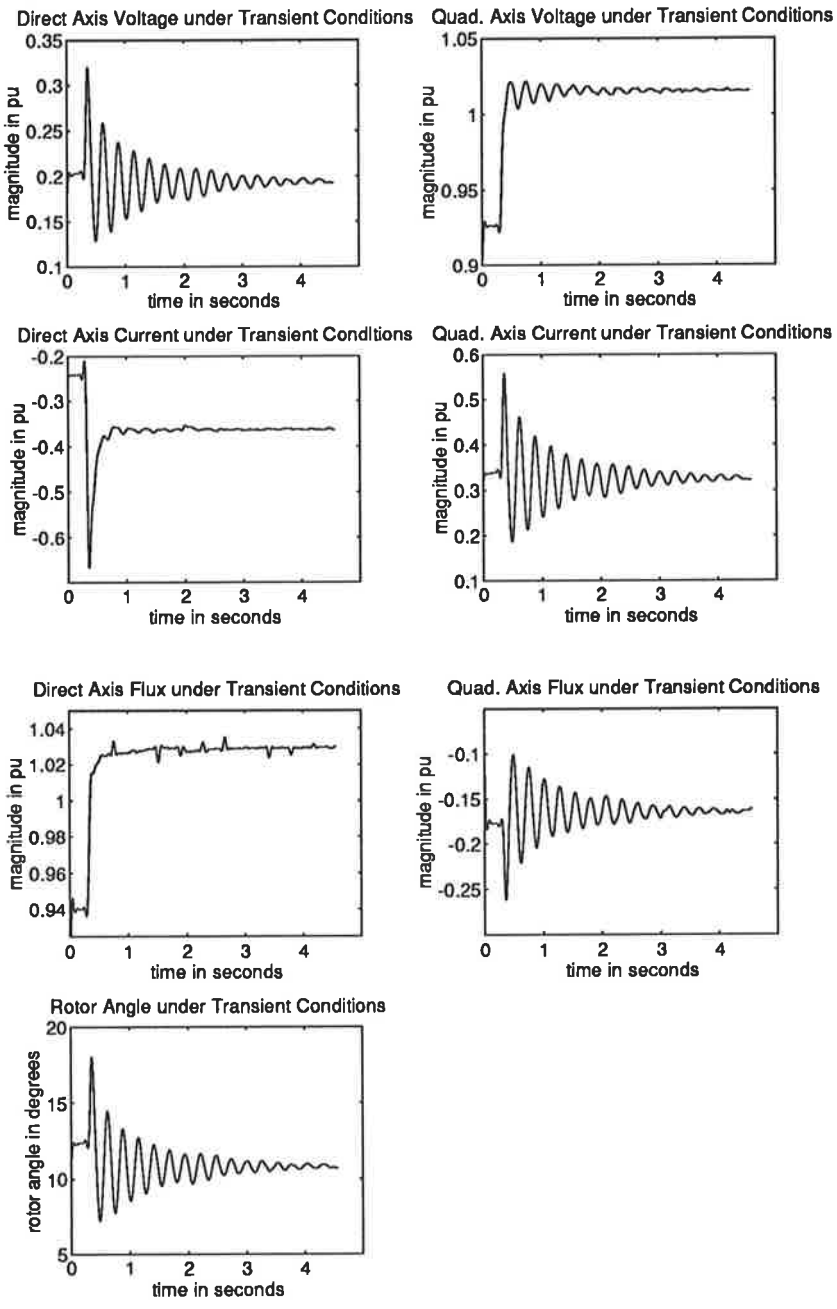

Figure 8.9: Step Reduction in the Line Impedance - Base monitoring system quantities

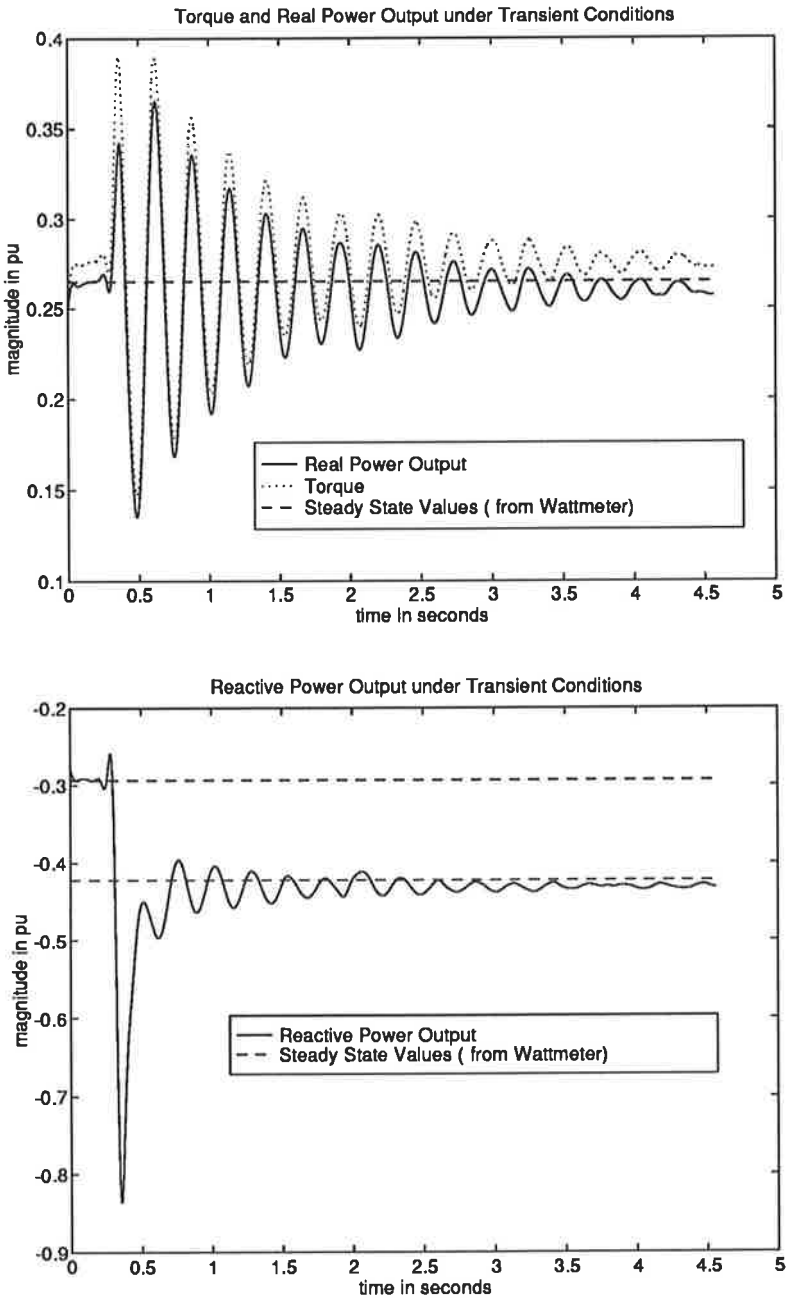

Figure 8.10: Step Reduction in the Line Impedance - Derived quantities

8.3.4 Analysis of Results

The various transient signals appear very good. There is no discontinuity in any of the signals with the signals exhibiting the typical exponentially decaying sinusoidal function to the step change. Hence depending on the control strategy being developed, any of the basic quantities measured by the measuring station, used on their own or combined to synthesis other signals like real power or electro-magnetic torque, would be suitable control signals.

Chapter 9

FREQUENCY RESPONSE TEST

9.1 Introduction

The last of the tests performed was a frequency response test. In this test, the frequency response of the direct axis flux, ψ_d, perturbed about some steady state operating point will be determined with respect to the synchronous machine's field excitation voltage, V_f. A gain/phase analyzer was used to perform this test. The analyzer has an oscillator that can be programmed to discretely sweep through a wide range of frequencies. Using this oscillator as the source of the perturbations, the analyzer can then be used to automatically calculate the frequency response at any 2 nodes in the circuit, ψ_d and V_f in this case, for that entire range of frequencies.

The machine set up used was as shown in Figure: 9.1. The isolating amplifier was used to set the steady state operating condition of the machine. The oscillator which is part of the gain/phase analyzer then produces a perturbation of the field excitation voltage. The tests were performed with the machine at various operating conditions, open circuit and on load.

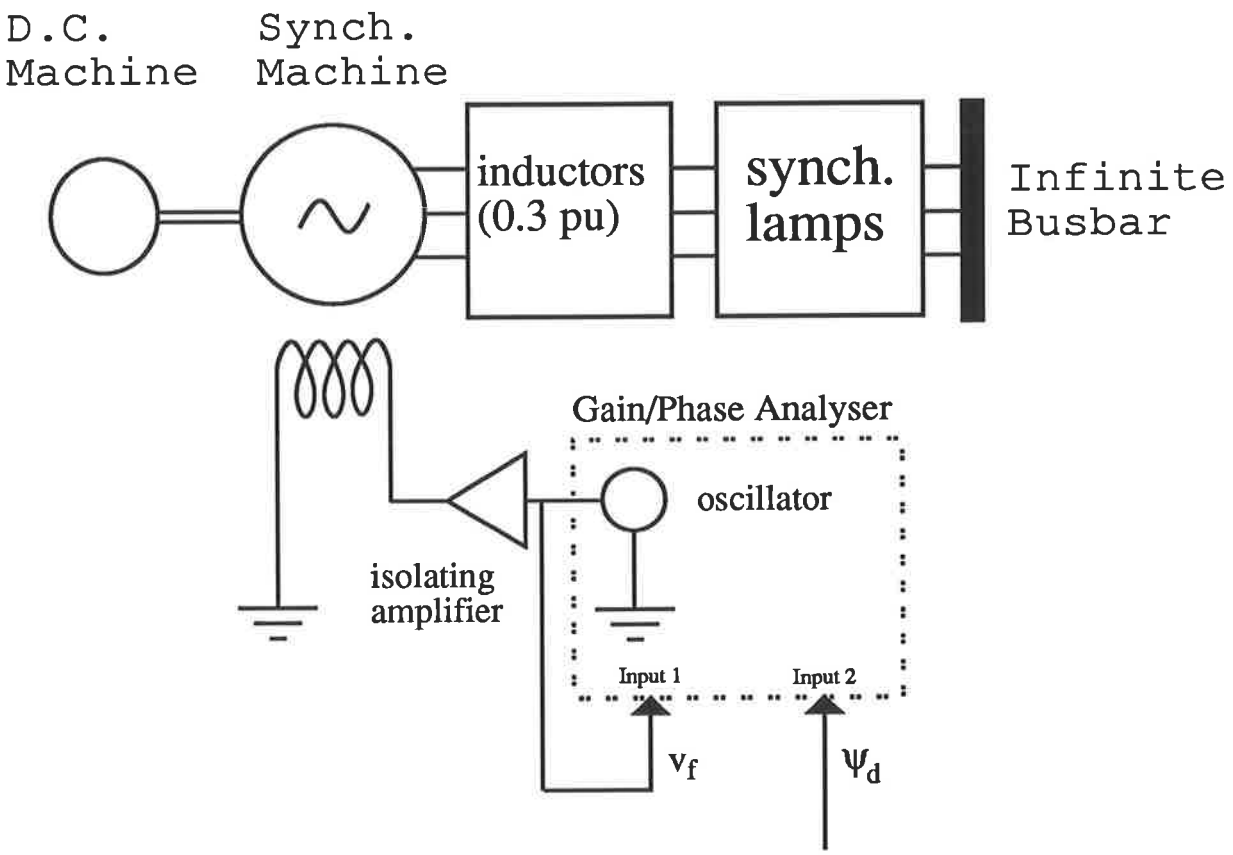

Figure 9.1: Machine set-up for the frequency response test

9.2 Frequency Response Test on Open Circuit

With the machine on open circuit, the frequency of the machine response was determined with the machine operating at 4 operating conditions, as detailed in Table: 9.1. A 1 Volt variable frequency perturbation was super-imposed

V_f	ψ_d
5 Volts	0.345 pu
10 Volts	0.630 pu
20 Volts	1.027 pu
30 Volts	1.223 pu

Table 9.1: Operating Condition for the open circuit frequency response test

onto these steady state levels. The results obtained are shown in Figure: 9.2.

The results show an abnormality centered at 25Hz. This effect is due to the rich frequency composition of the air-gap flux signal. The frequency components of concern here are not the 50Hz harmonics but the 75Hz and 125Hz components. These frequencies, when they are passed trough Park's transform, get down shifted to a 25Hz component.

This abnormality at 25Hz can be removed by filtering these frequency components. However, filtering these components is not as easy as it first appears. The major problem is the close proximity of the 75Hz component to the fundamental 50Hz frequency of the main signal. The bandwidth of the 3 identical low-pass filters, one for each phase, will have to be large enough so as not to effect the fundamental component, yet low enough sufficiently filter out the 75Hz component. Because of this bandwidth restriction, the low pass filters will probably have to be fairly high order filters. This will greatly increase the complexity of the transducer and in addition it may result in a sluggish transient response.

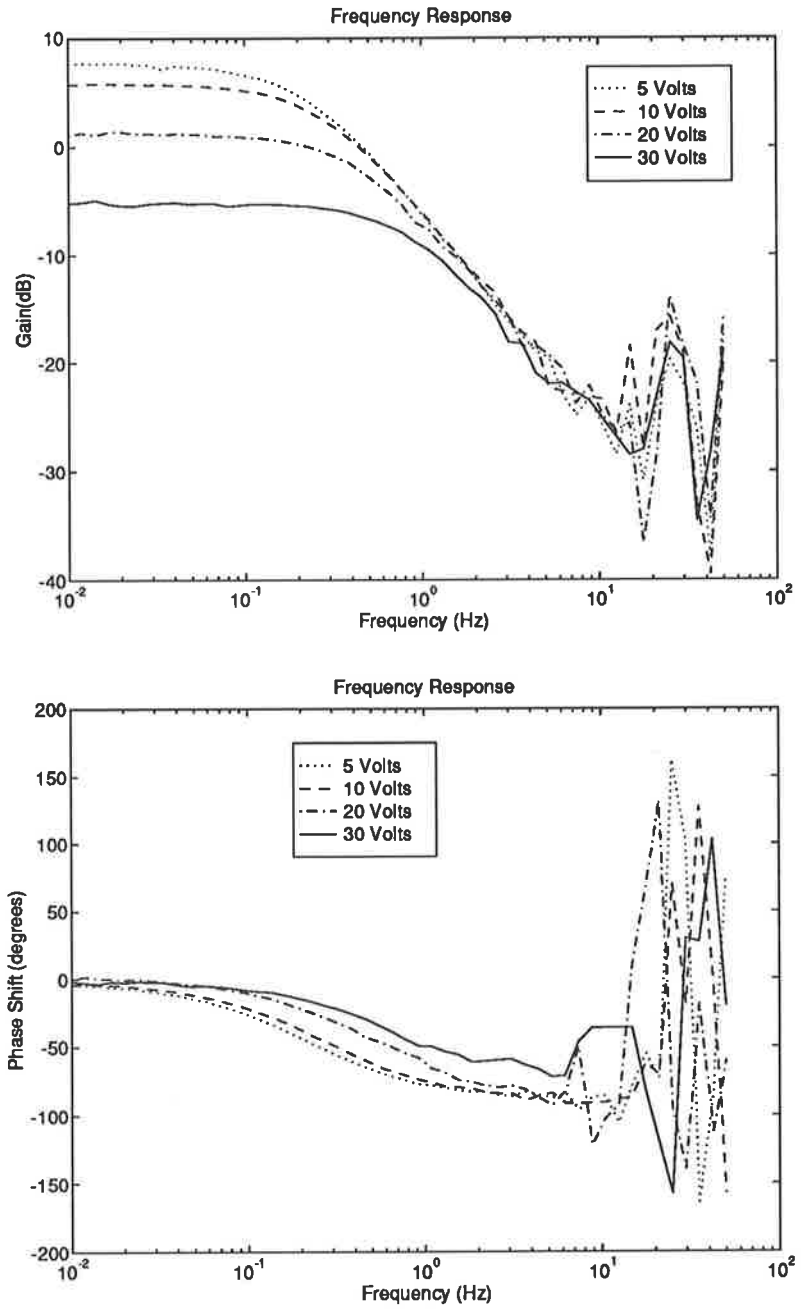

Figure 9.2: Frequency response of the machine on open circuit

Even with the above abnormality, there is plenty of information that can still be drawn from the results. Firstly, the effect of saturation is clearly evident from the gain curve. As the base value of the field excitation voltage is increased, the rotor core gets more saturated leading to a lower gain at low frequencies.

The phase curves start at 0^o and appear to level out at 90^o. This suggests that the frequency response represents a first order transfer function. A first order transfer function was fitted to the data of the $V_f = 5$ Volts case, as shown in Figure: 9.3, giving a pole corner frequency, fc, of 0.2027Hz (1.274 rad/sec). The first order transfer function of the system for this case is

$$\frac{\psi_d}{V_f}(s) = \frac{A}{s + 1.274} \tag{9.1}$$

Where

$$\frac{A}{1.274} = \text{the static gain of the system} \tag{9.2}$$

The value for the corner frequency can be equated to a machine parameter. Equation: 4.19 of [1], shown below as Equation: 9.3, shows the theoretical relationship between the direct axis flux linkage and the field excitation voltage.

$$\psi_d = \frac{X_d(\rho)}{\omega_o} * i_d + \frac{G(\rho)}{\omega_o} * u_f \tag{9.3}$$

The experimental results obtained here were with the machine on open circuit(i_d=0) and at synchronous speed(ω_o=1).

Therefore Equation: 9.3 can be re-written as

$$\frac{\psi_d}{u_f} = G(\rho) \tag{9.4}$$

Substituting the value of $G(\rho)$ obtained from Equation: 4.19 of [1].

$$\frac{\psi_d}{u_f} = \frac{1 + T_{kd}\rho}{(1 + T'_{do}\rho)(1 + T''_{do}\rho)} * \frac{X_{md}}{R_f} \tag{9.5}$$

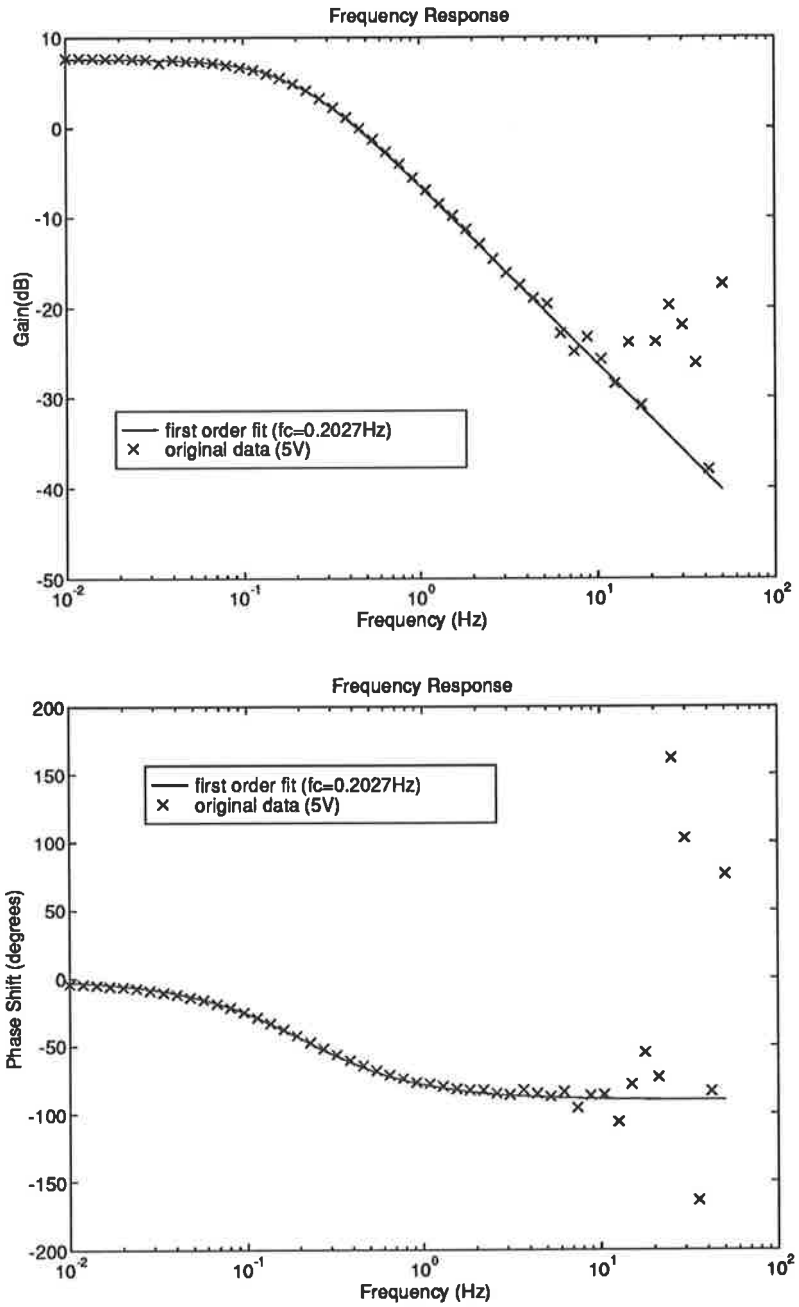

Figure 9.3: Parameter identification by curve fitting the frequency response curve

Where

$$\begin{aligned}
\rho &\equiv s \\
u_f &\equiv V_f \\
R_f &= \text{field resistance} \\
X_{md} &= \text{direct axis mutual reactance} \\
T_{kd} &= \text{direct axis damper leakage time constant} \\
T'_{do} &= \text{direct axis transient open circuit time constant} \\
T''_{do} &= \text{direct axis subtransient open circuit time constant}
\end{aligned}$$

Neglecting the higher order terms, Equation: 9.5 can be written as

$$\frac{\psi_d}{u_f} = \frac{1}{1+T'_{do}\rho} * \frac{X_{md}}{R_f} \tag{9.6}$$

$$= \frac{\frac{X_{md}}{R_f * T'_{do}}}{s+\frac{1}{T'_{do}}} \tag{9.7}$$

Equating the theoretical transfer function shown in Equation: 9.7 with the experimentally version shown in Equation: 9.1 yields

$$\frac{1}{T'_{do}} = 1.274 \tag{9.8}$$

$$T'_{do} = 0.7849s \tag{9.9}$$

For the other curves, simple first order transfer functions cannot be assigned due to the saturation. However, the pole corner frequency can still be determined from the phase curves. The frequency that corresponds to a shift of -45^o on the each phase curve is the pole corner frequency. The results are tabulated below in Table: 9.2. The pole corner frequency increases as the excitation voltage is increased. Hence, it can be concluded that the effect of increasing the excitation field voltage is firstly to increase the level and saturation in the rotor and secondly is to increase the pole corner frequency of the transfer function.

V_f	pole corner frequency
5 Volts	0.2027 Hz
10 Volts	0.2618 Hz
20 Volts	0.5107 Hz
30 Volts	0.7372 Hz

Table 9.2: First order poles from the frequency response test on an open circuit machine

9.3 Frequency Response Test on Load

For completeness, the frequency response was also measured with the machine on load. This was done for 2 different loading conditions, a leading and a lagging power factor case, as detailed in Table: 9.3. The results obtained

	Operating Condition 1 (leading pf)	Operating Condition 2 (lagging pf)
Real Power (P)	2.64 kW	2.66 kW
Reactive Power (Q)	-0.69 kVar	0.73 kVar
Excitation Field Current (I_{fd})	1.66 Amps	2.20 Amps
Excitation Field Voltage (V_f)	19.62 Volts	28.18 Volts
Line current (I_{line})	3.7 Amps	3.55 Amps
Terminal Voltage (V_t)	413 $Volts_{line-line}$	435 $Volts_{line-line}$
Infinite Busbar Voltage	417 $Volts_{line-line}$	417 $Volts_{line-line}$

Table 9.3: Machine operating conditions used for the frequency response test on load

are shown in Figure: 9.4. The frequency response curves are similar to the open circuit case with the abnormality at 25Hz still evident. For the lag case the gain at low values of frequency is lower than for the lead case. This is because the rotor core in the lag case is more saturated due to the larger field excitation voltage. As before, the frequency response curves here also seem to to represent a first order transfer function, with pole corner frequencies of

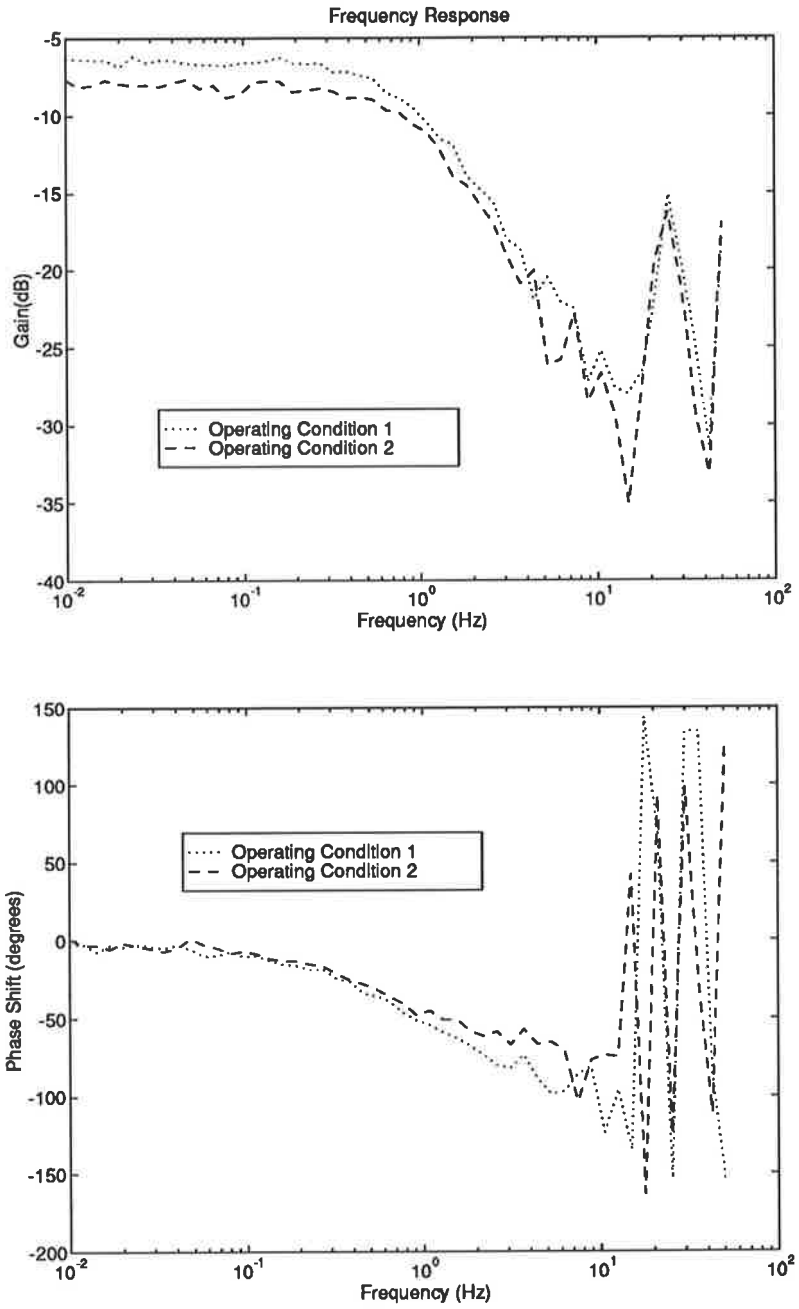

Figure 9.4: Frequency response of the machine on load

0.744 Hz for the first case and 0.8875 Hz for the second.

Chapter 10

CONCLUSION AND FURTHER RESEARCH

10.1 Conclusion

The work described in this thesis was the design and construction of a prototype monitoring system for synchronous generators. The monitoring system incorporated easy to measure quantities like line current and terminal voltage with 3 new features; the air-gap flux transducer, the Park's transform unit and the rotor angle transducer.

The design of the air-gap flux transducer was based on a design proposed for the vector control of induction motors [15]. This design was adapted for used with synchronous machines, with very good results. The air-gap flux signals were combined with the line current signals, to provide a measurement of the instantaneous electro-mechanical torque of the synchronous machine.

In the majority of work done on power systems, the machine quantities are expressed in Park's(d,q) frame of reference. A Park's transform unit was successfully incorporated into the measurement system. The 3-phase terminal voltage, line current and air-gap flux signals were able to be transformed, in

real time and at a rate of 8 times in a 50Hz cycle, into their equivalent direct and quadrature axis components.

The rotor angle is an important internal parameter of the synchronous generator and is a prime indicator of stability of the generator or a group of generators. The design for this transducer, was initially based on [2]. This design determines rotor angle by measuring the phase shift between a fixed point on the rotor shaft and a fixed point on a stator phase, the positive zero crossing, hence it has a sampling rate of 50Hz. However it was found that the unpredictable voltage unbalance that exists in the real world makes this design unsuitable. In a practical synchronous machine at steady state, the rotor angle is not a constant value but has a 100Hz ripple superimposed on it that is caused by the unbalance voltage, causing the positive zero crossing of the phase to be shifted. In light of this two possible solution to this problem was discussed. The first solution was an elegant design that used a phase-locked-loop to average out or balance the stator voltage zero crossings prior to feeding then into the rotor angle transducer. This method was however rejected as it was unable to measure the transient behaviour of the rotor angle. The second solution was a brute force method. A micro-controller was used to perform the basic design 6 times a cycle, on both the positive and negative zero crossing of each phase, or at a rate of 300Hz. This design measures the actual rotor angle; the desired mean of the signal together with the 100Hz ripple, which was then filtered out of the signal. This final implementation was tested and produced very good results.

The monitoring system was then subjected to a series of tests to determine its usefulness and to identify possible applications for the system. The first set of tests performed were with the synchronous machine operating under steady state conditions, principally in the single machine infinite busbar, SMIB, configuration. At various operating or load conditions, the quantities provided by the monitoring system were measured together with traditional measurements made with wattmeters and multimeters. These based quantities were used to calculate 3 other quantities, the real and reactive power and the electro-mechanical torque of the synchronous machine. The calculated measurements were compared with those generated conventionally with the wattmeters.

When the comparisons were made with the real and reactive powers, they was good agreement between the two sets of results. In conventional theory, the torque of the machine if often equated with the real power output of the machine. This was shown to be incorrect. The effect of the stator resistance, which in most cases can be assumed to be insignificant, was found be very significant. In reality, the torque of the machine is higher than the real power output of the machine due to the power loss in the stator resistance.

It was also demonstrated that the measurements could be used for parameter identification studies. The complete self inductance of the machine in both the direct, L_d, and quadrature, L_q, axes were calculated at the various load conditions. The effect of the saturation in the direct axis inductance at high direct axis flux levels was observed. The expected absence of saturation in the quadrature was also observed.

The last steady test that was performed demonstrates the the versatility and the power of the monitoring station. By changing the code that represents 0^o in the Park's transform of the 3-phase air-gap flux signal, it was possible to obtain a quantitative description of the spatial distribution of the flux in the rotor. The spatial flux distribution was determined for these operating conditions; with the machine on open circuit and with the rotor unsaturated and saturated and on load. The expected shift of the spatial distribution of the machine when on load towards the quadrature axis when compared to the open circuit case was observed. An unexpected result was obtained when the 2 open circuit spatial distributions were compared. The was a shift of the distribution of the saturated case when compared to the unsaturated case, probably caused by a non-uniform saturation across the pole face.

The transient capabilities of the monitoring system was also investigated. Two type of tests were performed, the first being a test to determine the dynamic parameters of the synchronous generator and the second being a test to verify that the transient signals are suitable for use as control signals as part of a feedback control loop. The dynamic parameters of the synchronous machine were obtained by the sudden 3-phase short circuit test as described in [13]. The monitoring system performed flawlessly and the machine's dynamic parameters were easily derived from the experimental data.

The monitoring system is to be eventually used as a part of an integrated system for synchronous generators. One of its tasks is the provision of suitable signals to be used as part of a control strategy for the generator. This application of the synchronous generator was investigated by subjecting 2 step changes to the operating condition of the laboratory test generator, a step change in shaft torque and a step change in external line inductance. In both tests, the monitoring system was able to synthesize the machine quantities to describe the transient accurately and without any noticeable discontinuity.

The last of the tests performed was a frequency response test. The frequency response of the direct axis flux, ψ_d, was determined with respect to the field excitation voltage at various operating conditions, with the synchronous machine on open circuit and with the rotor at various stages of saturation and with the machine operating under 2 loading conditions, with a leading and lagging power factor. The effect the rotor saturation had on the frequency response in the open circuit case was very obvious from the data. The frequency response experimental data suggested that a first order transfer function can be used to describe these frequency response. The frequency response for the load case also exhibited similar behaviour.

10.2 Further Research

The monitoring system has been tested and was found to be very effective in many applications. In terms of further work, other than some minor modifications to make the various designs more elegant, no more design work is required for the monitoring system. Work should however be done to use the measuring system, utilizing many of the unique features, to research synchronous machine behaviour and control. Two of these applications have been identified and are detailed here.

The first application is for parameter identification. A parameter identification test was performed in chapter 7 on the effect rotor saturation had on the direct and quadrature self inductance. In that test a qualitative description of the saturation effect was given. It would be useful to perform this test again but with more data points and hence it will be possible to obtain a

quantitative and hence more thorough description of these inductance values.

In the thesis, mention was made to the usefulness of using internal machine parameters, like the electro-mechanical torque or rotor angle, as part of an integral control strategy for synchronous generator. Hence it would very useful to research and experimentally verify the effectiveness of such a control strategy when compare to what is presently available.

Appendix A

AIR-GAP FLUX TRANSDUCER

A.1 Circuit Diagram

The air-gap flux transducer is implemented in hardware by utilizing standard analogue design techniques. The full circuit diagram is shown in Figure: A.1. There is a point to note in Figure: A.1. It is the $6.8M\Omega$ resistors, R14, R18 and R22. These resistors are used to compensate the integrator against d.c. offsets in the input signals, that will saturate it. These resistors result in the integrators acting as large gain amplifiers at low frequencies. The small d.c bias hence gets amplified to a large d.c. output bias. The $100K\Omega$ pots, POT10, POT11 and POT12, are used to prevent the integrators from saturating by removing the bulk of this output bias. The simple low-pass filters that follow the integrators, removes what bias remains.

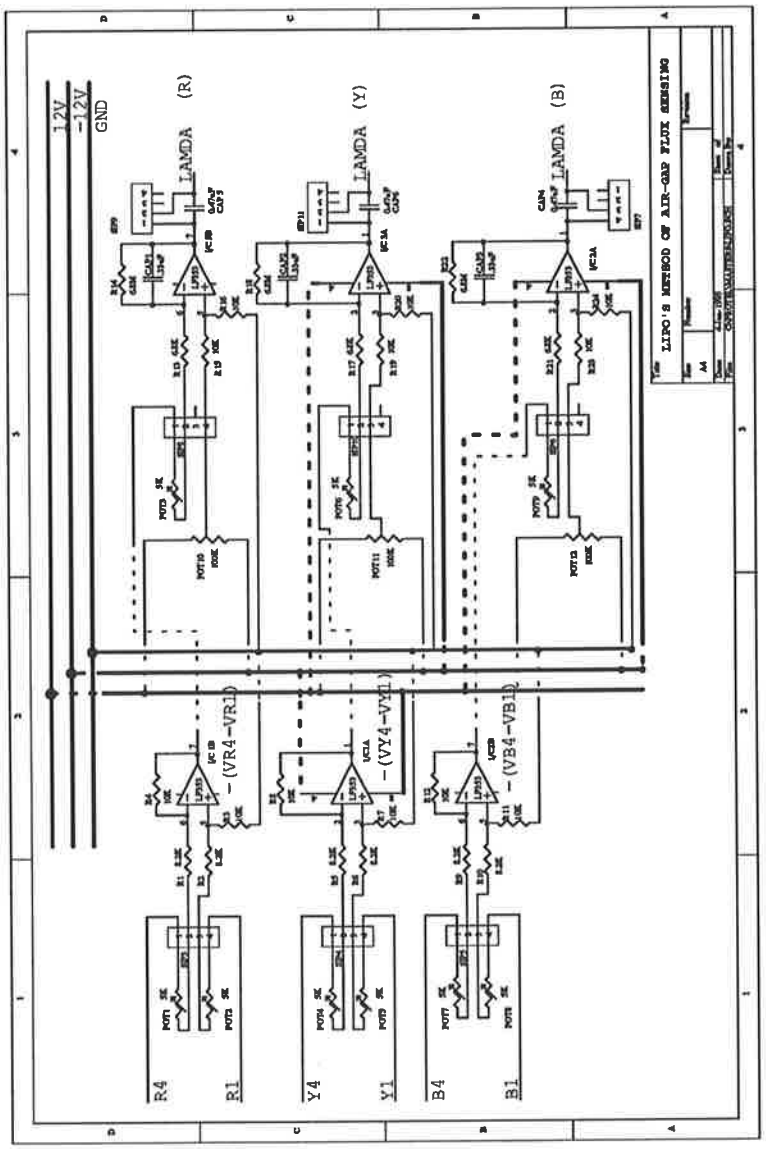

Figure A.1: Full Circuit Diagram of the Air-Gap Flux Transducer

A.2 Calibrating the Air-Gap Flux Transducer

The calibration process that was followed for the air-gap flux transducer is detailed below.

1. Make R1 the reference voltage.
2. Put in a 50Hz, $2V_{rms}$ voltage from a signal generator for R1.
3. Ground I/P R4.
4. Adjust the POT2 and POT3 until the output of the RED phase subtractor and integrator is a 50Hz, $2V_{rms}$ signal respectively. This sets the gain of that subtractor and integrator to have a gain of 1 @50Hz.
5. Input the same signal for both R1 and R4.
6. Adjust the POT1 until the RED phase subtractor is zero.
7. The RED phase is now calibrated.
8. Ground R4, Y4 and B4.
9. Input the same 50Hz, $2V_{rms}$ voltage for R1, Y1 and B1.
10. Adjust the POT5 and POT6, for the YELLOW phase, and POT8 and POT9, for the BLUE phase, until the O/P of the other 2 subtractors and integrators match those of the RED phase.
11. Input the same signal for Y1, Y4, B1 and B4.
12. Adjust the POT4, for the YELLOW phase, and POT 7, for the BLUE phase, until the O/P at the respective subtractors is zero.
13. View the O/P of all 3 phases just before the d.c coupled capacitors, CAP5, CAP6 and CAP4.
14. Adjust the 100K pot, POT10, for the RED phase, POT11, for the YELLOW phase and POT12, for the BLUE phase until the O/P of the respective integrators is $\approx 0V_{rms}$.
15. View the O/P after the d.c. couple capacitor. It should be the air gap flux voltage without any d.c. bias.

Appendix B

PARK'S TRANSFORM UNIT

B.1 Circuit Diagrams

The Park's transform unit is made up of both digital and analogue components. The digital part of the circuit is used to provide the triggering pulses, or control signals, for the rest of the unit. It had to generate the signals required for the sample and hold devices and the analogue multiplexers. A detailed circuit diagram of this part of the unit is shown in Figure: B.1. The reference code, or code that represents 0^{o} electrical, as used in the Park's transformation matrices, is set by the 8-bit dip switch. This reference code is compared with the codes generated by the shaft encoder. The shaft encoder codes are converted from a gray code to a binary code prior to comparison to aid the comparison process. The bit comparators produce a pulse every 45^{o}electrical and 360^{o}electrical from the reference position as set with the dip switches. These pulses are fed into a counter to produce a 3 bit word identifying the position of the shaft in 45^{o}electrical intervals.

Two LM393 based buffers were placed between the bit comparators and the counter. This was done to rectify a practical problem that resulted in the counter counting false triggers.

The sample and hold circuit works in a similar way. The only difference be-

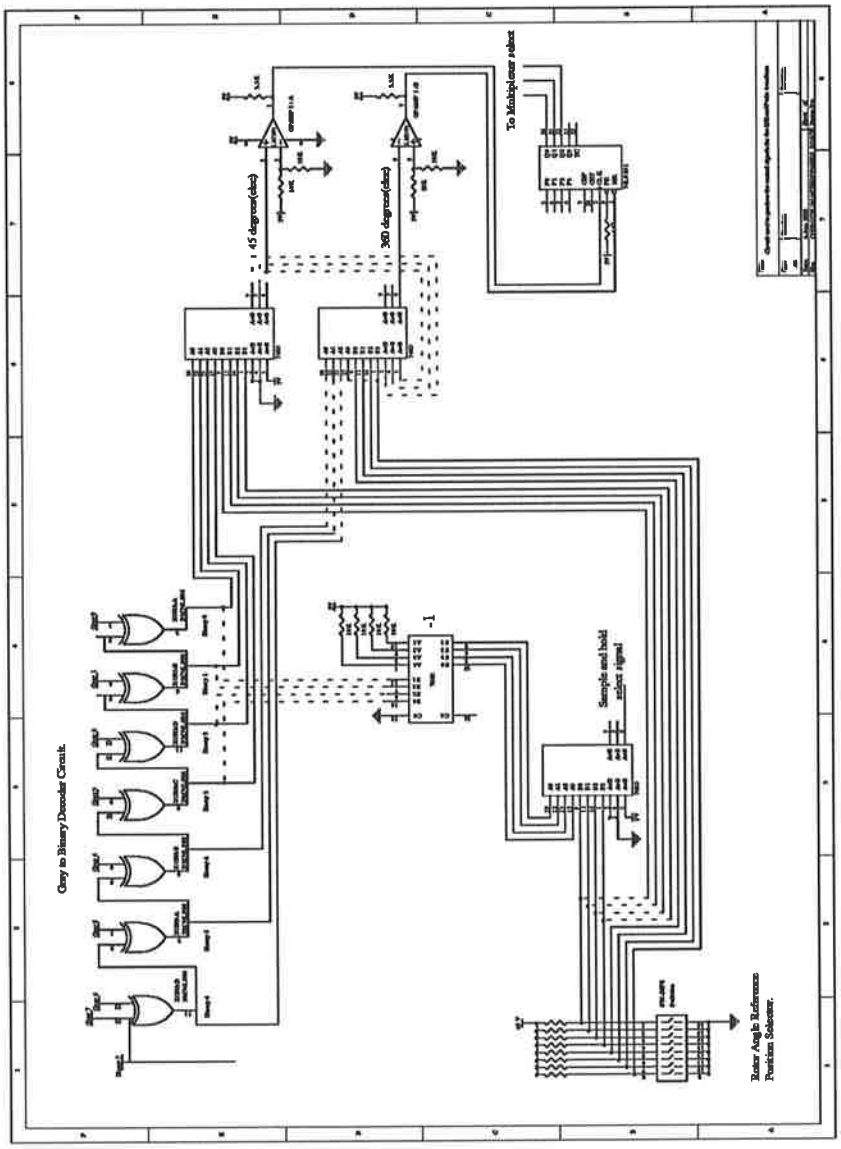

Figure B.1: Digital Part of the Parks Transform Unit

ing that instead of producing the 45°electrical pulses by comparing the shaft encoder codes to the reference code, it compares it to the code one before the reference. Hence the sample and hold circuit will begin its hold phase just as the 45°electrical Parks transform triggering pulse arrives. The comparison was made with a code that is 1 count less rather than the expected one count more because of the fact that the shaft encoder counts backwards.

The analogue part of the circuit was designed using standard analogue design techniques. The first transform of Park's transform, the 3-phase stationary to 2-phase stationary frame of reference, was performed with the circuit shown in Figure: B.2. The second transform, the 2-phase stationary to 2-axis rotating frame of reference, was performed using the circuits shown in Figure: B.3 and Figure: B.4. Figure: B.3 generates the transformation matrix coefficients which are then multiplexed in Figure: B.4 to complete Park's transform.

B.2 Calibrating The Park's Transform Unit

The calibration process that was followed for the Park's transform unit is detailed below.

1. Set the select line for all 3 sample/hold devices to logic "1" to put them in the sample mode.
2. I/P 5.657V @50Hz into the RED I/P. Ground the other 2 inputs.
3. Adjust pot 1 until the O/P md = 1.884V
4. Adjust pot 6 until the O/P md(-1) = 1.884V
   Adjust pot 7 until the O/P md(-0.707) = 1.332V
   Adjust pot 8 until the O/P md(0.707) = 1.332V
5. Ground all mux address lines
   Adjust pot 12 until the O/P d = 3.767V
6. Ground mux address lines A and C and put address line B to logic "1"
   Adjust pot 14 until the O/P q = 3.767V

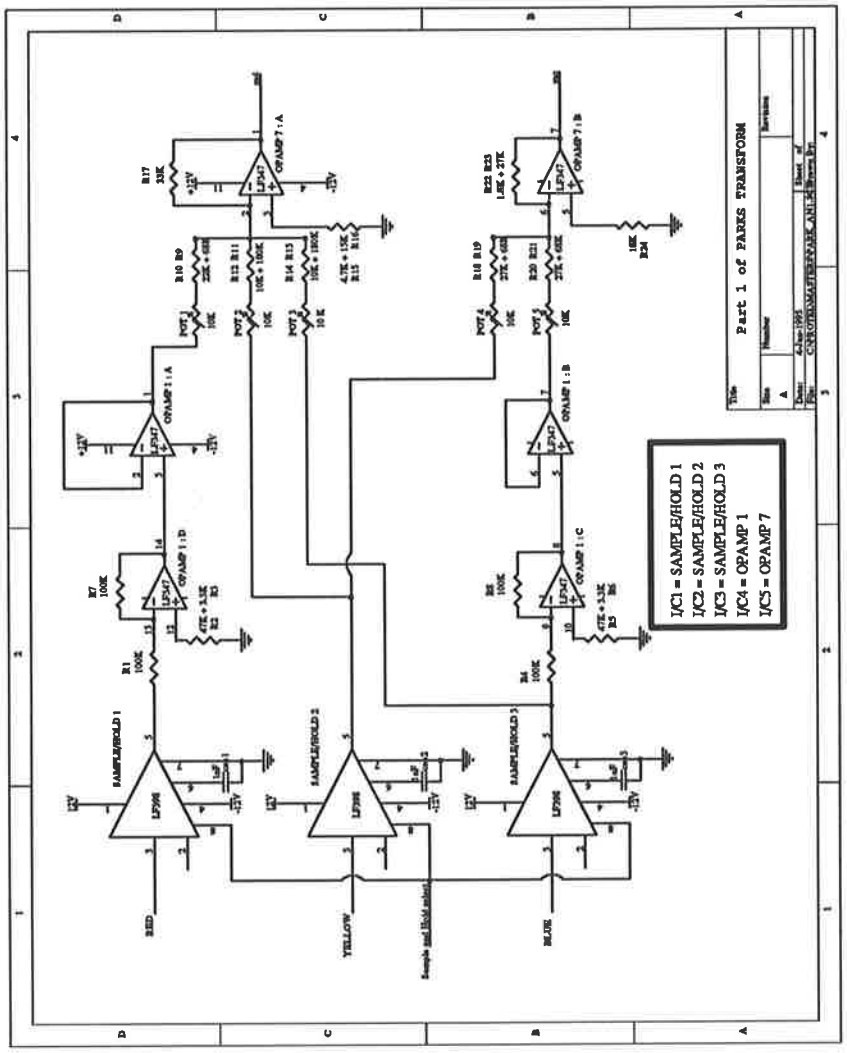

Figure B.2: Analogue Part (Pt: 1) of the Parks Transform Unit

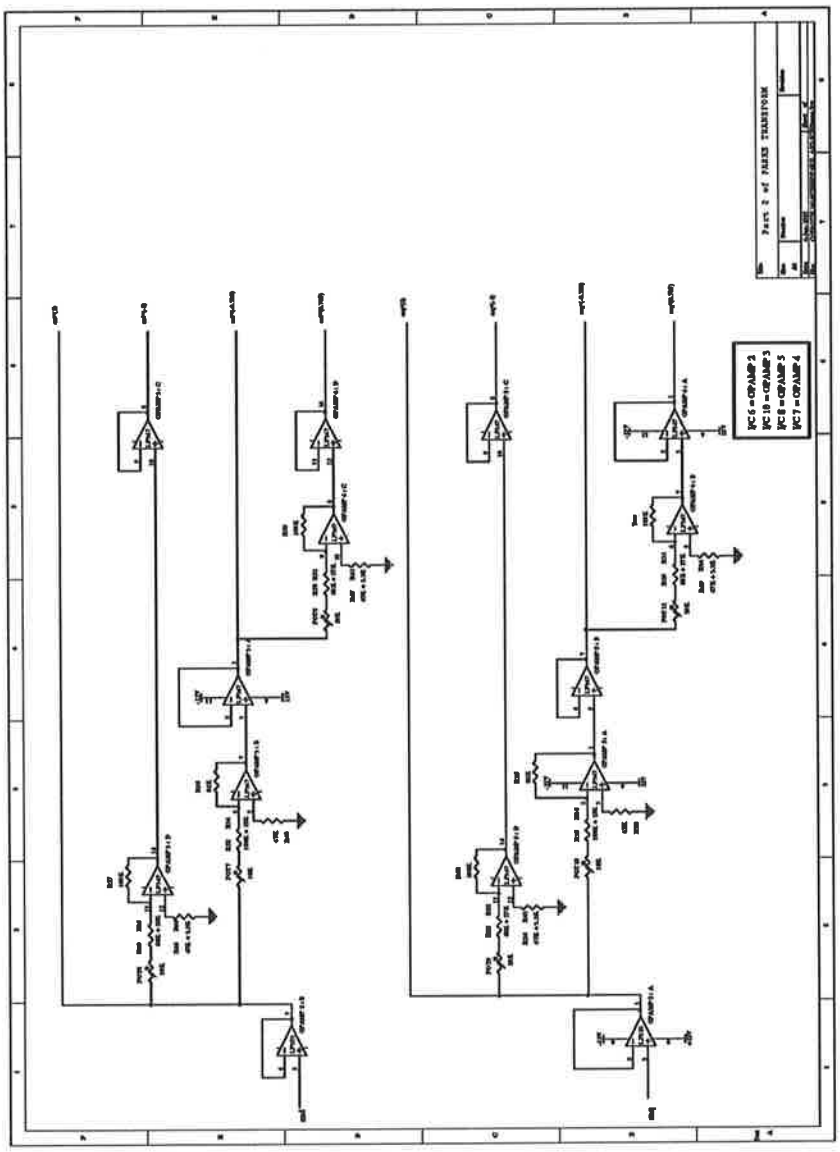

Figure B.3: Analogue Part (Pt: 2) of the Parks Transform Unit

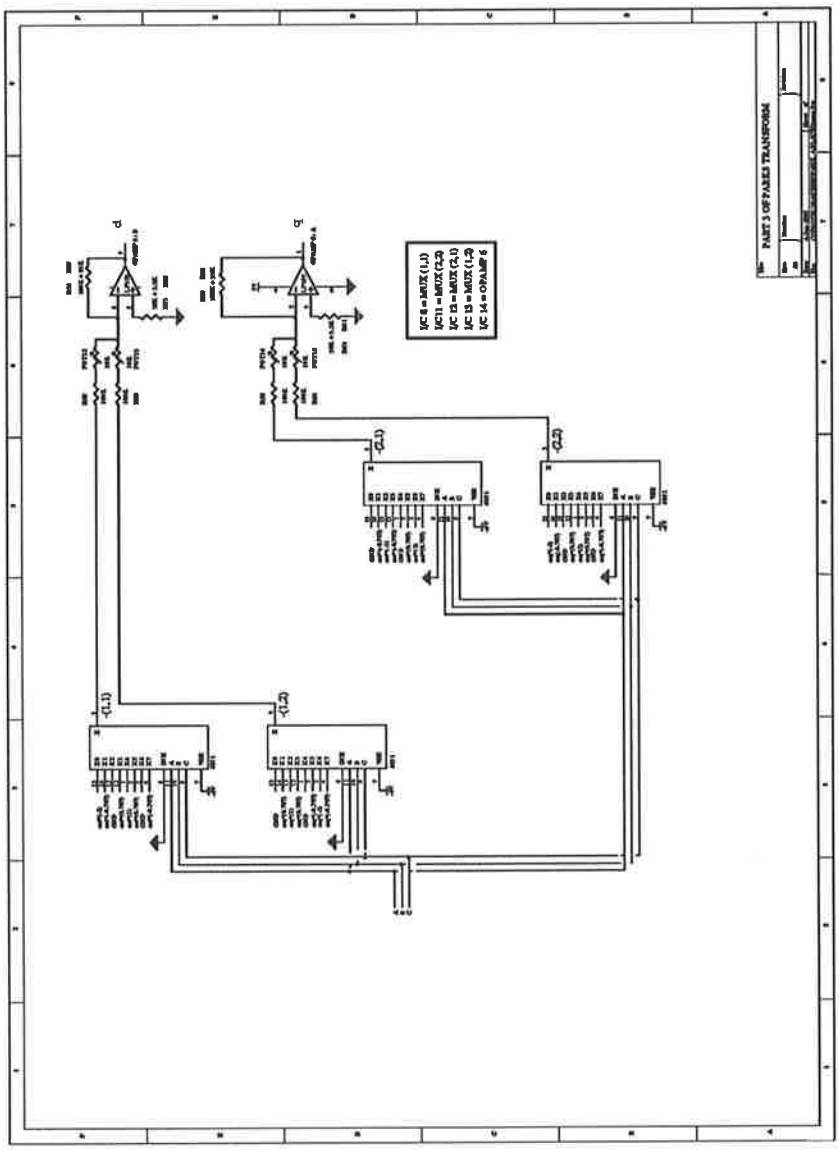

Figure B.4: Analogue Part (Pt: 3) of the Parks Transform Unit

7. I/P 5.657V @50Hz into the YELLOW I/P. Ground the other 2 inputs.

8. Adjust pot 2 until the O/P md = 0.942V
   Adjust pot 4 until the O/P mq = 1.633V

9. Adjust pot 9 until the O/P mq(-1) = 1.633V
   Adjust pot 10 until the O/P mq(-0.707) = 1.155V
   Adjust pot 11 until the O/P mq(0.707) = 1.155V

10. Ground all mux address lines
    Adjust pot 15 until the O/P q = 3.266V

11. Ground mux address lines A and C and put address line B to logic "1"
    Adjust pot 13 until the O/P d = 3.266V

12. I/P 5.657V @50Hz into all I/Ps
    Adjust pot 3 until the O/P md = 0V
    Adjust pot 5 until the O/P mq = 0V

Appendix C

ROTOR ANGLE TRANSDUCER

C.1 Circuit Diagram

The full circuit diagram of the rotor angle transducer is shown in Figure: C.1.

C.2 Source Code

The program for the micro-controller was written in assembly language. A full listing of the code is included below. The assembly code for the 68HC11 microcontroller is fairly straight forward. However, there 2 aspects that need clarification.

1. The free running counter in the microcontroller is a 16 bit counter. The digital count representing the phase shift is made by subtracting the value of the counter, when the desired edge on the zero crossing detector is detected, by the value of the counter determined by the datum pulse from the shaft encoder. If the counter does not count

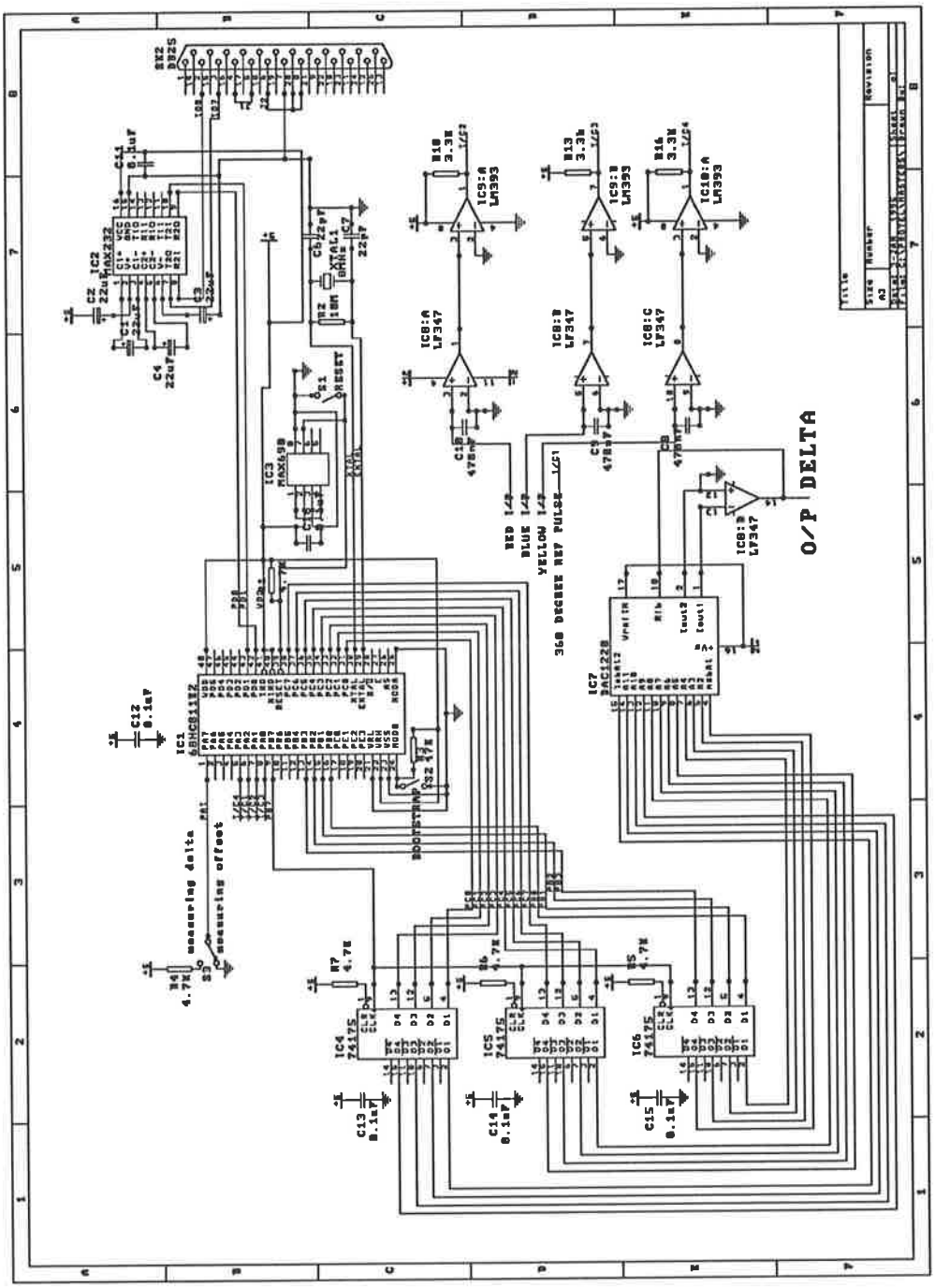

Figure C.1: Full Circuit Diagram of the Rotor Angle Transducer

more than 2^{16} between these pulses, the subtracting process is a simple 16 bit subtraction with no need to worry about overflows or carries. Because of this the frequency of the free running counter is reduced, in software, by a factor of 16 from 8MHz to 500kHz.

2. There is a interrupt mask in the 68HC11 called HPRIO. This mask sets the highest priority interrupt. This mask must be set to an interrupt that is being enable. If this mask is set to an interrupt that is not enabled, the microcontroller will crash on arrival of any of the enabled interrupts.

```
*************************************************************
*
* Source code used to impliment the rotor angle
* transducer with the 68HC11 micro-controller
*
*************************************************************

*EQUATES
PORTA     EQU    $1000   * I/P-O/P PORTA
PORTC     EQU    $1003   * I/P-O/P PORTC
PORTB     EQU    $1004   * O/P PORTB
PORTE     EQU    $100A   * I/P PORTE
DDRC      EQU    $1007   * DATA DIRECTION PORTC
TCNT      EQU    $100E   * TIMER COUNTER 16 BIT NUMBER
TIC1      EQU    $1010   * TIMER INPUT CAPTURE 1 16 BIT
TIC2      EQU    $1012   * TIMER INPUT CAPTURE 2 16 BIT
TIC3      EQU    $1014   * TIMER INPUT CAPTURE 3 16 BIT
TIC4      EQU    $101E   * TIMER INPUT CAPTURE 4 16 BIT
TCTL2     EQU    $1021   * TIMER CONTROL REGISTER 2
TMSK1     EQU    $1022   * TIMER INTERRUPT MASK REGISTER 1
TFLG1     EQU    $1023   * TIMER INTERRUPT FLAG REGISTER 1
TMSK2     EQU    $1024   * TIMER INTERRUPT MASK REGISTER 2
PACTL     EQU    $1026   * PULSE ACCUMULATOR ADDRESS REGISTER
HPRIO     EQU    $103C   * HIGHEST PRIORITY INTERRUPT

RAMBS     EQU    $0000   * START OF RAM
```

```
PAREA     EQU    $F800   * START OF PROGRAM AREA

*RAM
          ORG    RAMBS
PROD1     RMB    1       * XMUL PRODUCT
PROD2     RMB    1       * XMUL PRODUCT
PROD3     RMB    1       * XMUL PRODUCT
PROD4     RMB    1       * XMUL PRODUCT
FACTA     RMB    2       * XMUL MULTIPLICATION FACTOR
FACTB     RMB    2       * XMUL MULTIPLICATION FACTOR

REF       RMB    2       * REF TIME
W         RMB    2       * ROTOR ANGLE SCALING FACTOR
C         RMB    1       * CONTROL FLAG INDICATING IF MEASURING OFFSET
PNR       RMB    1       * CONTROL FLAG INDICATING WHICH EDGE MEASURING
PNY       RMB    1       * CONTROL FLAG INDICATING WHICH EDGE MEASURING
PNB       RMB    1       * CONTROL FLAG INDICATING WHICH EDGE MEASURING

OFFRP     RMB    2       * OFFSET DELTA RED POSITIVE
OFFRN     RMB    2       * OFFSET DELTA RED NEGATIVE
OFFYP     RMB    2       * OFFSET DELTA YELLOW POSITIVE
OFFYN     RMB    2       * OFFSET DELTA YELLOW NEGATIVE
OFFBP     RMB    2       * OFFSET DELTA BLUE POSITIVE
OFFBN     RMB    2       * OFFSET DELTA BLUE NEGATIVE

TOPRAM    EQU    RAMBS+$FF * TOP OF RAM


*SET UP INTERRUPT VECTOR TABLE
  ORG     $FFEE
  FDB     SVIC1

  ORG     $FFEC
  FDB     SVIC2

  ORG     $FFEA
  FDB     SVIC3
```

```
  ORG    $FFE0
  FDB    SVIC4

*START MAIN PROGRAM
*INITIALIZATION
  ORG    PAREA       * START OF PROGRAM AREA
  LDS    #TOPRAM     * LOAD STACK POINTER
  SEI

  LDAA   #%11111111 * CONFIGURE PORTC AS O/P
  STAA   DDRC

  LDAA   #%00000100
  STAA   PACTL       * CONFIGURE PIN AS I/C 4

  LDAA   #%01010101 * DETECT RISING EDGE ON I/C 1, 2, 3 & 4
  STAA   TCTL2

  LDAA   #%00001111  * ENABLE INTERRUPT FOR I/Cs
  STAA   TMSK1

  LDAA   #%11111111  * RESET ALL FLAGS
  STAA   TFLG1

  LDAA   #%00001000  * SET I/C 1 = HIGHEST PRIORITY INTERRUPT
  STAA   HPRIO

  LDAA   #%00000000
  STAA   C           * LOAD INITIAL VALUE FOR C
  STAA   PNR         * LOAD INITIAL VALUE FOR PNR
  STAA   PNY         * LOAD INITIAL VALUE FOR PNY
  STAA   PNB         * LOAD INITIAL VALUE FOR PNB

  LDAA   #%00000011  * SET CLOCK PRESCALER = 16
  STAA   TMSK2
```

```
  CLI                 * ENABLE INTERRUPT


MAIN:     WAI                 * WAIT FOR INTERRUPT

          LDAA   PORTA        * CHECK IF MSB OF PORTA
          ANDA   #%10000000   * IS SET. IF IT IS NOT SET
          STAA   C            * MEASURING OFFSET
          BRA    MAIN
*****************************************************************
* INTERRUPT SEVICE ROUTINES
*****************************************************************

*****************************************************************
* SVIC1 IS THE INTERRUPT SEVICE ROUTINE USED WHEN THE 360 DEGREE
* REF PULSE IS DETECTED ON I/C 1
*****************************************************************
SVIC1:    LDD    TIC1         * READ TIME OF PULSE
          SUBD   REF          * - PREVIOUS REF=PULSES IN ONE CYCLE
          XGDX                * TRANSFER RESULT TO INDEX REGISTER X
          LDD    #$0FFF       * $0FFF = 2^12
          FDIV
          STX    W            * W=(2^12)/(IC1-REF)
          STX    FACTB        * EXTRA LINE HERE AS XMUL USES FACTB
*                             * AS A VARIABLE. CAN BE REMOVED LATER
*                             * WHEN XMUL IS MODIFIED
          LDD    TIC1         * READ TIME OF PULSE
          STD    REF          * STORE THIS VALUE AS NEW REF

          LDAA   #%00000100
          STAA   TFLG1        * RESET INTERRUPT FOR I/C 1

          RTI                 * RETURN FROM INTERRUPTS

*****************************************************************
* SVIC2 IS THE INTERRUPT SEVICE ROUTINE USED WHEN THE RED PHASE
* ZERO CROSSING IS DETECTED
```

```
*****************************************************************

SVIC2:    LDD    TIC2        * READ TIME OF PULSE
          SUBD   REF         * -REF = PULSES IN DELTA
          STD    FACTA       * STORE THE RESULT IN FACTA
          JSR    XMUL        * JUMP TO THE 16 BIT MULTIPLYING ROUTINE
          LDAA   PROD1       * LOAD THE TOP 2 BYTES.  THESE REPRESENT
          LDAB   PROD2       * THE WHOLE NUMBER, WITH THE OTHER 2 BYTES
*                            * REPRESENTING THE FRACTIONAL PART
          BRSET  PNR $01 NEG_EDGER

POSI_EDGER: BRCLR  C %10000000 FLAGSETRP  *"0"=MEASURING OFFSET

MINUSRP:   SUBD   OFFRP        * SUBTRACT OFFSET

           JSR    OUT_PUT
           BRA    CLEARIC2

FLAGSETRP: STD    OFFRP      * IF C="0" LOAD DELTA=DELTA_OFFSET
           BRA    MINUSRP

*****************************************************************************
NEG_EDGER: BRCLR  C %10000000 FLAGSETRN  *"0"=MEASURING OFFSET

MINUSRN:  SUBD   OFFRN        * SUBTRACT OFFSET

          JSR    OUT_PUT
          BRA    CLEARIC2

FLAGSETRN: STD    OFFRN       * IF C="0" LOAD DELTA=DELTA_OFFSET
           BRA    MINUSRN


CLEARIC2: LDAA   #%00000010
          STAA   TFLG1       * RESET INTERRUPT FOR I/C 2

          LDAA   TCTL2
```

```
          EORA    #%00001100       * DETECT THE OPPOSITE EDGE AS BEFORE
          STAA    TCTL2

          INC     PNR
          BRSET   PNR $02 OVERFLOWR

          RTI                 * RETURN FROM INTERRUPT

OVERFLOWR: CLR     PNR        * IF PN="2" RESET IT BACK TO ZERO
           RTI

*****************************************************************
* SVIC3 IS THE INTERRUPT SEVICE ROUTINE USED WHEN THE YELLOW PHASE
* ZERO CROSSING IS DETECTED
*****************************************************************

SVIC3:    LDD     TIC3         * READ TIME OF PULSE
          SUBD    REF          * -REF = PULSES IN DELTA
          STD     FACTA        * STORE THE RESULT IN FACTA
          JSR     XMUL         * JUMP TO THE 16 BIT MULTIPLYING ROUTINE
          LDAA    PROD1        * LOAD THE TOP 2 BYTES.  THESE REPRESENT
          LDAB    PROD2        * THE WHOLE NUMBER, WITH THE OTHER 2 BYTES
*                              * REPRESENTING THE FRACTIONAL PART
          BRSET   PNY $01 NEG_EDGEY

POSI_EDGEY: BRCLR  C %10000000 FLAGSETYP  *"0"=MEASURING OFFSET

MINUSYP:   SUBD    OFFYP         * SUBTRACT OFFSET

           JSR     OUT_PUT
           BRA     CLEARIC3

FLAGSETYP: STD     OFFYP      * IF C="0" LOAD DELTA=DELTA_OFFSET
           BRA     MINUSYP

*****************************************************************************
NEG_EDGEY: BRCLR  C %10000000 FLAGSETYN  *"0"=MEASURING OFFSET
```

```
MINUSYN:    SUBD    OFFYN        * SUBTRACT OFFSET

            JSR     OUT_PUT
            BRA     CLEARIC3

FLAGSETYN: STD      OFFYN       * IF C="0" LOAD DELTA=DELTA_OFFSET
            BRA     MINUSYN


CLEARIC3: LDAA    #%00000001
          STAA    TFLG1       * RESET INTERRUPT FOR I/C 3


          LDAA    TCTL2
          EORA    #%00000011       * DETECT THE OPPOSITE EDGE AS BEFORE
          STAA    TCTL2

          INC     PNY
          BRSET   PNY $02 OVERFLOWY

          RTI               * RETURN FROM INTERRUPT

OVERFLOWY: CLR     PNY       * IF PN="2" RESET IT BACK TO ZERO
           RTI

*****************************************************************
* SVIC4 IS THE INTERRUPT SEVICE ROUTINE USED WHEN THE BLUE PHASE
* ZERO CROSSING IS DETECTED
*****************************************************************

SVIC4:      LDD     TIC4        * READ TIME OF PULSE
            SUBD    REF         * -REF = PULSES IN DELTA
            STD     FACTA       * STORE THE RESULT IN FACTA
            JSR     XMUL        * JUMP TO THE 16 BIT MULTIPLYING ROUTINE
            LDAA    PROD1       * LOAD THE TOP 2 BYTES.  THESE REPRESENT
            LDAB    PROD2       * THE WHOLE NUMBER, WITH THE OTHER 2 BYTES
```

```
*                              * REPRESENTING THE FRACTIONAL PART
          BRSET   PNB $01 NEG_EDGEB

POSI_EDGEB: BRCLR  C %10000000 FLAGSETBP  *"0"=MEASURING OFFSET

MINUSBP:    SUBD   OFFBP        * SUBTRACT OFFSET

            JSR    OUT_PUT
            BRA    CLEARIC4

FLAGSETBP: STD     OFFBP      * IF C="0" LOAD DELTA=DELTA_OFFSET
            BRA    MINUSBP

*************************************************************************
NEG_EDGEB: BRCLR  C %10000000 FLAGSETBN  *"0"=MEASURING OFFSET

MINUSBN:    SUBD   OFFBN        * SUBTRACT OFFSET

            JSR    OUT_PUT
            BRA    CLEARIC4

FLAGSETBN: STD     OFFBN      * IF C="0" LOAD DELTA=DELTA_OFFSET
            BRA    MINUSBN

CLEARIC4: LDAA    #%00001000
          STAA    TFLG1        * RESET INTERRUPT FOR I/C 4


          LDAA    TCTL2
          EORA    #%11000000      * DETECT THE OPPOSITE EDGE AS BEFORE
          STAA    TCTL2

          INC     PNB
          BRSET   PNB $02 OVERFLOWB

          RTI               * RETURN FROM INTERRUPT
```

```
OVERFLOWB: CLR    PNB       * IF PN="2" RESET IT BACK TO ZERO
           RTI

*************************************************************************
OUT_PUT:  ANDA    #%00001111  * CLEAR 4 MSB
          STAA    PORTB       * O/P RESULT TO PORT B AND C
          STAB    PORTC
          NOP
          NOP
*************************************************************************
*          BSET   PORTB #%10000000  * THE MSB IS USED TO TRIGGER THE D-A
*  cannot use bset --> it does not work
*************************************************************************
          ORA     #%10000000         * THE MSB IS USED TO TRIGGER THE D-A
          STAA    PORTB
          RTS
*************************************************************************
*                         GMATH.ASM
*
*                       Copyright 1988
*                            by
*                       James C. Shultz
*
* The source code for this General Math package for the
* MC68HC11 may be freely distributed under the rules of
* public domain.
*************************************************************************
*********
* XMUL() - 16 BIT BY 16 BIT MULTIPLY, PRODUCT = 32 BITS
*          Input -  16 bits are in FACTA (hi-byte) &
*          FACTA+1 (lo-byte),with the other 16 bits in
*          FACTB (hi-byte) & FACTB+1 (lo-byte)
*          The result is in PROD1 thru PROD4 with the low
*          byte being in PROD4
*********
XMUL:    PSHA                    *SAVE ACCA
         PSHB                    *SAVE ACCB
```

```
        LDD     #$0000          *GET ZERO
        STD     PROD1           *CLEAR PRODUCT
        LDAA    FACTA+1         *GET LOW BYTE
        LDAB    FACTB+1         *GET LOW BYTE
        MUL                     *MULTIPLY
        STD     PROD3           *SAVE
        LDAA    FACTA+1         *GET LOW BYTE
        LDAB    FACTB           *GET HIGH BYTE
        MUL                     *MULTIPLY
        ADDD    PROD2           *SUM INTO PRODUCT
        STD     PROD2           *SAVE
        BCC     XMU10           *CHECK FOR CARRY
        INC     PROD1           *DO CARRY
XMU10:  LDAA    FACTA           *GET HIGH BYTE
        LDAB    FACTB+1         *GET LOW BYTE
        MUL                     *MULTIPLY
        ADDD    PROD2           *SUM INTO PRODUCT
        STD     PROD2           *SAVE
        BCC     XMU20           *CHECK FOR CARRY
        INC     PROD1           *DO CARRY
XMU20:  LDAA    FACTA           *GET HIGH BYTE
        LDAB    FACTB           *GET HIGH BYTE
        MUL                     *MULTIPLY
        ADDD    PROD1           *SUM INTO PRODUCT
        STD     PROD1           *SAVE
XMU50:  PULB                    *RESTORE ACCB
        PULA                    *RESTORE ACCA
        RTS
```

C.3 Start-Up Procedure

The micro-controller has 2 modes of operation. The first is the bootstrap mode, which is when the program code is downloaded into the micro-controller's EEPROM, and the second is when it is executing the downloaded program. To put the micro-controller into bootstrap mode, the bootstrap switch, S2, is

closed. The micro-controller is then reset by activating the single-pole-single-throw(spst) momentary reset switch, S1. The micro-controller is then ready to receive the program via the DB25 socket. To start running the program, it is a simple task of first opening the bootstrap switch and then resetting the micro-controller. Activating the reset switch initializes micro-controller and sets the program counter to the base address of the EEPROM to begin running the program.

Appendix D

MATLAB CODE USED IN SIMULATIONS

D.1 parks.m

```
%#################################################################
%
% MATLAB routine parks.m used to simulated the Park's Transform
% Unit designed and constructed in this work
%
%#################################################################

clc  % clear command window
clg  % clear graph window
clear
echo off
%#################################################################
% Input variables
%
disp(' Now for the boring bit ... input of parameters')
c=input('How many sine wave cycle do we model? [3] : ');
```

```
if isempty(c)
  c=3;    % default number of sine wave cycles required
end
%
disp(' ')
disp(' ')
disp(' How many sampling points per cycle do we model?')
disp('The number has to be >= 128 and a multiple of 128')
s=input('You choice is? [128] : ');
if isempty(s)
  s=128;   % minimum = 128 -- default value for the number
           %of sampling points per cycle
end
%
%#####################################################################
t=0:.02/s:.02*c;            % t=time in seconds
%#####################################################################
%
disp(' ')
disp(' ')
disp('If the supplies are unbalanced, there will be a negative')
disp('voltage sequence.')
disp(' ')
disp(' How big is the negative voltage sequence as a fraction of')
disp(' positive sequence?')
n=input('You choice is? [0.025] : ');
if isempty(n)
   n=0.025;  % default value for the negative voltage sequence
end
disp(' ')
disp(' ')
disp('What is the phase shift (in degrees) between the +ve and')
disp('-ve sequence?')
disp('+ve rotor angle => generating ')
delta_t_raw=input('You choice is? [0] : ');
if isempty(delta_t_raw)
   delta_t_raw=0;  % default for rotor angle
```

```
end
delta_t=delta_t_raw/180*pi;
end
%
disp(' ')
disp(' ')
disp('What is the rotor angle (in degrees) of the system?')
disp('+ve rotor angle => generating ')
disp('If a constant rotor angle is needed choose option 1')
disp('Choose option 2 for a varying rotor angle with a user defined signal')
disp('Choose option 3 for a varying rotor angle with a signal defined by ')
disp('the matlab routine signal.m')
choice=input('You choice is? [3] : ');
if isempty(choice)
   choice=3;  % default for choice
end
if choice == 1
disp('What constant rotor angle do you require?')
delta_const=input('Your choice (in degrees) is? [0] : ');
if isempty(delta_const)
    delta_const=0;  % default for delta_const
end
for i=1:1:c*s+1
  delta_raw(i)=delta_const;
end

elseif choice == 2
disp('What is the equation of delta (in degrees) in the time')
disp('domain that you require, eg sin(2*pi*2*t)')
delta_raw=input('Your choice is ? : ');
else
signal
end
delta=delta_raw/180*pi;

%
%#####################################################################
```

```
% Defining a 3 phase +ve sequence sine wave @50Hz
%
t=0:.02/s:.02*c;
sin50_Rf=sin(2*50*pi*t + delta);
sin50_Yf=sin(2*50*pi*t-2*pi/3 + delta);
sin50_Bf=sin(2*50*pi*t-4*pi/3 + delta);
%

%
%#####################################################################
% Defining a 3 phase -ve sequence sine wave @50Hz
% whose magnitude is n times the +ve sequence
% and shifted by delta_t
%
t=0:.02/s:.02*c;
sin50_Rb=n*sin(2*50*pi*t+delta_t);
sin50_Yb=n*sin(2*50*pi*t+2*pi/3+delta_t);
sin50_Bb=n*sin(2*50*pi*t+4*pi/3+delta_t);
%

%
%#####################################################################
% Adding the +ve sequence to the -ve sequence
%
sin50_R=sin50_Rf+sin50_Rb;
sin50_Y=sin50_Yf+sin50_Yb;
sin50_B=sin50_Bf+sin50_Bb;
%
%
%
plot(t,sin50_R,'-r',t,sin50_Y,'-g',t,sin50_B,'-b')
title('Plot of a 3 phase unbalanced system')
xlabel('time (seconds)')
ylabel('Magnitude')
text(0.02*c,sin50_R(.02*c+1),'R'),
text(0.02*c,sin50_Y(.02*c+1),'Y'),
text(0.02*c,sin50_B(.02*c+1),'B')
```

```
grid
pause(5)
%
%#################################################################
% Perform sample and hold
%
step_size=s/8;   % number of samples in each step
 for i=1:1:s*c+1
  if rem(i,step_size) == 1
   R(i)=sin50_R(i);
   Y(i)=sin50_Y(i);
   B(i)=sin50_B(i);
  elseif rem(i,step_size) == 0
   R(i)=sin50_R(i);
   Y(i)=sin50_Y(i);
   B(i)=sin50_B(i);
  else
   R(i)=R(i-1);
   Y(i)=Y(i-1);
   B(i)=B(i-1);
  end
 end
plot(t,R,'-r',t,Y,'-g',t,B,'-b')
title('Plot of a sample/hold 3 phase unbalanced system')
xlabel('time (seconds)')
ylabel('Magnitude')
text(0.02*c,R(.02*c+1),'R'),
text(0.02*c,Y(.02*c+1),'Y'),
text(0.02*c,B(.02*c+1),'B')
grid
pause(5)
%
%#################################################################
% Part 1 of Parks transform
% 3 phase stationary --> 2 phase stationary
%
md=0.666*R-0.333*(Y+B);
```

```
mq=0.577*(B-Y);
plot(t,md,'-r',t,mq,'-b')
title('Plot of sample/hold md and mq ')
xlabel('time (seconds)')
ylabel('Magnitude')
text(0.02*c,md(.02*c+1),'md'),text(0.02*c,mq(.02*c+1),'mq')
grid
pause(5)
%
%#####################################################################
% Part 2 of Parks transform
% 2 phase stationary --> 2 phase rotational
%
%################################################
% Generating the transformation matrix elements
%################################################
%
for i=1:1:s*c+1
 dummy=fix(i/step_size);
  dummy2=rem(dummy,8);
   if dummy2 == 0
    M1_1(i)=1;
    M1_2(i)=0;
    M2_1(i)=0;
    M2_2(i)=1;
   elseif dummy2 == 1
    M1_1(i)=0.707;
    M1_2(i)=-0.707;
    M2_1(i)=0.707;
    M2_2(i)=0.707;
   elseif dummy2 == 2
    M1_1(i)=0;
    M1_2(i)=-1;
    M2_1(i)=1;
    M2_2(i)=0;
   elseif dummy2 == 3
    M1_1(i)=-0.707;
```

```
    M1_2(i)=-0.707;
    M2_1(i)=0.707;
    M2_2(i)=-0.707;
   elseif dummy2 == 4
    M1_1(i)=-1;
    M1_2(i)=0;
    M2_1(i)=0;
    M2_2(i)=-1;
   elseif dummy2 == 5
    M1_1(i)=-0.707;
    M1_2(i)=0.707;
    M2_1(i)=-0.707;
    M2_2(i)=-0.707;
   elseif dummy2 == 6
    M1_1(i)=0;
    M1_2(i)=1;
    M2_1(i)=-1;
    M2_2(i)=0;
   elseif dummy2 == 7
    M1_1(i)=0.707;
    M1_2(i)=0.707;
    M2_1(i)=-0.707;
    M2_2(i)=0.707;
   end
end
%
%################################################
% Matrix multiplication
%################################################
%
d=md.*M1_1 + mq.*M1_2;
q=md.*M2_1 + mq.*M2_2;
plot(t,d,'-r',t,q,'-b')
title(['Plot of d and q -- n = ',num2str(n)])
xlabel('time (seconds)')
ylabel('Magnitude')
text(0.02*c,d(.02*c+1),'d'),text(0.02*c,q(.02*c+1),'q')
```

```
pause(5)
%
%#####################################################################
```

D.2 rotor5_1.m

```
%#################################################################
%
% MATLAB routine rotor5_1.m used to simulated the Rotor Angle
% Transducer designed and constructed in this work
%
%#################################################################
clc  % clear command window
clg  % clear graph window
clear
echo off
%#################################################################
% Input variables
%
disp(' Now for the boring bit ... input of parameters')
c=input('How many sine wave cycle do we model? [3] : ');
if isempty(c)
  c=3;    % default number of sine wave cycles required
end
%
disp(' ')
disp(' ')
disp(' How many sampling points per cycle do we model?')
disp('The number has to be >= 128 and a multiple of 128')
s=input('You choice is? [128] : ');
if isempty(s)
  s=128;   % minimum = 128 -- default value for the number
           %of sampling points per cycle
end
%
```

```
%#####################################################################
t=0:.02/s:.02*c;            % t=time in seconds
%#####################################################################
%
disp(' ')
disp(' ')
disp('If the supplies are unbalanced, there will be a negative')
disp('voltage sequence.')
disp(' ')
disp(' How big is the negative voltage sequence as a fraction of')
disp(' positive sequence?')
n=input('You choice is? [0.025] : ');
if isempty(n)
   n=0.025;  % default value for the negative voltage sequence
end
disp(' ')
disp(' ')
disp('What is the phase shift (in degrees) between the +ve ')
disp('and -ve sequence? ')
disp('+ve rotor angle => generating ')
delta_t_raw=input('You choice is? [0] : ');
if isempty(delta_t_raw)
   delta_t_raw=0;  % default for rotor angle
end
delta_t=delta_t_raw/180*pi;
end
%
disp(' ')
disp(' ')
disp('What is the rotor angle (in degrees) of the system?')
disp('+ve rotor angle => generating ')
disp('If a constant rotor angle is needed choose option 1')
disp('Choose option 2 for a varying rotor angle with a user defined signal')
disp('Choose option 3 for a varying rotor angle with a signal defined by ')
disp('the matlab routine signal.m')
choice=input('You choice is? [3] : ');
if isempty(choice)
```

```
   choice=3;  % default for choice
end
if choice == 1
disp('What constant rotor angle do you require?')
delta_const=input('Your choice (in degrees) is? [0] : ');
if isempty(delta_const)
    delta_const=0;  % default for delta_const
end
for i=1:1:c*s+1
  delta_raw(i)=delta_const;
end

elseif choice == 2
disp('What is the equation of delta (in degrees) in the time')
disp('domain that you require, eg sin(2*pi*2*t)')
delta_raw=input('Your choice is ? : ');
else
signal
end
delta=delta_raw/180*pi;

for i=1:1:c*s+1
delta_ini(i)=delta(1);
end
%
%

%#################################################################
% First pass of simulation to determine the initial rotor angle
%#################################################################
% Defining a 3 phase +ve sequence sine wave @50Hz
%
sin50_Rf=sin(2*50*pi*t - delta_ini);
sin50_Yf=sin(2*50*pi*t - 2*pi/3 - delta_ini);
sin50_Bf=sin(2*50*pi*t - 4*pi/3 - delta_ini);
%#################################################################
% Defining a 3 phase -ve sequence sine wave @50Hz
```

```
% whose magnitude is n times the +ve sequence
% and shifted by delta_t
%
%
sin50_Rb=n*sin(2*50*pi*t - delta_ini + delta_t);
sin50_Yb=n*sin(2*50*pi*t + 2*pi/3 - delta_ini + delta_t);
sin50_Bb=n*sin(2*50*pi*t + 4*pi/3 - delta_ini + delta_t);
%
%#####################################################################
% Adding the +ve sequence to the -ve sequence
%
R=sin50_Rf+sin50_Rb;
Y=sin50_Yf+sin50_Yb;
B=sin50_Bf+sin50_Bb;
%
%
%#####################################################################
% zero crossing detector of Red phase
 for i=1:1:c*s+1
  if R(i)>0
   R_zero_cross(i)=1;
  else
   R_zero_cross(i)=0;
  end
 end
%#####################################################################
% zero crossing detector of Yellow phase
 for i=1:1:c*s+1
  if Y(i)>0
   Y_zero_cross(i)=1;
  else
   Y_zero_cross(i)=0;
  end
 end
%#####################################################################
% zero crossing detector of Blue phase
 for i=1:1:c*s+1
```

```
  if B(i)>0
   B_zero_cross(i)=1;
  else
   B_zero_cross(i)=0;
  end
 end

%#####################################################################
% pulses from shaft encoder
%angle 0 degree = element 1,s+1,s*2 + 1,....s*c + 1
%angle 180 degree = element s/2,s/2+s,...s/2+s*(c-1)

for i=1:1:c*s+1
  if rem(i,s)==1
   ref(i)=1;
  else
   ref(i)=0;
  end
end
%#####################################################################
% count phase shift
% ###################
% Red phase positive edge
%
% intialise variables
   flag1=0;
   flag2=0;
%####################
    for i=1:1:c*s
     if ref(i+1)>ref(i)
      flag1=1;
      start=i;
     end

     if flag1==1
if R_zero_cross(i+1)>R_zero_cross(i)
  flag2=1;
```

```
  stop=i;
end
     end
     if flag1&flag2==1
delta_ini_posi_R=(stop-start)/s*360;
if delta_ini_posi_R>180
  delta_ini_posi_R=delta_ini_posi_R-360;
elseif delta_ini_posi_R<-180
  delta_ini_posi_R=delta_ini_posi_R+360;
end
break
     end
    end
% ###################
% Red phase -ve edge
%
% intialise variables
   flag1=0;
   flag2=0;
%####################
    for i=1:1:c*s
     if ref(i+1)>ref(i)
      flag1=1;
      start=i;
     end

     if flag1==1
if R_zero_cross(i+1)<R_zero_cross(i)
  flag2=1;
  stop=i;
end
     end
     if flag1&flag2==1
delta_ini_neg_R=(stop-start)/s*360 -180;
if delta_ini_neg_R>180
  delta_ini_neg_R=delta_ini_neg_R-360;
elseif delta_ini_neg_R<-180
```

```
  delta_ini_neg_R=delta_ini_neg_R+360;
end
break
     end
    end
%#########################################################################
% ####################
% Yellow phase positive
%
% intialise variables
   flag1=0;
   flag2=0;
%######################
    for i=1:1:c*s
     if ref(i+1)>ref(i)
      flag1=1;
      start=i;
     end

     if flag1==1
if Y_zero_cross(i+1)>Y_zero_cross(i)
  flag2=1;
  stop=i;
end
     end
     if flag1&flag2==1
delta_ini_posi_Y=(stop-start)/s*360 - 120;
% the offset for the +ve yellow phase is assumed = 120 degrees
if delta_ini_posi_Y>180
  delta_ini_posi_Y=delta_ini_posi_Y-360;
elseif delta_ini_posi_Y<-180
  delta_ini_posi_Y=delta_ini_posi_Y+360;
end
break
     end
    end
%#########################################################################
```

```
% ###################
% Yellow phase negative
%
% intialise variables
   flag1=0;
   flag2=0;
%####################
    for i=1:1:c*s
     if ref(i+1)>ref(i)
      flag1=1;
      start=i;
     end

     if flag1==1
if Y_zero_cross(i+1)<Y_zero_cross(i)
  flag2=1;
  stop=i;
end
     end
     if flag1&flag2==1
delta_ini_neg_Y=(stop-start)/s*360 - 300;
% the offset for the -ve yellow phase is assumed = 300 degrees
if delta_ini_neg_Y>180
  delta_ini_neg_Y=delta_ini_neg_Y-360;
elseif delta_ini_neg_Y<-180
  delta_ini_neg_Y=delta_ini_neg_Y+360;
end
break
     end
    end
%#########################################################################

% ###################
% Blue phase +ve
%
% intialise variables
   flag1=0;
```

```
   flag2=0;
%####################
    for i=1:1:c*s
     if ref(i+1)>ref(i)
      flag1=1;
      start=i;
     end

     if flag1==1
if B_zero_cross(i+1)>B_zero_cross(i)
  flag2=1;
  stop=i;
end
     end
     if flag1&flag2==1
delta_ini_posi_B=(stop-start)/s*360 -240;
% the offset for the +ve yellow phase is assumed = 240 degrees
if delta_ini_posi_B>180
  delta_ini_posi_B=delta_ini_posi_B-360;
elseif delta_ini_posi_B<-180
  delta_ini_posi_B=delta_ini_posi_B+360;
end
break
     end
    end
% ###################
% Blue phase negative
%
% intialise variables
   flag1=0;
   flag2=0;
%####################
    for i=1:1:c*s
     if ref(i+1)>ref(i)
      flag1=1;
      start=i;
     end
```

```
     if flag1==1
if B_zero_cross(i+1)<B_zero_cross(i)
  flag2=1;
  stop=i;
end
     end
     if flag1&flag2==1
delta_ini_neg_B=(stop-start)/s*360 -60;
% the offset for the -ve yellow phase is assumed = 60 degrees
if delta_ini_neg_B>180
  delta_ini_neg_B=delta_ini_neg_B-360;
elseif delta_ini_neg_B<-180
  delta_ini_neg_B=delta_ini_neg_B+360;
end
break
     end
    end
%#########################################################################
% Defining a 3 phase +ve sequence sine wave @50Hz
%
sin50_Rf=sin(2*50*pi*t - delta);
sin50_Yf=sin(2*50*pi*t - 2*pi/3 - delta);
sin50_Bf=sin(2*50*pi*t - 4*pi/3 - delta);
%#########################################################################
% Defining a 3 phase -ve sequence sine wave @50Hz
% whose magnitude is n times the +ve sequence
% and shifted by delta_t
%
%
sin50_Rb=n*sin(2*50*pi*t - delta + delta_t);
sin50_Yb=n*sin(2*50*pi*t + 2*pi/3 - delta + delta_t);
sin50_Bb=n*sin(2*50*pi*t + 4*pi/3 - delta + delta_t);
%
%#########################################################################
% Adding the +ve sequence to the -ve sequence
%
```

```
R=sin50_Rf+sin50_Rb;
Y=sin50_Yf+sin50_Yb;
B=sin50_Bf+sin50_Bb;
%
%
%#####################################################################
% zero crossing detector of Red phase
 for i=1:1:c*s+1
  if R(i)>0
   R_zero_cross(i)=1;
  else
   R_zero_cross(i)=0;
  end
 end
%#####################################################################
% zero crossing detector of Yellow phase
 for i=1:1:c*s+1
  if Y(i)>0
   Y_zero_cross(i)=1;
  else
   Y_zero_cross(i)=0;
  end
 end
%#####################################################################
% zero crossing detector of Blue phase
 for i=1:1:c*s+1
  if B(i)>0
   B_zero_cross(i)=1;
  else
   B_zero_cross(i)=0;
  end
 end
%#####################################################################
% count phase shift
% ###################

%
```

```
% intialise variables
   flag1=0;
%####################
    for i=1:1:c*s
     if ref(i+1)>ref(i)
      flag1=1;
      flag2_R_posi=0;
      flag2_R_neg=0;
      flag2_Y_posi=0;
      flag2_Y_neg=0;
      flag2_B_posi=0;
      flag2_B_neg=0;
      start=i;
     end
% ##########################
% Red phase positive
%
     if flag1==1
if R_zero_cross(i+1)>R_zero_cross(i)
  flag2_R_posi=1;
  stop_R_posi=i;
end
     end
     if flag1&flag2_R_posi==1
delta_meas_posi_R(i)=(stop_R_posi-start)/s*360;
if delta_meas_posi_R(i)>180
  delta_meas_posi_R(i)=delta_meas_posi_R(i)-360;
elseif delta_meas_posi_R(i)<-180
  delta_meas_posi_R(i)=delta_meas_posi_R(i)+360;
end
     elseif i==1
delta_meas_posi_R(i)=delta_ini_posi_R;
     else
delta_meas_posi_R(i)=delta_meas_posi_R(i-1);
     end
% ##########################
% Red phase negative
```

```
%
     if flag1==1
if R_zero_cross(i+1)<R_zero_cross(i)
  flag2_R_neg=1;
  stop_R_neg=i;
end
     end
     if flag1&flag2_R_neg==1
delta_meas_neg_R(i)=(stop_R_neg-start)/s*360 -180;
if delta_meas_neg_R(i)>180
  delta_meas_neg_R(i)=delta_meas_neg_R(i)-360;
elseif delta_meas_neg_R(i)<-180
  delta_meas_neg_R(i)=delta_meas_neg_R(i)+360;
end
     elseif i==1
delta_meas_neg_R(i)=delta_ini_neg_R;
     else
delta_meas_neg_R(i)=delta_meas_neg_R(i-1);
     end

%#####################################################
% yellow phase positive
%
     if flag1==1
if Y_zero_cross(i+1)>Y_zero_cross(i)
  flag2_Y_posi=1;
  stop_Y_posi=i;
end
     end
     if flag1&flag2_Y_posi==1
delta_meas_posi_Y(i)=(stop_Y_posi-start)/s*360 -120; % offset = 120 degrees
if delta_meas_posi_Y(i)>180
  delta_meas_posi_Y(i)=delta_meas_posi_Y(i)-360;
elseif delta_meas_posi_Y(i)<-180
  delta_meas_posi_Y(i)=delta_meas_posi_Y(i)+360;
end
     elseif i==1
```

```
delta_meas_posi_Y(i)=delta_ini_posi_Y;
     else
delta_meas_posi_Y(i)=delta_meas_posi_Y(i-1);
     end
%#####################################################
% yellow phase negative
%
     if flag1==1
if Y_zero_cross(i+1)<Y_zero_cross(i)
  flag2_Y_neg=1;
  stop_Y_neg=i;
end
     end
     if flag1&flag2_Y_neg==1
delta_meas_neg_Y(i)=(stop_Y_neg-start)/s*360 -300; % offset = 300 degrees
if delta_meas_neg_Y(i)>180
  delta_meas_neg_Y(i)=delta_meas_neg_Y(i)-360;
elseif delta_meas_neg_Y(i)<-180
  delta_meas_neg_Y(i)=delta_meas_neg_Y(i)+360;
end
     elseif i==1
delta_meas_neg_Y(i)=delta_ini_neg_Y;
     else
delta_meas_neg_Y(i)=delta_meas_neg_Y(i-1);
     end


%#####################################################################
% Blue phase positive
%

     if flag1==1
if B_zero_cross(i+1)>B_zero_cross(i)
  flag2_B_posi=1;
  stop_B_posi=i;
end
     end
```

```
     if flag1&flag2_B_posi==1
delta_meas_posi_B(i)=(stop_B_posi-start)/s*360 -240; % offset = 240 degrees
if delta_meas_posi_B(i)>180
  delta_meas_posi_B(i)=delta_meas_posi_B(i)-360;
elseif delta_meas_posi_B(i)<-180
  delta_meas_posi_B(i)=delta_meas_posi_B(i)+360;
end
     elseif i==1
delta_meas_posi_B(i)=delta_ini_posi_B;
     else
delta_meas_posi_B(i)=delta_meas_posi_B(i-1);
     end

%#####################################################################
% Blue phase negative
%

     if flag1==1
if B_zero_cross(i+1)<B_zero_cross(i)
  flag2_B_neg=1;
  stop_B_neg=i;
end
     end
     if flag1&flag2_B_neg==1
delta_meas_neg_B(i)=(stop_B_neg-start)/s*360 -60; % offset = 60 degrees
if delta_meas_neg_B(i)>180
  delta_meas_neg_B(i)=delta_meas_neg_B(i)-360;
elseif delta_meas_neg_B(i)<-180
  delta_meas_neg_B(i)=delta_meas_neg_B(i)+360;
end
     elseif i==1
delta_meas_neg_B(i)=delta_ini_neg_B;
     else
delta_meas_neg_B(i)=delta_meas_neg_B(i-1);
     end
```

```
%#########################################################################
%composite
%#########################################################################
    if flag1&flag2_R_posi==1
delta_measured(i)=delta_meas_posi_R(i);
   flag2_R_posi=0;
done_R_posi=1;

    elseif flag1&flag2_R_neg==1
delta_measured(i)=delta_meas_neg_R(i);
   flag2_R_neg=0;
done_R_neg=1;

    elseif flag1&flag2_Y_posi==1
delta_measured(i)=delta_meas_posi_Y(i);
        flag2_Y_posi=0;
done_Y_posi=1;

    elseif flag1&flag2_Y_neg==1
delta_measured(i)=delta_meas_neg_Y(i);
        flag2_Y_neg=0;
done_Y_neg=1;

    elseif flag1&flag2_B_posi==1
delta_measured(i)=delta_meas_posi_B(i);
flag2_B_posi=0;
done_B_posi=1;

    elseif flag1&flag2_B_neg==1
delta_measured(i)=delta_meas_neg_B(i);
flag2_B_neg=0;
done_B_neg=1;

    elseif i==1
delta_measured(i)=delta_raw(i);
% assume initial value is correct and = to initial value of transient
```

```
    else
delta_measured(i)=delta_measured(i-1);
    end

    if  done_R_posi & done_R_neg & done_Y_posi & done_Y_neg
         & done_B_posi & done_B_neg==1
flag1=0;
done_R_posi=0;
done_R_neg=0;
done_Y_posi=0;
done_Y_neg=0;
done_B_posi=0;
done_B_neg=0;
    end
  end
delta_measured(c*s+1)=delta_measured(c*s);       % fudge factor to define
                                                 % the last data point
delta_meas_posi_R(c*s+1)=delta_meas_posi_R(c*s); % fudge factor to define
                                                 % the last data point
delta_meas_neg_R(c*s+1)=delta_meas_neg_R(c*s);   % fudge factor to define
                                                 % the last data point
delta_meas_posi_Y(c*s+1)=delta_meas_posi_Y(c*s); % fudge factor to define
                                                 % the last data point
delta_meas_neg_Y(c*s+1)=delta_meas_neg_Y(c*s);   % fudge factor to define
                                                 % the last data point
delta_meas_posi_B(c*s+1)=delta_meas_posi_B(c*s); % fudge factor to define
                                                 % the last data point
delta_meas_neg_B(c*s+1)=delta_meas_neg_B(c*s);   % fudge factor to define
                                                 % the last data point


subplot(711)
plot(t,delta_meas_posi_R,t,delta_raw)   % ploting delta measured on the +ve
                                        % red edge

subplot(712)
```

```
plot(t,delta_meas_neg_R,t,delta_raw)     % ploting delta measured on the -ve
                                         % red edge

subplot(713)
plot(t,delta_meas_posi_Y,t,delta_raw)    % ploting delta measured on the +ve
                                         % yellow edge

subplot(714)
plot(t,delta_meas_neg_Y,t,delta_raw)     % ploting delta measured on the -ve
                                         % yellow edge

subplot(715)
plot(t,delta_meas_posi_B,t,delta_raw)    % ploting delta measured on the +ve
                                         % blue edge

subplot(716)
plot(t,delta_meas_neg_B,t,delta_raw)     % ploting delta measured on the -ve
                                         % blue edge

subplot(717)
plot(t,delta_measured,t,delta_raw)       % ploting delta measured on all the
                                         % edges as will be determined with
                                         % the micro-controller based
                                         % transducer
```

D.3 signal.m

```
%#################################################################
%
% MATLAB routine signal.m used to generate a transient rotor
% angle of the form 20+20*sin(2*pi*1*t)*(1+exp(-t)) for use with
% parks.m and rotor5_1.m
%
%#################################################################
```

```
%clc
%clear
%axis([1 2 3 4]);axis;
%echo off
%#####################################################################
% Input variables
%
%disp(' Now for the boring bit ... input of parameters')
%c=input('How many sine wave cycle do we model? [3] : ');
%if isempty(c)
%  c=3;    % default number of sine wave cycles required
%end
%
%disp(' ')
%disp(' ')
%disp(' How many sampling points per cycle do we model?')
%disp('The number has to be >= 128 and a multiple of 128')
%s=input('You choice is? [128] : ');
%if isempty(s)
%  s=128;   % minimum = 128 -- default value for the number
%           %of sampling points per cycle
%end

%t=0:.02/s:.02*c;

% ###########################################################################
% The above are commands used used to define the size of the signal
% In most cases they are not required as the definations are made in the
% main routine rotor5_1.m and parks.m
% ###########################################################################

sin1_Hz=sin(2*pi*1*t);                    % defining a 1Hz sine wave
exponential=20*(1+exp(-t));               % defining the exponential decay,
                                          % NB 20 = increase in delta
transient=20 + sin1_Hz .* exponential;    % multiplying the 2 above signals
                                          % together and adding the initial
                                          % value of 20.
```

```
% ##################################
% The above signals starts from a
% value of 20 and after the
% transient settles to a value of
% 40
% ##################################
pad=20 * ones(1,12.5*s);                % pad the start of the signal to
                                        % show the d.c. initial condition

paded_transient=[pad transient];        %
                                        % ##################################
for q=1:1:c*s+1                         % resize the signal so that it is
delta_raw(q)=paded_transient(q);        % the same size as the other
end                                     % signals in the main routine
                                        % ##################################

%subplot(311)                           % some commands used to plot the
%plot(t,sin1_Hz)                        % signal
%subplot(312)
%plot(t,exponential)
%subplot(313)
%plot(t,delta_raw)
```

Appendix E

LARGE-SIGNAL MACHINE TESTS

In the testing of the various transducers, calculations were made using the synchronous machine's large-signal machine parameters, to determine the validity and accuracy of the designs. The tests performed on the machine set in order to obtain these parameters are covered here.

E.1 Open and Short Circuit Tests

With the synchronous machine running at synchronous speed the open circuit and short circuit tests were performed. In the open circuit test, the relationship between the machine's open circuit terminal voltage and the field excitation current, I_f, is determined. Similarly, the short circuit test determines the relationship between the machine's line current and the field excitation current with the terminals short circuited. The results obtained are graphically represented in Figure: E.1.

From these results the unsaturated synchronous impedance, $Z_{s(unsat)}$, can be

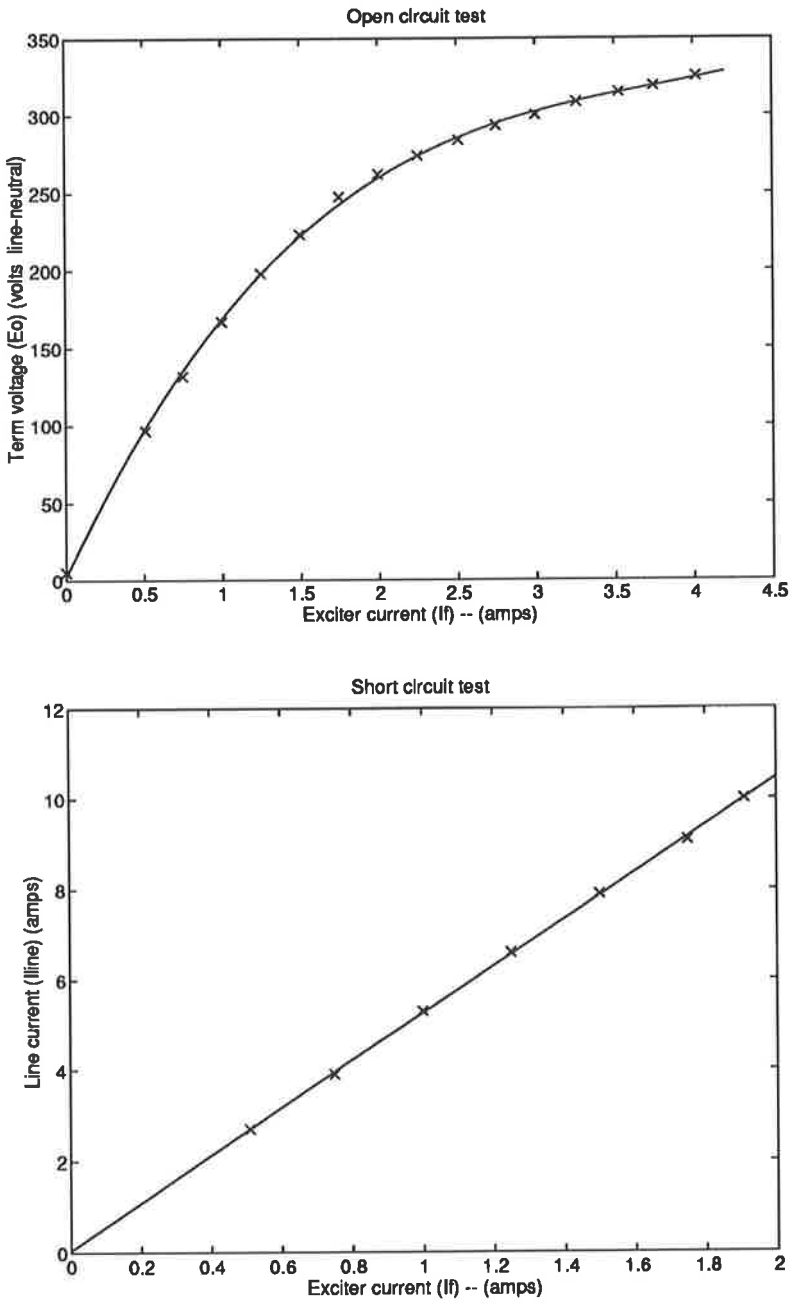

Figure E.1: Open and Short Circuit Test Results

calculated via Equation: E.1.

$$Z_{s(unsat)} = \frac{\text{slope of the linear section of the open circuit curve}}{\text{slope of the short circuit curve}} \quad \text{(E.1)}$$
$$= 27.6\Omega$$

$Z_{s(unsat)}$ is made up 2 components. The first is the unsaturated direct axis synchronous reactance, $X_{d(unsat)}$, and the second is the stator resistance, R_a. The stator resistance was measured to be 1.05Ω using a digital multimeter whose reading was multiplied by a factor of 1.05 to take into account the skin effect that exists in the stator conductors when under a.c. conditions. The unsaturated direct axis synchronous reactance can hence be calculated using Equation: E.2.

$$X_{d(unsat)} = \sqrt{Z^2_{s(unsat)} + R^2_a} \quad \text{(E.2)}$$
$$= 27.6\Omega$$

The effect of the resistance can be clearly seen to be insignificant when compared to the reactance.

E.2 Zero-Power-Factor Test

The zero power factor, zpf, test is used to determine the value of the direct axis leakage reactance, X_l, of the synchronous machine. The machine set was configured as shown in Figure: E.2. In the test, the variable inductors are varied, and at each value of this inductance, the field excitation current is varied to keep the machine line current constant, at 5 Amps in this case. The machine's terminal voltage is also measured at each of these points, hence providing a relationship between the terminal voltage and field excitation current at zero power factor. This is expressed graphically in Figure: E.3.

The shape of the zpf curve is the same as that of the open circuit curve, with the only difference being that it is shifted down and across. The down shifting is due to the voltage drop across the leakage inductance and the across shifting is due to the stator armature reaction. Poitier triangles are then drawn, as in Figure: E.3, giving

$$X_l = 1.72\Omega \quad \text{(E.3)}$$

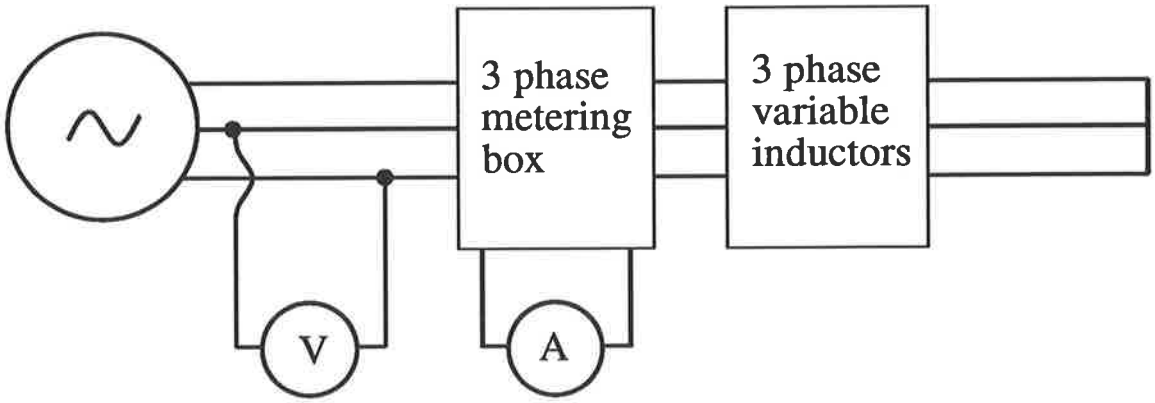

Figure E.2: Machine Set-up for the Zero Power Factor Test

E.3 Slip Test

In the slip test, a value for the quadrature axis unsaturated synchronous reactance, $X_{q(unsat)}$, is obtained by determining a relationship between this quantity and $X_{d(unsat)}$. The machine setup used for this test is as shown in Figure: E.4. The 2 quantities of interest in this test are the terminal voltage and line current signals. The line current is determined by measuring the voltage drop across the 50Ω resistor via an isolating transformer.

The machine is first run up to a speed that is very close to synchronous speed with the field excitation open circuit. A reduced voltage is then applied to the stator terminals. The synchronously rotating mmf produced by this voltage will rotate at a slightly different speed to the rotor. This results in an sinusoidally varying envelope being induced onto the terminal voltage and line current signals as the direct and quadrature axis periodically align with the rotating mmf. A maximum voltage signal and a minimum current signal occurs when the mmf is aligned with the direct axis. The reverse is true for the quadrature axis. The maximum and minimum value for the voltage and current signals were measured and used to determine the $X_{q(unsat)}$ as shown

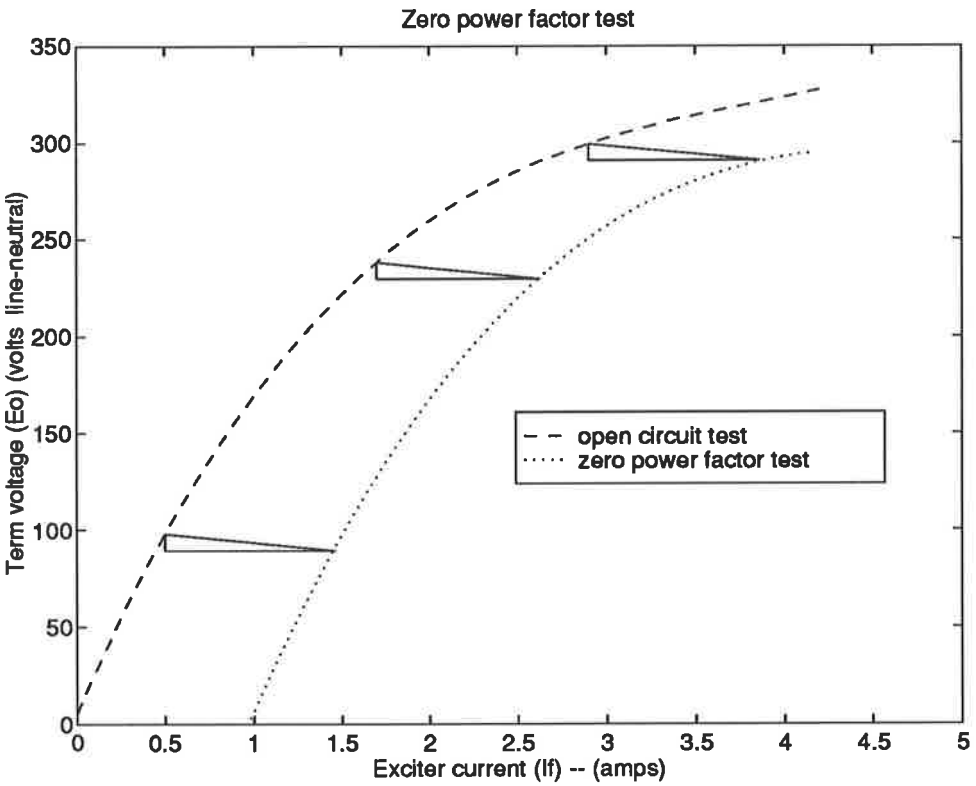

Figure E.3: Results of the Zero Power Factor Test

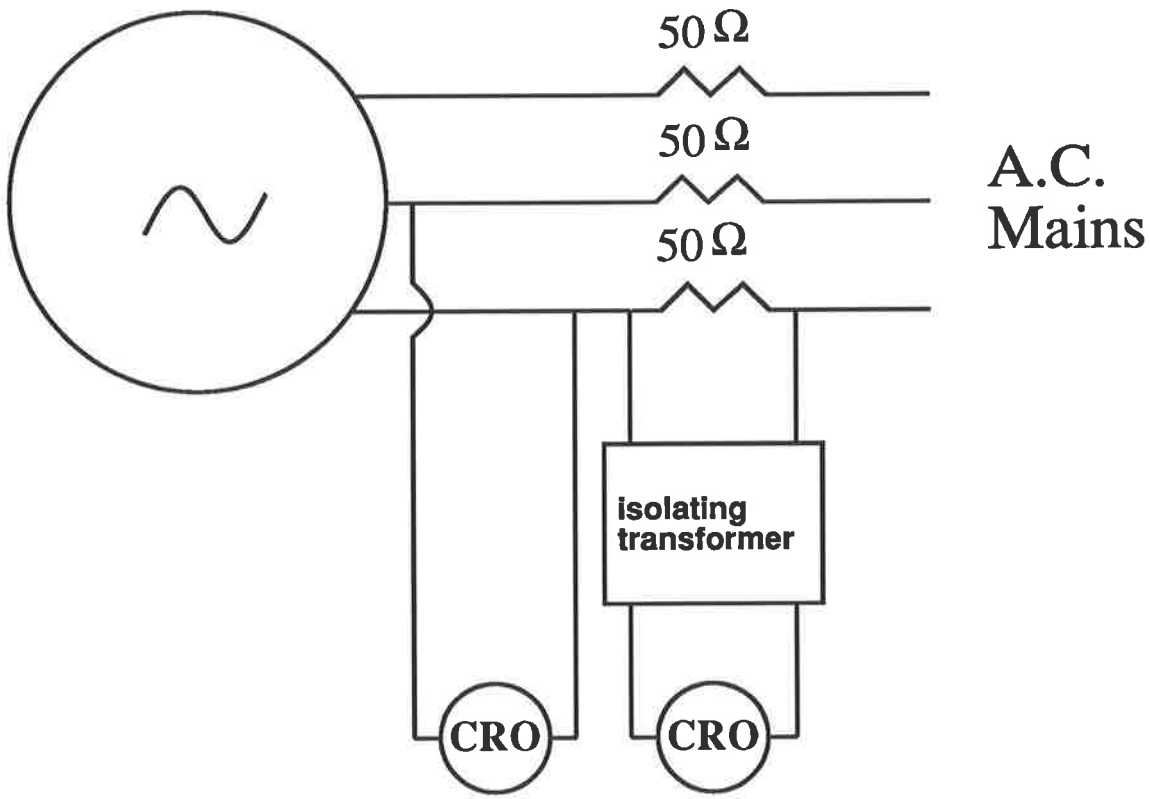

Figure E.4: Machine Set-up for the Slip Test

below in Equation: E.4.

$$\begin{aligned} X_{q(unsat)} &= X_{d(unsat)} * \frac{V_{min}}{V_{max}} * \frac{I_{min}}{I_{max}} \\ &= 13.1\Omega \end{aligned} \tag{E.4}$$

Only the ratio of the maximum and minimum of the current and voltage is required. Hence there is no need to obtain exact numerical values, and all that is required is to measure these quantities in terms of the generic scale of the CRO.

E.4 Summary of Results

The results obtained, in this appendix, are summarized below

$$\begin{aligned} X_{d(unsat)} &= 27.6\Omega \\ X_{q(unsat)} &= 13.1\Omega \\ X_l &= 1.72\Omega \\ R_a &= 1.05\Omega \end{aligned}$$

Appendix F

DETERMINING 1pu SYNCHRONOUS MACHINE FIELD EXCITATION CURRENT

The following quantities were determined from the large-signal machine tests, appendix E.

$$\begin{aligned} \text{unsaturated direct axis synchronous reactance, } X_d &= 27.6\Omega \\ \text{direct axis leakage reactance, } X_l &= 1.72\Omega \end{aligned}$$

The unsaturated mutual reactance between the field and the direct axis, X_{md}, can then be calculated as shown in Equation: F.1.

$$X_{md} = X_d - X_l \tag{F.1}$$

$$= 25.88\Omega$$
$$= 1.134pu$$

From the unsaturated portion of the open circuit characteristics

$$\text{terminal voltage, } V_t = 154V$$
$$= 0.371pu$$

when field excitation current, $i_{fd} = 0.464\text{A}$

But in per unit

$$V_q = V_t = X_{md} * i_{fd}$$
$$0.371 = 1.134 * i_{fd}(pu)$$

Therefore

$$i_{fd}(pu) = 0.327pu \equiv 0.464A$$

Therefore

1 per unit excitation current = 1.418A(d.c.)

Bibliography

[1] B. Adkins and R.G. Harley. *The General Theory of Alternating Current Machines: Application to Practical Problems.* Chapman and Hall, 1975.

[2] S.I. Ahson and M.H. Ali. A microprocessor-based scheme for torque-angle and speed measurement. *IEEE Trans Ind Elec*, IE-34(2):135–138, May 1987.

[3] J.D. Ainsworth. The phase-locked oscillator - a new control system for controlled static converters. *IEEE Trans Power Apparatus and Systems*, PAS-87:859–865, March 1968.

[4] I.M. Canay. Extended synchronous machine model for calculation of transient processes and stability. *Electr Mach and Electro-mech*, 1:137–150, 1977.

[5] IEEE Power Engineering Education Committe. *IEEE tutorial course on power system stabilization via excitation control*, 1980.

[6] M.E. Coultes and W. Watson. Synchronous machine model by standstill frequency response test. *IEEE Trans on Power Apparatus ans Systems*, PAS-100(4):1480–1489, April 1981.

[7] P.L. Dandeno, P. Kundur, A.T. Poray, and H.M. Zein El-Din. Adaption and validation of turbogenerator model parameters through on line frequency response measurements. *IEEE Summer Power Meeting*, paper 80(SM 576-9), 1980.

[8] P.L. Dandeno and A.T. Poray. Development of detailed turbogenerator equivalent circuits from stanstill frequency response measurements. *IEEE Summer Power Meeting*, paper 80(SM 575-1), 1980.

[9] F.P. DeMello and C. Concordia. Concepts of synchronous machine stability as affected by excitation control. *IEEE Trans*, PAS:316–329, April 1969.

[10] A.M. El-Serafi and Hamdy S. Khalil. A direct method for determining the dynamic behaviour of synchronous machines usingqunc response dataye fre. *IEEE PES Winter Meeting*, paper C 75(182-1), 1975.

[11] M.J. Gibbard and Q.H. Kean. Identification of excitation system parameters. *IEE Trans*, PAS-94:1201–1207, 1975.

[12] J.D. Hurley and H.R. Schwenk. Standstill frequency response modelling and evaluation by field tests on a 645 mva turbine generator. *IEEE Trans on Power Apparatus and Systems*, PAS-100(2):828–836, February 1981.

[13] IEEE. *IEEE Guide: Test Procedure for Synchronous Machines*, 1983.

[14] R.D. Land. *The identification of power system dynamics by pseudo-random ternary noise injection and cross correlation.* PhD thesis, University of Sydney, 1984.

[15] T.A. Lipo and K.C. Change. A new approach to flux and torque-sensing in induction machines. *IEEE Trans on Ind Appl*, 1A-22:731–737, July 1986.

[16] R.W. Merchant. *Recursive estimation using the bilinear operator with applications to synchronous machine parameter identification.* PhD thesis, The University of Adelaide, 1992.

[17] Motorola. *HC11 Reference Manual*, 1991.

[18] L. Salvatore and M. Savino. Experimental determination of synchronous machine parameters. *IEE Proc B Electr Appl,*, 128(4):212–218, 1981.

[19] G. Shackshaft and A.T. Poray. Implimenation of new approach to determination of synchronous-machine parameters from tests. *Proc IEE*, 124(12):1170–1178, December 1977.

[20] J. Webb and V. Gosbell. Stationary d.c. decay tests on a 50mw turbo generator to obtain q-axis parameters. *Trans IE Aust*, EE14(2):97–100, 1978.